Synthesis of lactic acid using hydrogen cyanide extracted from cassava (*Manihot esculenta*) leaves

By

Monga Ilunga

(Reg. No: 20809093)

Submitted in fulfilment of the requirements for the degree of

MASTER OF APPLIED SCIENCE

in

CHEMISTRY

in the

FACULTY OF APPLIED SCIENCES

at the

DURBAN UNIVERSITY OF TECHNOLOGY

Supervisor: Dr Vimla Paul

Co-supervisors: Dr Orpah Zinyemba

Dr Sudhakar Muniyasamy

DECLARATION

I, Monga Ilunga, hereby declare that the research work reported in this thesis, besides where indicated, is my original work and has not been presented for any degree to this or any other institution, and its only publication was in the form of conference presentations and journal publication as listed on page xviii.

Student Name: Monga Ilunga

Signature: Date: 12 May 2022

Supervisor Name: Dr. Vimla Paul

Signature Date: 12 May 2022

Co-supervisor Name: Dr. Orpah Zinyemba

Signature: Date: 12 May 2022

Co-supervisor Name: Dr. Sudhakar Muniyasamy

Signature: Date: 12 May 2022

DEDICATION

To my Lord and Saviour Jesus Christ, for being the rock on which I stand. Your unconditional love, faithfulness and guidance have seen me through everything.

To my mother Christiane Ngoy Mavungu Mukala, for your love and support. You showed me that I could achieve anything I set my mind to.

To the late Alain Monga Ngoi Musoboi (Father) and Yvan Monga Maloba (Brother). You both never said goodbye or that you were going. Only God knows why you were gone before I even realized it. You will forever live through my memories.

To my husband Jean-Marie Mwepu Mbuya and my son Yannis Serge Kilobo Mbuya. Your love, support and patience throughout this journey inspired me to push and never give up. Thank you for everything – I love you.

To my siblings, Freddy, Carole, Alex, Magalie and Vanessa. You guys supported me and encouraged me through it all. Best cheerleading squad ever!!!!

ACKNOWLEDGEMENTS

It is by no means possible that I would have made it without the support of the following set of inspirational people in my life. Foremost, I extend my deepest gratitude to **God Almighty** for providing me with the wisdom, peace, strength and good health that enabled me to undertake this research. **To God be the Glory!** For He said in *Luke 1:37*

"For nothing will be impossible with God".

I convey my heartfelt gratitude and appreciation to my supervisor **Dr. Vimla Paul** and co-supervisors **Dr. Orpah Zinyemba** and **Dr. Sudhakar Muniyasamy** for their guidance, patience, assistance, and encouragement throughout this long journey. You never gave up on me despite the many challenges and setbacks that I faced.

To my DUT family, I would like to thank all the staffs at the department of Chemistry for shaping me into the scientist I am today. Special thanks to Mr S. R. Chetty for his continuous support. You have instilled in me the love of meticulous laboratory work. Mrs Dervani Naicker (Avy), thank you for the experimental insight.

To my second family in the department of Chemical Sciences at the University of Johannesburg. Thank you to everyone for having me and making me feel welcome for the past four years. Special thanks to Mr Meshack Thivhani, Mr Christopher Kgatshe, and Dr. Batsile Mogudi for providing training and assistance with the instrumets. I would further like to thank Mr Mutshi Nwamadi, Mr Siyasanga Mpelane and Ms Orienda Sebabi for their experimental assistance at the Spectrum Analytical Facility.

Finally, I would like to thank the National Research Foundation (NRF) for the financial support.

TABLES OF CONTENTS

DECLARATION ii
DEDICATION iii
ACKNOWLEDGEMENTS iv
TABLES OF CONTENTS v
LIST OF FIGURES ix
LIST OF TABLES xii
LIST OF ACRONYMS AND SYMBOLS xiii
RESEARCH OUTPUTS xviii
ABSTRACT xix
CHAPTER 1: INTRODUCTION 1
1.1 Background information 1
1.2 Statement of the problem and justification 3
1.3 Research hypothesis 4
1.4 Research objectives 5
1.5 Research Methodology 5
1.6 Significance of the study 5
1.7 Scope and limitations of the study 6
1.8 Outline of the thesis 6
CHAPTER 2: LITERATURE REVIEW 7
2.1 LACTIC ACID 7
2.1.1 Introduction 7
2.1.2 Lactic Acid Properties 7
2.1.3 Production Technologies 8
2.1.3.1 Chemical Synthesis 8
2.1.3.2 Carbohydrate Fermentation 9
2.1.3.2.1 Raw materials for lactic acid production 9
2.1.3.2.2 Microorganisms for lactic acid production 10
2.1.3.2.3 Fermentation media 10
2.1.3.2.4 Fermentation methods 11
2.1.3.3 Catalytic conversion 11
2.1.4 Applications Areas of Lactic Acid 14
2.2 HYDROGEN CYANIDE 15
2.2.1 Introduction 15

2.2.2 Hydrogen cyanide properties 16
2.2.3 Production Technologies 17
2.2.3.1 Industrial processes 17
2.2.3.1.1 Andrussow process 17
2.2.3.1.2 The Blausaure Methane Anlage (BMA) process 18
2.2.3.1.3 Sohio process 18
2.2.3.1.4 Shawinigan process 19
2.2.3.2 Natural sources of hydrogen cyanide 19
2.2.3.2.1 Fungi 21
2.2.3.2.2 Algae 21
2.2.3.2.3 Animals 21
2.2.3.2.4 Plants 22
2.2.4 Application Areas of Hydrogen cyanide 23
2.3 CASSAVA 23
2.3.1 Introduction 23
2.3.2 Cassava Production 25
2.3.3 Cyanogenic nature of cassava 27
2.3.4 Factors affecting the cyanide content of cassava 31
2.3.4.1 Seasonal conditions 31
2.3.4.2 Soil type 31
2.3.4.3 Cassava cultivar 31
2.3.4.4 Altitude 31
2.3.4.5 Age of cassava crop 32
2.3.5 Analysis of cyanogenic glucosides 32
2.3.5.1 Direct determination of cyanogenic glucosides 32
2.3.5.2 Indirect determination of cyanogenic glucosides 32
2.3.5.2.1 Extraction of cyanogens from plant materials 33
2.3.5.2.2 Hydrolysis of cyanogenic glucosides to cyanide 33
2.3.5.2.3 Analysis of endogenous cyanide 34
2.3.6 Uses of cassava, impact of cyanide in cassava processing effluent and cyanide 39
2.3.6.1 Cassava uses 40
2.3.6.1.1 Cassava roots 40
2.3.6.1.2 Cassava leaves 40
2.3.6.1.3 Cassava stems 41
2.3.6.2 Impact of cyanide in cassava processing effluent 41

2.3.6.3 Cyanide remediation 42
CHAPTER 3: MATERIALS AND METHODS 43
3.1 Materials 43
3.1.1 Sample collection 43
3.1.2 Chemicals and Preparation of reagents 43
3.1.2.1 Absorbing solutions 43
3.1.2.2 Sodium cyanide standard solutions 43
3.1.2.3 Reagents for the alkaline titration method 44
3.1.2.4 Reagent for the spectrophotometric method (alkaline picrate method) 45
3.1.2.5 Reagents for the determination of sodium carbonate and sodium hydroxide in 45
3.1.2.6 Reagents for racemic lactic acid synthesis 46
3.2 Methods 46
3.2.1 Extraction of hydrogen cyanide from cassava leaves 46
3.2.1.1 Optimization of maceration time and temperature, and recovery time 46
3.2.1.2 Release of hydrogen cyanide from plant material 46
3.2.1.3 Recovery of released hydrogen cyanide 47
3.2.2 Quantification of extracted hydrogen cyanide 48
3.2.2.1 Alkaline titration method (Titrimetric method) 48
3.2.2.2 Alkaline picrate method (Spectrophotometric method) 49
3.2.3 Determination of sodium carbonate and sodium hydroxide in sodium cyanide 51
3.2.4 Drying of sodium cyanide solution 53
3.2.5 Synthesis of racemic lactic acid 54
3.2.5.1 Addition of hydrogen cyanide/Preparation of DL-lactonitrile 54
3.2.5.2 Hydrolysis by hydrochloric acid 55
3.2.5.3 Esterification (Fischer esterification) 55
3.2.5.4 Hydrolysis by acidified water 56
3.2.6 Structural confirmation of synthesised products 56
3.2.6.1 Attenuated Total Reflectance - Fourier Transform Infrared Spectroscopy (ATR-FTIR) 56
3.2.6.2 X-ray diffraction analysis (XRD) 56
3.2.6.3 Scanning Electron Microscopy with Energy Dispersive X-Ray spectroscopy (SEM-EDS) 57
3.2.6.4 ^{1}H Quantitative nuclear magnetic resonance (^{1}H QNMR) 57
3.2.7 Statistical analysis 58
CHAPTER 4: RESULTS AND DISCUSSION 59
4.1 Comparative study using two different analytical methods 59

4.2 Optimization of hydrogen cyanide extraction from cassava leaves 62
4.2.1 Optimization of maceration time 62
4.2.2 Optimization of maceration temperature 63
4.2.3 Optimization of recovery time 64
4.3 Saturation of absorbing solution with naturally produced hydrogen cyanide 65
4.4 Determination of sodium carbonate and residual sodium hydroxide in sodium cyanide salt 66
4.5 Characterization of sodium cyanide prepared using HCN gas extracted from cassava leaves 68
4.5.1 Attenuated total reflectance- Fourier transform infrared spectroscopy (ATR-FTIR) 68
4.5.2 X-ray diffraction analysis (XRD) 70
4.5.3 Scanning electron microscopy with energy dispersive x-ray spectroscopy (SEM/EDS) 72
4.6 Synthesis of racemic lactic acid 74
4.6.1 Addition of hydrogen cyanide/Preparation of DL-lactonitrile (Step 1) 75
4.6.1.1 Attenuated total reflectance- Fourier transform infrared spectroscopy (ATR-FTIR) 76
4.6.1.2 ^{1}H Quantitative nuclear magnetic resonance (^{1}H QNMR) 77
4.6.2 Hydrolysis by hydrochloric acid (Step 2) 78
4.6.2.1 Attenuated total reflectance- Fourier transform infrared spectroscopy (ATR-FTIR) 79
4.6.2.2 ^{1}H Quantitative nuclear magnetic resonance (^{1}H QNMR) 80
4.6.3 Esterification (Step 3) 81
4.6.3.1 Attenuated total reflectance- Fourier transform infrared spectroscopy (ATR-FTIR) 82
4.6.3.2 ^{1}H Quantitative nuclear magnetic resonance (^{1}H QNMR) 84
4.6.4 Hydrolysis by acidified water (Step 4) 86
4.6.4.1 Attenuated total reflectance- Fourier transform infrared spectroscopy (ATR-FTIR) 87
4.6.4.2 ^{1}H Quantitative nuclear magnetic resonance (^{1}H QNMR) 89
CHAPTER 5: CONCLUSIONS AND RECOMMENDATIONS 91
5.1 Conclusions 91
5.2 Recommendations 93
REFERENCES 94

LIST OF FIGURES

Figure 2.1: Chemical structure of L (+)-lactic acid and D (-)-lactic acid.....8

Figure 2.2: Common chemicals derived from lactic acid.....15

Figure 2.3: Biosynthetic pathway of cyanogenic glycoside from amino acid 20

Figure 2.4: Some cyanogens found in bacteria 21

Figure 2.5: Hydrolysis of cyanogenic glycosides 22

Figure 2.6: Worldwide spread of cassava 24

Figure 2.7: Propagation methods of cassava.....26

Figure 2.8: World cassava production (a), major producers (b), major importers (c) and major exporters (d) for 2017.....27

Figure 2.9: Location of cyanogenic glucosides and linamarase enzyme in plant cell 28

Figure 2.10: Chemical structures of cyanogenic glucosides found in cassava.....28

Figure 2.11: Hydrolysis of cyanogenic glucosides.....29

Figure 2.12: Synthesis of cyanogenic glucosides in cassava 30

Figure 3.1: Release of hydrogen cyanide gas (cyanogenesis) from cassava leaves.....47

Figure 3.2: Hydrogen cyanide recovery under vacuum at 35 °C–40 °C.....47

Figure 3.3: Titration set up.....49

Figure 3.4: Formation of sodium isopurpurate.....49

Figure 3.5: Samples preparation for UV analysis 51

Figure 3.6: Steps of drying process.....54

Figure 4.1: Typical standard calibration curve for the spectrophotometric determination of HCN 61

Figure 4.2: HCN concentration (mg/Kg) at different maceration times 63

Figure 4.3: HCN concentration (mg/Kg) at different maceration temperatures 64

Figure 4.4: % HCN recovered at different times under vacuum at 35 °C – 40 °C 65

Figure 4.5: Saturation of 5.1064 mol/L NaOH absorbing solution over time with HCN gas extracted from cassava leaves 66

Figure 4.6: ATR-FTIR spectra of sodium cyanide 69

Figure 4.7: ATR-FTIR spectra of sodium carbonate 70

Figure 4.8: X-ray diffraction patterns of sodium cyanide 71

Figure 4.9: X-ray diffraction patterns of sodium carbonate 72

Figure 4.10: SEM images and EDS spectra of (a) control NaCN, (b) green NaCN, (c) control Na_2CO_3 and (d) precipitated Na_2CO_3 73

Figure 4.11: Synthesis of DL-lactonitrile 76

Figure 4.12: ATR-FTIR spectra of control and synthesised DL-lactonitrile 77

Figure 4.13: ^{1}H QNMR (500 MHz, DMSO-d6) spectra of (a) control DL-lactonitrile, (b) synthesised DL-lactonitrile, (c) solvent only and (d) 37% HCl 78

Figure 4.14: Hydrolysis of synthesised DL-lactonitrile 79

Figure 4.15: ATR-FTIR spectra of control and crude racemic lactic acid 80

Figure 4.16: ^{1}H QNMR (500 MHz, D_2O) spectra of (a) control racemic lactic acid and (b) crude racemic lactic acid 81

Figure 4.17: Esterification of crude racemic lactic acid 82

Figure 4.18: ATR-FTIR spectra of control and impure methyl-DL-lactate 83

Figure 4.19: Purification of impure methyl-DL-lactate 83

Figure 4.20: ATR-FTIR spectra of control and purified methyl-DL-lactate.....84

Figure 4.21: ^{1}H QNMR (500 MHz, D_2O) Spectra of (a) control methyl-DL-lactate, (b) impure methyl-DL-lactate and (c) purified methyl-DL-lactate.....86

Figure 4.22: Hydrolysis of purified methyl-DL-lactate with acidified water.....87

Figure 4.23: ATR-FTIR spectra of control and pure racemic lactic acid.....88

Figure 4.24: ATR-FTIR spectra of control and recovered methanol.....88

Figure 4.25: ^{1}H QNMR (500 MHz, D_2O) spectrum of synthesised racemic lactic acid.....89

Figure 4.26: ^{1}H QNMR (500 MHz, D_2O) spectra of (a) control methanol and (b) extracted methanol.....90

LIST OF TABLES

Table 3.1: Preparation of test solutions for method comparison and cyanide recovery studies 44

Table 3.2: Preparation of standards for the spectrophotometric method 44

Table 3.3: Dilution of standard test solutions 50

Table 3.4: Preparation of cyanide solutions for UV analysis 50

Table 3.5: Volumes of HCl solution used to titrate Na_2CO_3 and NaOH in the NaCN solution 53

Table 4.1: Hydrogen cyanide concentration in standard solutions as determined by two different methods 59

Table 4.2: Absorbance values 61

Table 4.3: Estimation of Na_2CO_3 and residual NaOH in sodium cyanide 67

Table 4.4: Density and weight of synthesised compounds 75

LIST OF ACRONYMS AND SYMBOLS

%	Percentage
°C	Degree Celsius
µg/mL	Microgram per litre
µL	Microlitre
^{1}H QNMR	Proton Quantitative Nuclear Magnetic Resonance
Å	Armstrong
A	Peak area
Ag/AgCl	Silver/Silver chloride
$AgNO_3$	Silver nitrate
Al	Aluminium
APTMS	3-aminoproyltrimethoxysilane
aq.	Aqueous
ATR-FTIR	Attenuated Total Reflectance - Fourier Transform Infrared Spectroscopy
$Ba(OH)_2$	Barium hydroxide
BMA	Blausaure Methane Anlage
C	Carbon
$Ca(OH)_2$	Calcium hydroxide
CH_3COOH	Acetic acid
CL	Confidence level
cm^{-1}	Per centimetre
CN^-	Cyanide ion
CNGs	Cyanogenic Glycosides
Co(II)	Cobalt ion
CO_2	Carbon dioxide
CO_3^{2-}	Carbonate
Conc.	Concentration

Cu^{2+}	Cupric ion
CuCTAB/MgO	Cetyltrimethylammonium bromide (CTAB) capped copper supported on magnesia
CuO/ZrO_2	Copper oxide supported on Zirconium dioxide
D_2O	Deuterium oxide
D-LA	D (-) - lactic acid
DL-LA	Racemic lactic acid
DMF	Dimethylformamide
DMSO-*d6*	Deuterated Dimethyl Sulfoxide
Er/deAlβ-2	Erbium-grafted de-aluminated β zeolite
$ErCl_3$	Erbium trichloride
Er-K10	Erbium-exchanged montmorillonite K10
FA	Formic acid
FE-SEM	Field Emission Scanning Electron Microscope
FIA	Flow injection analysis
g/g	Gram per gram
g/L	Gram per litre
g/L.h	Gram per litre per hour
g/mL	Gram per millilitre
g/mol	Gram per mole
GC-MS	Gas Chromatography Mass Spectrometry
H^+	Hydrogen ion
H_2CO_3	Carbonic acid
H_2O	Water
H_2SO_4	Sulphuric acid
H_3PO_4	Orthophosphoric acid
$H_6[PV_3Mo_9O_{40}]$	Keggin-type POM switchable catalyst
HCl	Hydrochloric acid
HCN	Hydrogen cyanide

HCO_3^-	Bicarbonate
HCOOH	Formic acid
HPLC-DAD	High-Performance Liquid Chromatography with Diode-Array Detection
HPLC-RI	High-Performance Liquid Chromatography with Refractive Index Detection
HPLC-UV	High-Performance Liquid Chromatography with Ultraviolet Visible Detection
ICDD	International Centre for Diffraction Data
Int	Integral
IS	Internal Standard
ISE	Ion-Selective Electrode
K_2CrO_4	Potassium chromate
$K_5[V_3W_3O_{19}]$	Lindqvist-type POM switchable catalyst
KI	Potassium iodide
KOH	Potassium hydroxide
LA	Lactic Acid
LC-MS/MS	Liquid Chromatography-tandem Mass Spectrometry
liq.	Liquid
L-LA	L (+) – lactic acid
M	molar concentration (Molarity)
mg/Kg	Milligram per kilogram
mg/L	Milligram per litre
mg/mL	Milligram per millilitre
MHz	Megahertz
min	Minutes
mmol/L	Millimole per litre
mol/L	Mole per litre
MPa	Megapascal
Mw	Molecular weight

n	Number of ^{1}H atoms
N	Number of signal within the target analyte
N_2	Nitrogen
Na	Sodium
Na_2CO_3	Sodium carbonate
Na_2HCO_3	Sodium bicarbonate
Na_2SiO_3	Sodium silicate
NaCl	Sodium chloride
NaCN	Sodium cyanide
NaOH	Sodium hydroxide
NH_4OH	Ammonium hydroxide
Ni(II)	Nickel ion
nm	Nanometre
O	Oxygen
OH^-	Hydroxide
P	Purity
PDDLA	Poly-DL-lactic acid
PDLA	Poly-D-lactic acid
PLA	Poly Lactic Acid
PLLA	Poly-L-lactic acid
POM	Polyoxometalate
ppm	Parts per million
RPLC	Reversed-Phase Liquid Chromatography
rpm	Revolutions per minute
SA	South Africa
SEM-EDS	Scanning Electron Microscopy with Energy Dispersive X-Ray Spectroscopy
$SEM_{stat.}$	Standard Error of the Mean
Sn	Tin

SO_2	Sulphur dioxide
SPE	Solid Phase Extraction
SSA	Sub-Saharan Africa
std	Standard
t	Target analyte
TLC	Thin Layer Chromatography
USA	United State of America
V	Volume
W	Weight
W/V	Weight per volume
XRD	X-Ray Diffraction
ZrO_2	Zirconium oxide
ΔH	Enthalpy change
δ	Delta

RESEARCH OUTPUTS

Publications

Authors: Ilunga Monga, Vimla Paul, Sudhakar Muniyasamy and Orpah Zinyemba

Year: May 2022

Title: Green synthesis of Sodium Cyanide using Hydrogen Cyanide extracted under vacuum from Cassava (*Manihot esculenta* Crantz) leaves

Status: submitted

Conferences (oral presentations)

3rd International Conference on Composites, Biocomposites and Nanocomposites held at the Nelson Mandela Bay Stadium, Port Elizabeth, South Africa, 7th – 9th November 2018. "Synthesis of lactic acid using hydrogen cyanide extracted from cassava (*Manihot esculenta*) leaves".

The annual SACI Postgraduate Research Colloquium, 7th July 2021 (online). "Green synthesis of DL-lactic acid using hydrogen cyanide extracted from cassava (*Manihot esculenta* crantz) leaves". (1st Place: MSc oral).

Faculty of Applied Sciences Research Day 2021 (online), 25th November 2021. "Green synthesis of DL-lactic acid using hydrogen cyanide extracted from cassava (*Manihot esculenta* crantz) leaves".

ABSTRACT

Racemic lactic acid (2-hydroxypropanoic acid) has gained interest in the food and non-food industries and in producing biodegradable and biocompatible lactic acid polymers. Although racemic lactic acid is conveniently synthesised by chemical synthesis via the DL-lactonitrile route, it can also be produced by the fermentation process provided that suitable micro-organisms and substrates are used. However, regardless of the sustainability issues associated with the fermentation process, it is the preferred production method since the chemical process relies on fossil fuel resources. In this context, this study aims to extract hydrogen cyanide (HCN) from cassava (*Manihot esculenta* Crantz) leaves and then use it to chemically produce racemic lactic acid.

Cassava leaves were chosen as a natural source of HCN since they release 20 times more HCN than the tubers. HCN is produced by endogenous enzymes (linamarase and hydroxynitrile lyase) hydrolysing the cyanogenic glucosides (linamarin and lotaustralin). Following 120 minutes of maceration at 30 °C, the released HCN was extracted for 45 minutes under vacuum at 35 °C – 45 °C and collected in 400 mL of 5.104 mol/L sodium hydroxide (NaOH) solution (absorbing solution) to give sodium cyanide (NaCN) solution. The extraction process was repeated until saturation of the absorbing solution was achieved. The final concentration of NaCN solution determined by the alkaline picrate method was found to be 4.0421 mol/L.

Furthermore, the sodium carbonate (Na_2CO_3) and residual NaOH content in control and sample sodium cyanide solutions were also determined. The Na_2CO_3 content was 0.72 % in the control NaCN solution and 2.49 % in the sample NaCN solution. The residual sodium hydroxide content was 2.61 % in the control sodium cyanide solution and 4.20 % in the prepared sodium cyanide solution.

79.241 g of NaCN crystals (0.19 % yield, green NaCN) were obtained from 42.750 kg of fresh cassava leaves. The suggested approach was successful in preparing NaCN, as evidenced by X-Ray Diffraction (XRD), Attenuated Total Reflectance-Fourier Transform Infrared Spectroscopy (ATR-FTIR), and Scanning Electron Microscopy with Energy Dispersive X-Ray Spectroscopy (SEM-EDS) results. Control and green NaCN both contained sodium carbonate impurities, as shown by these spectral techniques. Titration tests revealed that the latter was 0.61 % and 2.29 % in control and green NaCN, respectively. In addition, titration studies indicated that the residual NaOH content in control NaCN was 1.63 % and 4.68 % in green

NaCN. The high carbonate content can be explained by the reaction between residual sodium hydroxide and atmospheric CO_2. Reproducibility and repeatability tests were done to evaluate the reliability of the hydrogen cyanide extraction method.

Racemic lactic acid was synthesised using a four-step process. 73 mL of DL-lactonitrile (2-hydroxypropanenitrile) (81.1 % yield, 59.7 % pure) was prepared by reacting 75 mL of acetaldehyde with hydrogen cyanide generated in-situ from green sodium cyanide (62.190 g in 150 mL of Milli-Q water) in the presence of 37 % hydrochloric acid (100 mL). 35 mL of crude racemic lactic acid (84.1 % yield, 14.9 % pure) was prepared by hydrolysing 40 mL of DL-lactonitrile with 8 mol/L hydrochloric acid (40 mL). Crude racemic lactic acid underwent a two-step purification process in the presence of concentrated sulphuric acid (5 mL), used as the catalyst. 35 mL of crude lactic acid was first esterified with excess methanol (50 mL) to produce 32 mL of methyl DL-lactate (methyl 2-hydroxypropanoate) (71.6 % yield, 46.1 % pure). The ester was then hydrolysed with excess water (20 mL) to give 22 mL of purified racemic lactic acid (88.0 % yield, 56.0 % pure). The identity of the synthesised products was confirmed by comparing them against control samples using ^{1}H Quantitative Nuclear Magnetic Resonance (^{1}H QNMR) and ATR-FTIR. Their purity was determined by ^{1}H QNMR, using dimethylformamide as the internal standard. The overall yield of synthesised racemic lactic acid was 43.0 %.

CHAPTER 1: INTRODUCTION

1.1 Background information

Cassava (*Manihot esculenta* Crantz) is a perennial crop that originated in Latin America and was later introduced into Africa and Asia by European traders between the 16th and 19th centuries (Burns et al., 2010, Omomowo et al., 2015, Wilberforce and Ngele, 2016). Even though almost 100 species of *Manihot* genus are reported, *Manihot esculenta* Crantz is the only commercially cultivated (Wangari, 2013). Cassava is the third most important source of energy in the tropics after rice and maise, and the fifth most important food source after maise, rice, wheat and potato (Guédé et al., 2013). It is a staple food for more than half of a billion people in tropical regions of Africa, Asia and Latin America (Burns et al., 2010, Diallo et al., 2014, Omotayo et al., 2015). Globally, according to the Food and Agriculture Organization of the United Nations publications catalogue ((FAO), November 2018), approximately 276 million tonnes of cassava were produced in 2017; which is a 0.3 % decrease from 2016, with Africa, Asia and Latin America producing 57 %, 32 %, and 11 % of the total, respectively. The top five national producers are Nigeria, followed by Thailand, Brazil, Ghana and Indonesia. These data of cassava production show the importance of cassava in the African continent, where it is primarily cultivated for consumption as a human foodstuff.

Cassava is admirably tolerant to drought and nutrient-deficient soil; hence it is often referred to as "the drought, war and famine crop" in most developing countries (Burns et al., 2010). Cassava is primarily cultivated for its enlarged starch-filled roots (tubers) rich in carbohydrates and minerals. The leaves, which provide an inexpensive and rich source of proteins, omega-3 fatty acids, fibres, minerals and vitamins, are also consumed in some regions. (Burns et al., 2010, Pereira et al., 2016, FRI, 2012). Nevertheless, cassava has attracted attention as a raw material for a wide range of industrial applications such as the production of bioethanol, textile, bioplastics, pharmaceuticals, paper and animal feed (Omomowo et al., 2015, Wilberforce and Ngele, 2016). The cassava production in South Africa is a relatively recent development, with the commercial exploitation only starting in 1948 (Nuwamanya et al., 2016). Cassava is commercially grown for its high-quality starch in the provinces of Limpopo, Mpumalanga and Northern KwaZulu-Natal, where it is called Mutumbula (Tshivenda), Muthupula (Xitsonga) or Unjumbula (isiZulu) ((DAFF), 2010). It is also grown as a secondary crop by subsistence

farmers (Amelework et al., 2021). However, its versatility is limited by its toxicity (Amelework et al., 2021).

Cassava (also called *manioc*, *manihot*, *tapioca* or *yucca*) is an essential food crop for humans whose toxicity is associated with cyanogenic glycosides (CNGs) presence in all edible parts. These CNGs are molecules of sugar attached to a cyanide group (Wangari, 2013). They are secondary metabolites produced by at least 2650 plants species (Cho et al., 2013, Saunders, 2012, Ubwa et al., 2015), where they act as defence mechanisms against herbivore and pathogen attack (FRI, 2012). Cassava contains two cyanogenic glycosides called cyanogenic glucosides (cyanogens) since glucose is the sugar molecule. They are namely linamarin and small amounts of lotaustralin. When the plant tissue is damaged, they release toxic hydrogen cyanide gas (HCN) in cyanogenesis. Upon disruption of the plant tissue, the cyanogens come into contact with linamarase, an endogenous enzyme that breaks them into glucose and cyanohydrins. The cyanohydrins are subsequently hydrolysed in a second reaction to release HCN, acetone (from linamarin) and a small amount of butanone (from lotaustralin) (Burns et al., 2010, Wilberforce and Ngele, 2016, Guédé et al., 2013, Diallo et al., 2014, Pereira et al., 2016, Ngugi et al., 2015, Zidenga et al., 2017). These cyanogens are distributed throughout the cassava plant except the seed, with the highest concentrations accumulating in the leaves (Burns et al., 2010, FRI, 2012, Ubwa et al., 2015, Lambri et al., 2013, Montagnac et al., 2009, Umuhozariho M et al., 2014) where they are synthesised before being transported to the root (Wangari, 2013).

The different cassava varieties are distinguished by their cyanide content. This difference in cyanide concentration can be caused by the location, plant age, or environment. The variety of species with low cyanide content is sweet cassava. They contain a high concentration of free sugars, and those with high cyanide content are referred to as bitter cassava (Burns et al., 2010, Ubwa et al., 2015). A variety without cyanide has never been naturally observed (Nhassico et al., 2008). Environmental factors such as drought, low soil fertility and pest attack can affect the bitterness of cassava (Ubwa et al., 2015, Tivana, 2012), resulting in this variety being more readily available and cheaper (Wangari, 2013).

The consumption of unprocessed cassava is toxic to humans since the fatal dose of ingested HCN is relatively low, ranging from 0.5 to 3.5 mg/kg body weight (Burns et al., 2010). Cassava

intoxication can either be acute or chronic. The symptoms observed from acute intoxication include death, rapid respiration, drop in blood pressure, rapid pulse, dizziness, stomach pains, vomiting, and mental confusion (Nyirenda, 2021). The symptoms associated with chronic intoxication include goitre, the swelling of the neck or larynx resulting from enlargement of the thyroid gland, and cretinism, dwarfism, mental retardation and also konzo, an irreversible paralysis of the legs, which occurs mainly in children (Nhassico et al., 2008, Nyirenda, 2021).

From environmental management and sustainable perspective, the processing of non-dried cassava plants into different products generates large volumes of wastewater. The particularity of this wastewater is its cyanide content, which makes it highly poisonous. Therefore, if allowed to flow freely, this contaminated water will pollute the soil and subsequently poison the receiving water (Omomowo et al., 2015, Eletta et al., 2016). Given the serious threat posed by this contaminated wastewater on human livelihood, environment and aquatic life (Omomowo et al., 2015, Chibueze Izah et al., 2018); and the increasing demand for the cassava; there is a compelling need for removing the cyanide prior to releasing it in the environment.

Concerns over the escalating global and environmental problems have incited researchers to develop greener production methods (Abdel-Rahman et al., 2013). The main attraction of these greener methods is the use of renewable raw materials during the production processes. Consequently, cassava could be used as a raw material for producing any product that requires HCN in its production process since it releases HCN ranging from 1 to 2000 mg/Kg HCN equivalent (Nyirenda, 2021, Burns et al., 2010). As a result, adding value to the cyanide produced by processing the cassava plant is beneficial, particularly in terms of environmental sustainability. Of these products, racemic lactic acid (DL-LA) is one of the most important owing to its extensive use in the food, pharmaceutical, cosmetic and chemical industries (Sitompul et al., 2016).

1.2 Statement of the problem and justification

The chemical synthesis of the DL-LA monomer was prevalent until 1990 when the fermentation process was developed due to the increased costs of global energy and environmental problems associated with carbon emission (Komesu et al., 2017b, Lasprilla et al., 2012). However, owing to the disadvantages associated with the fermentation method, such as the use of food carbohydrates as substrates, contamination problems and end-product

inhibition (Abdel-Rahman and Sonomoto, 2016), there is urgency in using cheap renewable raw materials that do not compete with food security during the chemical synthesis of DL-LA. Hence, this will allow us to overcome the lack of interest associated with the chemical synthesis of DL-LA.

Moreover, since the starting materials of the chemical synthesis route, namely acetaldehyde and HCN, are typically derived from petroleum or natural gas, it is crucial to find an alternative route for their production to reduce the global energy environmental problems (Akoetey, 2015). Currently, acetaldehyde can be produced at an industrial scale from bio-ethanol (Sekab, 2021). It is possible to transform the fossil fuel-based chemical process into a cost-effective and environmentally friendly process if HCN is also produced from inexpensive renewable resources. Therefore, due to the increasing interest in DL-LA over the last few years and its application in the medical field for drug delivery (Borandeh et al., 2021), there is an urgency in using materials derived from renewable sources in its production process. The principal renewable sources of HCN are the plants where it occurs as cyanogenic glycosides.

The cassava plant, known to contain HCN in all parts, produces a relatively high concentration of HCN ranging from 1 to 2000 mg/Kg HCN equivalent (Nyirenda, 2021, Burns et al., 2010) from the enzymatic hydrolysis of cyanogenic glucosides (linamarin and lotaustralin), is a good candidate for cheap renewable HCN source. The status of the cassava plant as an inexpensive source of HCN is further supported by the fact that it is the staple food of approximately 800 million people in tropical countries and is a raw material in many industries (Burns et al., 2010, Diallo et al., 2014, Omotayo et al., 2015). These industries need to process cassava to remove the toxic cyanogenic glucosides. Thus producing large amounts of cyanide-rich wastewater, which instead of being discharged as effluent into waterways, where it creates environmental problems, can instead be collected and used to synthesise valuable products. This research work reports on the removal of HCN from cassava leaves and its subsequent use for DL-LA production using a chemical synthesis method.

1.3 Research hypothesis

Cassava leaves contain cyanogenic glucosides, which, when hydrolysed, produce a considerable amount of HCN. The latter was extracted and used to synthesise DL-LA.

1.4 Research objectives

The research was carried out to investigate the possibility of using cassava leaves as a natural source of HCN for the chemical synthesis of DL-LA. An extraction method was developed by optimising extraction parameters (maceration temperature and time and HCN recovery time) for the complete release of HCN from cassava leaves by autolysis. The concentration of HCN liberated from cassava leaves and collected in an aqueous sodium hydroxide (NaOH) solution (absorbing solution) was determined using the most effective cyanide determination method. This method was identified after comparing titrimetric (alkaline titration) and spectrophotometric (alkaline picrate solution) methods.

1.5 Research Methodology

This section only outlines a brief methodology that was used throughout this research. HCN released from cassava leaves using the optimum extraction parameters and extracted under vacuum between 35 °C and 40 °C was collected in the absorbing solution to be converted to sodium cyanide (NaCN). The NaCN crystals (green NaCN) were obtained after drying the prepared cyanide solution. The identity, the crystal structure and purity of green NaCN was confirmed against control NaCN salt by attenuated total reflectance-fourier transform infrared spectroscopy (ATR-FTIR), x-ray diffraction analysis (XRD) and scanning electron microscopy with energy dispersive x-ray spectroscopy (SEM-EDS). HCN generated in-situ from green NaCN was reacted with acetaldehyde in the presence of concentrated hydrochloric acid (HCl) to produce DL-lactonitrile. Crude DL-LA was prepared by hydrolysing DL-lactonitrile with dilute HCl. The crude DL-LA was purified by esterification with methanol, then hydrolysis using water acidified with concentrated sulphuric acid (H_2SO_4) (Komesu et al., 2017b). The reliability of the HCN extraction method was determined by reproducibility and repeatability tests. In contrast, the validity of the DL-LA synthesis method was achieved by comparing the structure of the synthesised products against control samples using ^{1}H-NMR and ATR-FTIR. The former spectral technique was also used to determine their purity.

1.6 Significance of the study

The information in this research on the extraction of HCN from cassava leaves will be crucial for synthesising other valuable chemicals. The HCN extraction method developed can be applied to any cyanogenic plant. The use of naturally produced HCN allows converting the once unsustainable chemical synthesis method of LA into a green method. In addition, such

information will be critical towards informing farmers on the potential of cassava wastewater as a secondary source of income.

1.7 Scope and limitations of the study

This work involved investigating DL-LA production by chemical synthesis process using HCN extracted from cassava leaves bought from local markets. This study was only limited to cassava leaves, although the cassava root (tuber) and other plant materials could have been used since about 2600 plant species are known to produce HCN. Other cyanogenic plant species that could have been used are lima bean, bitter almond, sorghum, linseed and bamboo shoots.

1.8 Outline of the thesis

The thesis is divided into five chapters. Chapter one will include the background information, statement of the problem and justification of the research, research hypothesis, and research objectives, brief description of the research methodology, the significance of the research, and the research's scope and limitations. Chapter two will include a comprehensive literature review comprising definitions, other synthesis routes and cyanide removal treatment methods. The literature review was crucial in providing the guidelines for the research project. In chapter three, materials and significant factors affecting HCN extraction from cassava leaves needed in the DL-LA production by a chemical process and the detailed methodology used will be discussed. The research findings for optimum HCN extraction and its subsequent use in DL-LA production by the chemical process will be presented in chapter four. Parameters such as maceration temperature and time, HCN recovery time, and the most effective method for cyanide determination will be investigated in detail and discussed in chapter four. The findings of the research projects will be concluded in chapter five, and some recommendations for future studies will also be included.

CHAPTER 2: LITERATURE REVIEW

2.1 LACTIC ACID

2.1.1 Introduction

Lactic acid (intended as the two *L* and *D* isomers together with the racemic mixture), or 2-hydroxypropionic acid, is the most widely occurring hydroxycarboxylic acid (Komesu et al., 2017b, Ameen and Caruso, 2017). It is a natural organic acid that has mainly gained interest in the food and non-food industries, including producing biodegradable and biocompatible lactic acid polymers (PLA) (Komesu et al., 2017b, Abdel-Rahman et al., 2013, Sobrun et al., 2012). PLA uses range from packaging to foams and fibres (Abdel-Rahman et al., 2013) and manufacturing of biomedical devices (Acosta et al., 2005, Lasprilla et al., 2012, Narayanan et al., 2016). Lactic acid, also known as milk acid, was first discovered in 1780 by the Swedish chemist Carl Wilhelm Scheele, but Charles E. Avery achieved its first commercial production in 1881 at Littleton, Massachusetts, USA (Komesu et al., 2017b, Narayanan et al., 2004, Boontawan, 2010).

The global lactic acid market was estimated to be USD 2.9 billion in 2018 and is expected to reach USD 10.06 billion by 2025, growing at 19.43 % from 2019 to 2025. Increasing petroleum prices and the development of new uses and products, such as reinforcement of PLA with other materials, positively drive the expansion of the lactic acid market. The three largest regional markets for lactic acid are North America, the Asia Pacific and Europe (Research, 2019).

2.1.2 Lactic Acid Properties

These two functional groups, alcohol and acid, allow lactic acid to undergo various chemical reactions. The main classes of these reactions are condensation, oxidation, substitution, and reduction (Rashid, 2008). Lactic acid (LA) can be found as a white crystalline solid when anhydrous or as a clear to yellowish liquid when melted or dissolved in water (Komesu et al., 2017b, Rashid, 2008). It is odourless, sour in taste, soluble in water, ether, and alcohol, but insoluble in chloroform (Komesu et al., 2017b, Rashid, 2008). LA exists in two optically active isomeric forms (Figure 2.1), L (+)-lactic acid (L-LA) and D (-)-lactic acid (D-LA), and in racemic form (DL-LA), which is a mixture of L (+)-lactic acid and D (-)-lactic acid (Komesu et al., 2017b, Ameen and Caruso, 2017, Abdel-Rahman and Sonomoto, 2016).

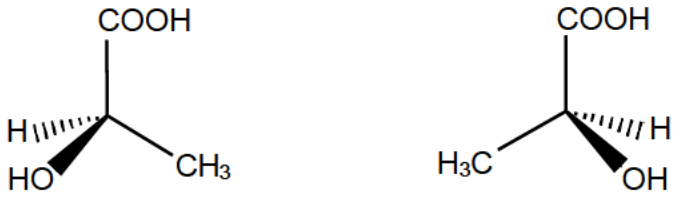

L(+)-lactic acid D(-)-lactic acid

Figure 2.1: Chemical structure of L (+)-lactic acid and D (-)-lactic acid

The optically active isomers behave differently in living tissues (Komesu et al., 2017b). The L isomer is the biological isomer as it is naturally produced in the human body during muscle contraction (Komesu et al., 2017b, Ameen and Caruso, 2017). Hence, its commercial production is more developed than the D isomer and the racemic form (Akoetey, 2015).

2.1.3 Production Technologies

Lactic acid (LA), a naturally occurring organic acid found in plants, microorganisms, and animals (Komesu et al., 2017b), can be produced by either chemical synthesis from petroleum products, coal, and natural gas, by microbial fermentation of carbohydrates (Komesu et al., 2017b, Ameen and Caruso, 2017, Eiteman and Ramalingam, 2015, Shen et al., 2021, Karande et al., 2016) or catalytic conversion (Shen et al., 2021). Currently, most LA is industrially manufactured via microbial fermentation of carbohydrates (Shen et al., 2021, Subramanian et al., 2015, Coelho et al., 2011, Karande et al., 2016).

2.1.3.1 Chemical Synthesis

The production of Lactic acid (LA) using the chemical synthesis process only produces racemic lactic acid (DL-LA) (Komesu et al., 2017b, Sobrun et al., 2012, Ghaffar et al., 2014). Although there are several different routes used for the chemical production of LA, the hydrolysis of DL-lactonitrile by strong acids is the most preferred commercial method (Ameen and Caruso, 2017, Krishna et al., 2018). This method was developed in 1863 by the German chemist Johannes Wislicenus (Komesu et al., 2017a) because of the need for heat-stable LA in the baking industries (Ghasemi et al., 2009, Wee et al., 2006, Karande et al., 2016). The other chemical routes for LA synthesis are base-catalysed degradation of sugars, oxidation of propylene glycol, nitric acid oxidation of propylene, hydrolysis of 2-Chloropropionic Acid and the reaction of acetaldehyde, carbon monoxide, and water at high temperatures and pressure.

LA was first industrially produced by the chemical process in 1963 by the company Monsanto based in Texas, USA (Komesu et al., 2017b). Two other companies, namely, Sterling Chemicals Inc. (USA), which stopped production in the early 1990s, and Musashino Chemical (Japan), also used the DL-lactonitrile route to produce LA. They changed their production process to fermentation to overcome the drawbacks such as dependence on fossil fuels, price of raw materials, and the impurity of the product associated with the chemical process (Komesu et al., 2017b).

Since the chemical synthesis always leads to racemic lactic acid (DL-LA), and only one of the lactic acid isomers is desired for many specific applications, a chiral resolution must be factored in the cost if either D- or L- lactic acid isomers are the intended products. Chromatographic methods, chemical resolution and the combination of chemo- and biocatalysis are considered the means for chiral resolution of racemic lactic acid (Zhang et al., 2018). However, this can be bypassed by using biotechnological processes based on fermentation.

2.1.3.2 Carbohydrate Fermentation

Worldwide lactic acid (LA) from the fermentation process accounts for approximately 90 % of the total LA production (Komesu et al., 2017b, Lasprilla et al., 2012, Coelho et al., 2011, Lopes et al., 2012, Karande et al., 2016). The popularity of this production method is because it is eco-friendly, comparatively fast, has superior yields, and can produce stereospecific isomer, namely L-lactic acid (L-LA), D-lactic acid (D-LA) and racemic mixture (DL-LA), depending on the microorganism used (Reddy et al., 2008, Masutani and Kimura, 2014).

The biological degradation of a substrate by a population of microorganisms into the desired product, such as lactic acid, constitute the basis of any fermentation process (Komesu et al., 2017b). LA fermentation process is influenced by factors such as raw materials, fermentation media, microorganisms and fermentation method (Komesu et al., 2017b, Krishna et al., 2018).

2.1.3.2.1 Raw materials for lactic acid production

The choice of raw material depends on its price, availability, purity (Krishna et al., 2018, Ghaffar et al., 2014), rapid fermentation rate, high yields and little or no formation of by-products (Ghaffar et al., 2014). Some of the renewable raw materials used in LA production are refined materials such as carbohydrates (Komesu et al., 2017b, Krishna et al., 2018), starchy materials such as rice, cassava and maise (Komesu et al., 2017b), cellulosic materials such as wood (Krishna et al., 2018), lignocellulosic materials (Komesu et al., 2017b), agricultural

residues such as corn cob, cassava bagasse, beet molasses, sugarcane press mud and carrot waste (Krishna et al., 2018) and industrial wastes such as whey and molasses (Komesu et al., 2017b).

2.1.3.2.2 Microorganisms for lactic acid production

Microorganisms are indispensable in the production of lactic acid (LA). Hence, they must always be available and cheap (Krishna et al., 2018). Microorganisms used for LA production can be classified into bacteria, fungi and yeast (Komesu et al., 2017b, Abdel-Rahman et al., 2013, Krishna et al., 2018). Each microorganism has one or more advantages over the others, such as a wide raw materials range, better yield and productivity, reduction of nutritional requirements, or improved optical purity of LA (Abdel-Rahman et al., 2013). Various LA manufacturers have utilised genetic engineering methods to improve LA yield and optical purity (Abdel-Rahman et al., 2013, Krishna et al., 2018).

The criteria of selection of the ideal microorganisms to use depends on:

- The type of raw material to be fermented since the microorganisms' metabolism is dependent on the carbon source (Komesu et al., 2017b).
- The form of the final fermentation product, i.e. L (+)- lactic acid, D (-)- lactic acid or DL- lactic acid (racemic form) (Maślanka et al., 2015).

2.1.3.2.3 Fermentation media

The fermentation media is as essential as the microorganism is in any fermentation process. It can account for almost 50 % of the whole production process (Klaic et al., 2014). The type of nutrient media depends on the nutritional growth requirements of the specific microorganism to be used during lactic acid production (Basu et al., 2015).

Nutritional requirements are in turn classified as

a) Essential nutrients, when they are indispensable to the growth of bacteria, and no growth will be detected in their absence (Hayek and Ibrahim, 2013).

b) Simulatory nutrients, when they improve bacteria growth and decrease growth is measured in their absence (Hayek and Ibrahim, 2013).

c) Unessential nutrients, when they do not affect the growth of bacteria, do not influence the growth of bacteria, neither improve nor inhibit (Hayek and Ibrahim, 2013).

2.1.3.2.4 Fermentation methods

The selection of fermentation methods is governed by the type or nature of the substrate, microorganism growth, and viscosity of the fermentation broth (Abdel-Rahman et al., 2013). The most common fermentation methods used for lactic acid production are batch, continuous, fed-batch (Abdel-Rahman et al., 2013, Krishna et al., 2018, Bayitse, 2015) and repeated fermentations (Bayitse, 2015). The choice of fermentation mode also depends on the costs of the substrate and the costs involved with each fermentation process (Komesu et al., 2017b).

About the abovementioned requirements for lactic acid by bio-fermentation process, extensive research has been conducted using various raw materials, fermentation media, microorganisms, and different methods. For example, Yun et al. (2004) produced 129 g DL-LA/L using a newly isolated strain of *Lactobacillus Sp*. RKY2 by fermenting rice bran supplemented with whole rice in batch fermentation at 36 ºC and pH 6. Trontel et al. (2010) did a batch fermentation at 40 ºC and pH 5.5 and used amylolytic lactic acid bacterium *Lactobacillus amylovorus* DSM 20531^T to ferment glucose, sucrose, and starch to DL-LA. They produced DL-LA ranging from 10.08 g/L to 18.56 g/L.

Calabia and Tokiwa (2007) obtained maximum DL-LA yields of 84 g/L, 107 g/L and 120g/L from sugar beet juice, sugarcane molasses, and sugarcane juice, respectively, using the JCM 1148 strain of *L. delbrueckii* in batch fermentation. Budsabathip (2013) managed to ferment several carbohydrate sources to DL-LA using bacterial strains isolated from soils, plant bark, and root. They produced DL-LA ranging from 55.30 g/L to 77.31 g/L and productivity between 0.76 g/L and 1.07 g/L.h. However, Orozco et al. (2014) utilised lactose from powdered milk to produce DL-LA yield ranging from 0.52 g/g to 0.99 g/g using different microorganism strain in a batch system. Furthermore, they obtained a final concentration of 80.95 g/L DL-LA aqueous solution through microfiltration, nanofiltration and reverse osmosis membranes.

2.1.3.3 Catalytic conversion

Although the majority of the chemical catalytic systems (chemocatalytic processes) produce DL-LA (Li et al., 2019), they have gained more interest since they use biomass resources as raw materials. They also emerge as a promising alternative method for overcoming the sustainability issues (such as low productivity and need for high price enzymes) associated

with the current fermentation processes (Zhang et al., 2018, Li et al., 2017, Wang et al., 2013). The two most important types of biomass are wood and agricultural products or crops such as cassava, wheat, maise and rice (Bayitse, 2015).

Numerous studies have been done on the catalytic conversion of biomass to lactic acid (LA) in water or organic solvents, using different homogeneous or heterogeneous catalysts (Zhang et al., 2018, Wang et al., 2013, Li et al., 2017, Sánchez et al., 2012). In recent years, the hydrothermal conversion of different biomass has been extensively investigated. Kishida et al. (2006) conducted 13 experiments on several substrates for 10 minutes using NaOH catalyst under different hydrothermal reaction conditions and reported LA yields ranging from 0 % to 39.9 %. Kong et al. (2008) obtained an LA yield of 9.51 % from glucose using Co(II) catalyst while stirring at a speed of 400 rpm at 300 °C for 2 minutes. They also reported a yield of 6.62 % from microcrystalline cellulose using Ni(II) catalyst under the same conditions.

Several researchers investigated the hydrothermal reaction conditions at 300 °C for 1 minute. Jin and Enomoto (2008) and Yan et al. (2010) reported LA yields of 28 % and 20 %, respectively, from glucose using 0.32 mol/L calcium hydroxide ($Ca(OH)_2$) catalyst. However, Yan's research group only obtained a yield (27 %) closed to the one reported in Jin and Enomoto's study when they used 2.5 mol/L NaOH as the catalyst. LA yields of 43.5 % with 2.5 mol/L NaOH and 46 % with 2 mol/L potassium hydroxide (KOH) from fructose were reported by Ma et al. (2010). Duo et al. (2016) reported a LA yield of 30 % from glucose using Na_2SiO_3 catalyst.

Lei et al. (2014), Wang et al. (2015) and Wang et al. (2016) used the same hydrothermal reaction conditions of 240 °C under 2Mpa N_2 for 30 minutes in 30 mL of water and produced LA of 91.1 %, 67.6 % and 58 % yield, respectively. Lei and co-workers used 0.1 g cellulose and 0.05 g $ErCl_3$ catalyst, while both Wang research groups used 0.3 g of cellulose but a different catalyst. 0.1 g of Er-K10 catalyst was used in the 2015 study, while 0.1 g of Er/deAlβ-2 catalyst was used in the 2016 study. $ErCl_3$ grafted on the mesoporous silica (MCM-41) surface was used to produce LA from cellulose with a yield of 64 % (Tallarico et al., 2019). They performed an ultrasound pre-treatment to reduce the cellulose crystallinity before producing LA by microwave-assisted conversion at 220 °C for 90 minutes.

Wang et al. (2014) conducted 10 experiments to produce LA using 25 mmol/L glucose over 100 mmol/L polymer catalysts. The reactions were done under N_2 and 50 mmol/L aqueous

alkaline solutions at 100 °C for 30 minutes. They reported LA yields ranging from 7 % to 65.5 %. Orazov and Davis (2015) reported LA yields ranging from 3.9 % to 88.4 % after conducting 30 experiments using different substrates, catalysts and reaction conditions.

Yang et al. (2015) achieved a maximum LA yield of 42 % and 30 % by hydrothermal treatment of xylose and xylan, respectively, in alkaline water between 160 and 240 °C at 0 to 100 % O_2 pressure, and 0.5 to 4 catalyst to biomass weight ratio with ZrO2 catalyst. Yang et al. (2016) reported a LA yield of 94.6 % from 10 mL of 1.4 mol/L glycerol using 0.2g 30 %CuO/ZrO_2 catalyst in alkaline water (1:1 NaOH/glycerol molar ratio) at 180 °C and 1.4 MPa N_2 for 8 hours.

The use of modified (CuCTAB/MgO) and unmodified magnesium oxide (MgO) as catalysts was investigated by Choudhary et al. (2015) and He et al. (2016), respectively. A maximum LA yield of 70 % was reported when glucose was reacted with CuCTAB/MgO in the presence of NaOH at 120 °C for 1 hour. On the other hand, a maximum LA yield of 79.7 % was obtained by treating dissolved hemicelluloses derivatives with 0.5 g of MgO at 220 °C for 1 hour.

Li et al. (2017) and Kuy and Boonyarattanakalin (2019) investigated the use of barium hydroxide ($Ba(OH)_2$) as a catalyst for the production of lactic acid. In the study conducted in 2017b, LA yields of 95.4 % and 83.5 % were reported from 0.025 mol/L glucose and 0.1 mol/L fructose, respectively, in the presence of 0.25 mol/L catalyst under N_2 at 1 bar after 48 hours of reaction at room temperature. However, only 53.95±0.8 % LA yield was reported in the study done in 2019. LA was produced from cassava starch with 0.15 mol/L catalyst at 240 °C after 60 minutes.

Dong et al. (2016) and Shen et al. (2021) investigated the efficiency of modified Sn – Beta to catalyse the conversion of biomass to LA. Dong and co-workers reported a LA yield of 54 % from the sucrose in water without a base using Zn – Sn – Beta catalyst. The reaction was done under ambient air pressure at 190 °C for 2 hours. However, only 37 % LA yield was reported by Shen's research group. They used *Scenedesmus* algae as a substrate. The substrate was pre-treated in an ice bath ultrasound before mixing it with 3-aminopropyltrimethoxysilane (APTMS)-modified Sn-Beta catalyst. The one-step catalysis reaction was carried out for 5 hours at 190 °C using 50 µL of APTMS, 240 mg of Sn-Beta zeolite catalyst and 30 mg of *Scenedesmus* /mL.

Recently, the use of switchable catalysts has gained momentum. These catalysts are characterised by their ability to produce different products under the same reaction conditions when used in a different gas atmosphere. Voss et al. (2020) reported a maximum LA yield of 40 % from glyceraldehyde within 1 hour at 160 °C under N_2 in a one reactor setup. The Keggin-type polyoxometalate (POM) $H_6[PV_3Mo_9O_{40}]$ switchable catalyst was used. They obtained formic acid (FA) at a yield of 42 % when they performed the same experiment under an oxygen (O_2) atmosphere. They reported a maximum LA yield of 18 % under the N_2 atmosphere and a maximum FA yield of 16 % under the O_2 atmosphere from glyceraldehyde using the Lindqvist-type POM $K_5[V_3W_3O_{19}]$ under the same reaction conditions.

2.1.4 Applications Areas of Lactic Acid

Over the years, lactic acid has attracted considerable attention as a chemical with many potential applications. It has found widespread application in the food, cosmetic, pharmaceutical and chemical industries (Komesu et al., 2017b, Abdel-Rahman and Sonomoto, 2016, Sobrun et al., 2012, Krishna et al., 2018). The ability of lactic acid to yield valuable chemicals (Figure 2.2) arises from the presence of two reactive functional groups, namely carboxylic and hydroxyl groups (Krishna et al., 2018). Depending on the application, one form of lactic acid, meaning L-lactic acid, D-lactic acid or DL-lactic acid, is preferred.

There has also been an increased demand for lactic acid as a feedstock for the production of biopolymer Poly-lactic acid (PLA) (Sobrun et al., 2012, Lasprilla et al., 2012, Krishna et al., 2018). Since lactic acid is a chiral molecule, the term poly-lactic acid refers to a family of polymers: pure Poly-L-lactic acid (PLLA), pure Poly-D-lactic acid (PDLA) or Poly-DL-lactic acid (PDLLA) (Lasprilla et al., 2012). Although lactic acid has attracted much interest in different fields, its use is still limited by the final production costs arising from the downstream processes (Komesu et al., 2017b).

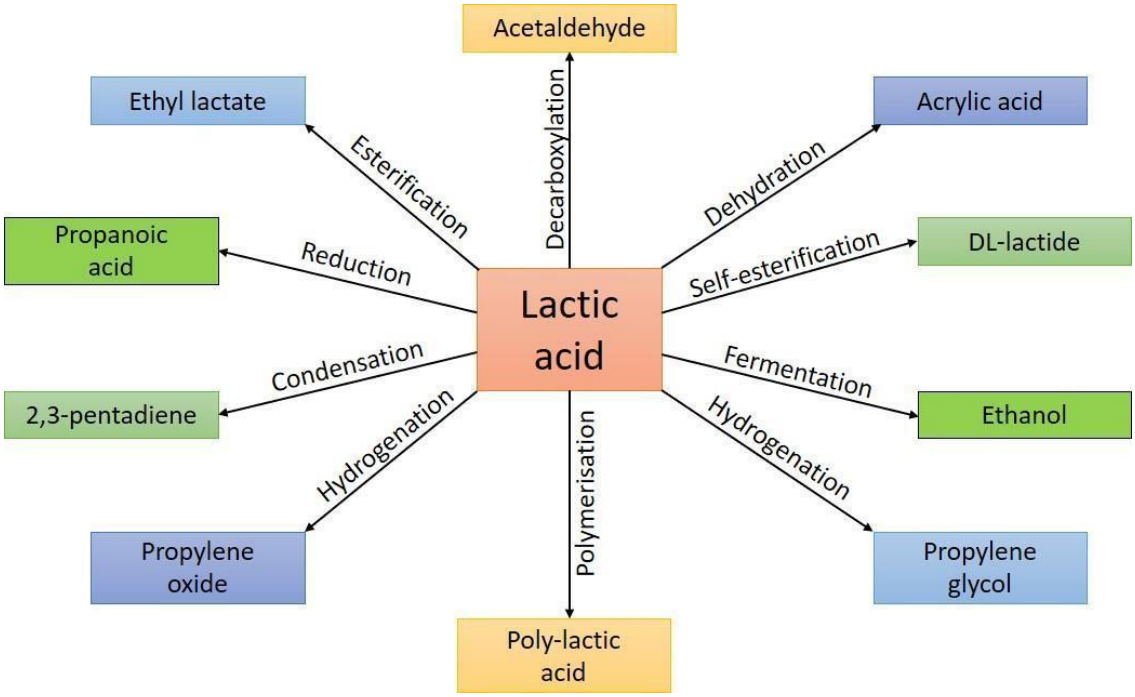

(Source: Adapted from Wee et al. (2006), Komesu et al. (2017b)).

Figure 2.2: Common chemicals derived from lactic acid

2.2 HYDROGEN CYANIDE

2.2.1 Introduction

Hydrogen cyanide (HCN), also called prussic acid, is a highly volatile and poisonous compound first isolated from a blue pigment (Prussian blue). HCN exists in the form of a toxic liquid or colourless gas (Gail et al., 2011).

Carl Wilhelm Scheele, a Swedish chemist, was the first to prepare HCN from Prussian blue in 1782 (Gail et al., 2011). HCN is among the most toxic substances known to man. It is lethal to humans at 1-2 mg/Kg body weight dosage. It acts by blocking the respiratory chain and preventing the aerobic organism from using oxygen (Bruckner et al., 2017).

Although poisonous, HCN is used in many industrial processes and is an invaluable precursor to numerous chemical compounds, including pharmaceuticals and polymers. The mining sector uses about 13 % of the total production of manufactured HCN, while the remaining 87 % are used in different industrial processes (Woffenden et al., 2008).

The global market of HCN is expected to reach a high Compound Annual Growth Rate (CAGR) of 1 % by 2028. The major factors driving the HCN market (DataMIntelligence, 2021) are:

- Increase demand for manufacturing sodium cyanide and potassium cyanide, needed in organic synthesis to produce nitriles and carboxylic acids, and the mining of silver and gold.

- Increase applications of HCN in Adiponitrile production, which is the precursor to manufacture nylon 66.

The global HCN market is segmented on application, region and production process (DataMIntelligence, 2021).

Currently, HCN is produced in significant quantities through several processes, such as Andrussow and Degussa processes, or recovered as a waste product from acrylonitrile manufacturing. It is also known to occur naturally in some plants and fruits with a pit (Saunders, 2012, Jaszczak et al., 2017) and in some animals (Saunders, 2012) as cyanogenic glycosides.

2.2.2 Hydrogen cyanide properties

Hydrogen cyanide (HCN), also called prussic acid, hydrocyanic acid or formonitrile, is a colourless or pale blue liquid or a colourless gas at higher temperatures. HCN is volatile and highly poisonous, with a faint bitter almond odour and a bitter, burning taste (Gail et al., 2011, Information, 2020). In the gas phase, it is flammable and potentially explosive. It has a very low boiling point of 25.6 °C and can readily be liquefied at room temperature (Information, 2020). HCN burns in oxygen or air with a blue flame according to the following reaction (Gail et al., 2011):

$$\underset{\text{Hydrogen Cyanide}}{2\,HCN} + \underset{\text{Oxygen}}{1.5\,O_2} \longrightarrow \underset{\text{Nitrogen}}{N_2} + \underset{\text{Carbon monoxide}}{2\,CO} + \underset{\text{Water}}{H_2O} \qquad (1)$$

Pure liquid HCN is known to polymerise into brown-black, amorphous polymers called azulmic acid. It is stabilised using a small amount of acid, such as 0.1 wt % orthophosphoric acid (H_3PO_4), 1-5 % formic acid (HCOOH) or acetic acid (CH_3COOH). 0.2 wt % Sulphur

dioxide (SO_2) stabilises gaseous HCN (Gail et al., 2011). HCN is best preserved as a cyanide ion (CN^-) in aqueous alkaline media ((EFSA), 2007). It is miscible in water in all ratios but is often made as a 96 % aqueous solution. It is also miscible with ethyl ether and ethanol (Information, 2020).

2.2.3 Production Technologies

Hydrogen cyanide originates both from manufactured (industrial) processes and natural sources.

2.2.3.1 Industrial processes

Hydrogen cyanide can be synthesised when enough energy is supplied to any system containing hydrogen, carbon and nitrogen (Gail et al., 2011). It is produced either by the Andrussow, the Blausaure Methane Anlage (BMA) or Shawinigan process. Furthermore, it can also be produced as a by-product in acrylonitrile manufacturing (Sohio process) (Gail et al., 2011).

2.2.3.1.1 Andrussow process

This process was developed around 1930 by L. Andrussow. It is the primary method for directly synthesising hydrogen cyanide (HCN). It involves the reaction of ammonia, methane and air over a platinum-rhodium or platinum-iridium gauze catalyst as shown in the following reaction (Gail et al., 2011) :

$$\underset{\text{Methane}}{CH_4} + \underset{\text{Ammonia}}{NH_3} + \underset{\text{Oxygen}}{1.5\ O_2} \xrightarrow{\text{Catalyst}} \underset{\text{Hydrogen Cyanide}}{HCN} + \underset{\text{Water}}{3\ H_2O} \quad (2)$$

$\Delta H = -474$ kJ/mol

This is an exothermic reaction taking place at a temperature above 1000 °C and around atmospheric pressure, with a gas velocity of 3 m/s going through the catalyst zone. In order to avoid decomposition of HCN by polymerisation, the gas produced is quickly cooled in a waste-heat boiler, which produces the steam used in the process. The HCN gas from the waste-heat boiler is washed with dilute sulphuric acid to remove unreacted ammonia.

The disadvantage of this method is its dependency on pure methane as raw material. This help to avoid the carburisation of the platinum catalyst. Another problem encountered with this process is the relatively low yield based on methane (60-70 %) and ammonia (70 %) and the

low HCN concentration in the product gas. Therefore, the recovery equipment must handle a large volume of gas.

2.2.3.1.2 The Blausaure Methane Anlage (BMA) process

This process involves the reaction of ammonia and methane in the absence of oxygen according to the following reaction (Gail et al., 2011):

$$\underset{\text{Methane}}{CH_4} + \underset{\text{Ammonia}}{NH_3} \xrightarrow{\text{Catalyst}} \underset{\text{Hydrogen cyanide}}{HCN} + \underset{\text{Hydrogen}}{3\,H_2} \quad (3)$$

$\Delta H = +252$ kJ/mol

This is an endothermic reaction requiring temperatures above 1200 °C and performed in highly heated alumina tube bundles. The inside of the tubes is coated with a thin layer of a particular platinum catalyst. The HCN gas leaving the alumina tubes is water-cooled to 300 °C in an aluminium chamber.

The main advantage of this process is the high HCN content of the gas produced. Thus allowing the reduction of the number of recovery steps, equipment size and cost. Another advantage is that 80-87 % of the ammonia and 90-94 % of the methane are used to produce HCN. In the event of limited methane supply, it is possible to directly carry out this process with methanol in a three-step reaction or with liquefied hydrocarbons or ethanol.

2.2.3.1.3 Sohio process

The hydrogen cyanide is produced as a by-product during the synthesis of acrylonitrile, as shown in the following reactions(Deepa et al., 2016) :

Main reaction

$$\underset{\text{Propene}}{2\,C_3H_6} + \underset{\text{Ammonia}}{2\,NH_3} + \underset{\text{Oxygen}}{3\,O_2} \longrightarrow \underset{\text{Acrylonitrile}}{2\,C_3H_3N} + \underset{\text{Water}}{6\,H_2O} \quad (4)$$

Side reactions

$$\underset{\text{Propene}}{2\,C_3H_6} + \underset{\text{Ammonia}}{3\,NH_3} + \underset{\text{Oxygen}}{3\,O_2} \longrightarrow \underset{\text{Acetonitrile}}{3\,C_2H_3N} + \underset{\text{Water}}{6\,H_2O} \quad (5)$$

$$\underset{\text{Propene}}{C_3H_6} + \underset{\text{Ammonia}}{3\,NH_3} + \underset{\text{Oxygen}}{3\,O_2} \longrightarrow \underset{\text{Hydrogen cyanide}}{3\,HCN} + \underset{\text{Water}}{6\,H_2O} \quad (6)$$

$$\underset{\text{Propene}}{2\,C_3H_6} + \underset{\text{Oxygen}}{9\,O_2} \longrightarrow \underset{\text{Carbon dioxide}}{6\,CO_2} + \underset{\text{Water}}{6\,H_2O} \quad (7)$$

A mixture of acrylonitrile, hydrogen cyanide, acetonitrile and carbon dioxide is formed. Hydrogen cyanide, one of the two significant by-products, is removed when the product stream is sent to the fractionator.

2.2.3.1.4 Shawinigan process

The Shawinigan process, also called the Fluohmic process, was developed in 1960 by Shawinigan Chemicals, now part of Gulf Oil Canada. It involves the reaction of hydrocarbon gases with ammonia in an electrically heated fluidised bed of coke (Gail et al., 2011).

The reaction vessel is made of a circular cavity constructed from alumina and silica carbide. The reactants, a mixture of ammonia and hydrocarbon (N/C ratio slightly > 1), is passed through a fluidised bed of coke heated by electrodes immersed in the bed.

The only difference between the chemical reaction of the Shawinigan process and the BMA process is that the Shawinigan process does not require any catalyst in its process, and the operating temperatures are kept above 1500 °C as shown in the following reaction:

$$\underset{\text{Ammonia}}{NH_3} + \underset{\text{Propane}}{C_3H_8} \longrightarrow \underset{\text{Hydrogen cyanide}}{3\,HCN} + \underset{\text{Hydrogen}}{7\,H_2} \quad (8)$$

2.2.3.2 Natural sources of hydrogen cyanide

The distribution of cyanide compounds is widespread in nature, where it is produced by several organisms such as fungi, bacteria, plants, algae (Veselá, 2015, Davis et al., 2017, Bhalla et al., 2017, Panou and Gkelis, 2020, Nyirenda, 2021, Yu, 2014) and some animals (Veselá, 2015, Davis et al., 2017, Bhalla et al., 2017). These cyanide compounds release hydrogen cyanide (HCN) through the cyanogenesis process (Veselá, 2015, Panou and Gkelis, 2020, Nyirenda, 2021). This process serves as a defensive and offensive mechanism (Panou and Gkelis, 2020).

The principal natural source of HCN is cyanogenic glycosides. They are produced by more than 2000 plants species (Veselá, 2015, Bhalla et al., 2017, Nyirenda, 2021, Yu, 2014, Zuk et al., 2020). The cyanogens are derived from amino acid precursors, as shown in the biosynthetic pathway depicted in Figure 2.3:

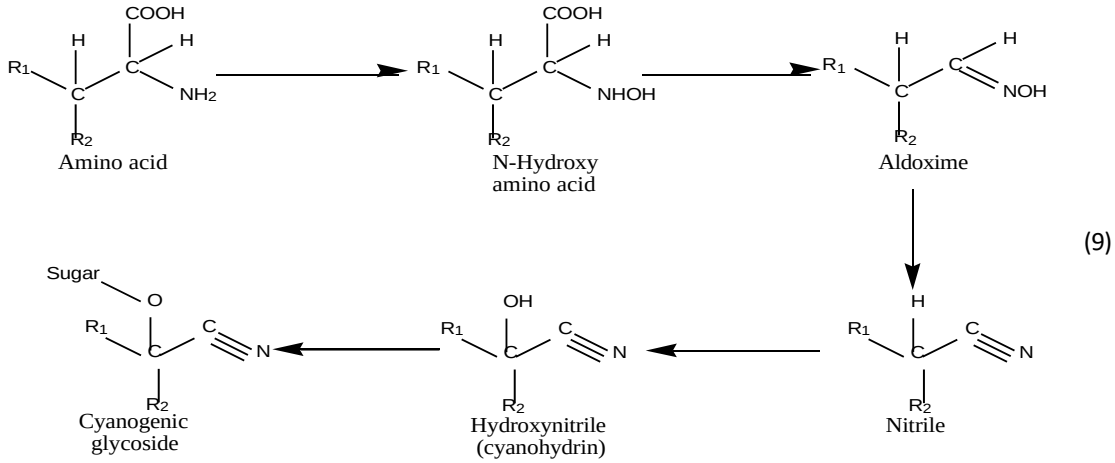

(9)

(Source: Adapted from Nyirenda (2021)).

Figure 2.3: Biosynthetic pathway of cyanogenic glycoside from amino acid

Many bacterial species produce cyanide. They secrete the cyanogenic compounds for antimicrobial purposes (Bhalla et al., 2017). The cyanogens produced by bacteria originate from amino acid glycine (Veselá, 2015). Some of the cyanogenic bacteria are: *Pseudomonas aeruginosa*, *Pseudomonas aureofaciens*, *Pseudomonas fluorescens* (Bhalla et al., 2017, Broderick et al., 2008), *Pseudomonas Chlororaphis*, *Chromobacterium violaceum* (Bhalla et al., 2017), *Anacystis nidulans*, *Nostoc muscorum* (Panou and Gkelis, 2020, Broderick et al., 2008), *Rhizobium leguminosarum*, *Solanum tuberosum* (Broderick et al., 2008) and *Plectonema* (Panou and Gkelis, 2020).

Glyoxylic acid cyanohydrin, pyruvic acid cyanohydrin (Figure 2.4), and several α-aminonitriles have been reported to be produced by several bacteria. They use these cyanide compounds to suppress competitive organisms (Veselá, 2015).

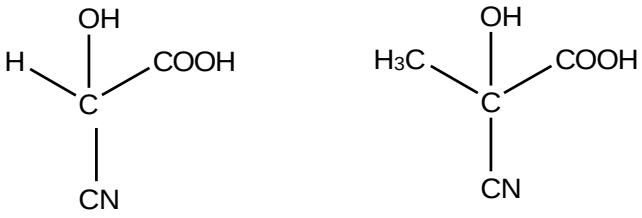

Glyoxylic acid cyanohydrin

Pyruvic acid cyanohydrin

Figure 2.4: Some cyanogens found in bacteria

2.2.3.2.1 Fungi

Cyanogenic fungal species secret cyanogens for antimicrobial purposes (Bhalla et al., 2017). The cyanogenic compounds produced by fungi are derived from amino acid glycine (Veselá, 2015). Several fungi species belonging to *Cortinariaceae*, *Agaricaceae*, *Rhodophyllaceae*, *Polyporaceae* and *Tricholomataceae* have produced cyanide compounds (Tewe and Iyayi, 1989).

Glyoxylic acid cyanohydrin, pyruvic acid cyanohydrin (Figure 2.4), and many α- aminonitriles have also been reported in several fungi. They use these cyanogen compounds to hinder competitive organisms (Veselá, 2015). Some cyanogenic fungi are *Aleurodiscus amorphous* and *Marasmius oreades* (Caspar and Spiteller, 2015).

2.2.3.2.2 Algae

Green algae *Chlorella Vulgaris* is the major alga known to undergo cyanogenesis (Veselá, 2015, Tewe and Iyayi, 1989). *Chlorella Vulgaris* is the alga in which cyanide production was first reported by Gewitz *et al*. in 1976 (Panou and Gkelis, 2020). Histidine is the amino acid precursor for the cyanide compounds produced by alga (Veselá, 2015, Panou and Gkelis, 2020). The algae produce hydrogen cyanide to deter predators (Davis et al., 2017).

2.2.3.2.3 Animals

Some species of centipedes and millipedes can produce hydrogen cyanide (HCN). These terrestrial invertebrates produce HCN as a chemical defence to stop predators (Bruckner et al., 2017, Davis et al., 2017). Arthropods, such as *Chilopoda*, *Diplopoda* and *Insecta*, also produce cyanogen glycosides to defend themselves against predators (Veselá, 2015). Sponges synthesise cyanogens compounds as antimicrobial agents (Veselá, 2015), while some insects synthesise cyanide compounds to help control their breeding behaviour (Bhalla et al., 2017).

2.2.3.2.4 Plants

More than 2000 plant species produce cyanogenic glycosides (Saunders, 2012, Veselá, 2015, Bhalla et al., 2017, Nyirenda, 2021, Zuk et al., 2020, Cho et al., 2013, Chaouali et al., 2013, Ubwa et al., 2015). These natural toxins of varied structures are secondary metabolites used by plants to fight off many threats, including bacteria, insects, fungi, and predators (Nyirenda, 2021). These cyanogens have been observed in many economically important crops (Veselá, 2015, Nyirenda, 2021, Abraham et al., 2016), including sorghum, cassava, peaches, cherries, butter beans (Chaouali et al., 2013, Nyirenda, 2021), bamboo, linseed and apricots (Chaouali et al., 2013).

Hydrogen cyanide (HCN) is released from cyanogenic compounds through a hydrolysis process called cyanogenesis (Figure 2.5) (Veselá, 2015, Panou and Gkelis, 2020, Nyirenda, 2021). HCN is formed when hydrolytic enzymes are released following the maceration of plant tissues or gut microflora after ingestion (Saunders, 2012, Nyirenda, 2021, Chaouali et al., 2013, Indrastuti et al., 2018).

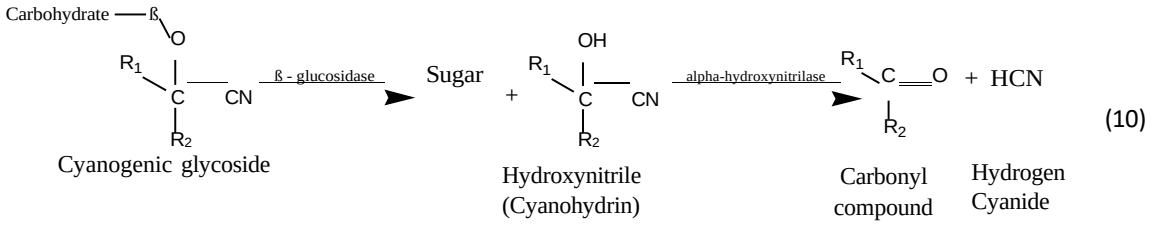

(10)

Figure 2.5: Hydrolysis of cyanogenic glycosides

Approximately 75 cyanogenic glycosides (Ndubuisi and Chidiebere, 2018), among which 25 are known to be synthesised in edible plants (Nyirenda, 2021, Bolarinwa et al., 2016). The majority of these toxins are believed to originate from only six amino acids, namely L-isoleucine, L-phenylalanine, L-valine, L-tyrosine, or L-leucine, and a nonprotein amino acid called cyclopentenyl-glycine (Bolarinwa et al., 2016). These cyanogenic glycosides are O-ß-glycosidic derivatives of α-hydroxynitriles, and based on their amino acid precursor, they can either be aliphatic, aromatic or cyclopentenoid (Ndubuisi and Chidiebere, 2018). A glycosidic linkage stabilises the unstable cyanohydrin portion of these toxins to either a single sugar residue (cyanogenic monosaccharides), two sugar residues (cyanogenic disaccharides) or three sugar residues (cyanogenic trisaccharides) (Ndubuisi and Chidiebere, 2018).

All the HCN used in the world originate from industrial processes that rely on fossil resources. Therefore, concerning the decreased availability of fossil fuel reserves and the serious environmental concerns caused by their utilisation, it is crucial to find alternative routes for its production. In this context the production of HCN as sodium cyanide (NaCN) from renewable resources such as cassava was investigated by Attahdaniel et al. (2013) and Attahdaniel et al. (2020). NaCN, a hygroscopic white crystalline or granular powder, is known to release HCN in the presence of acids (ECETOC, 2007).

In 2013, Attahdaniel research group prepared NaCN from cassava. The HCN released by acid hydrolysis was collected in 3.6 mol/L NaOH absorbing solution. The NaCN solution was dried at a temperature between 60 °C and 70 °C to give NaCN crystal with a maximum yield between 4.27 % and 5.90 %. Two hydrolysis methods for HCN release from cassava, namely direct and acid hydrolysis, were compared in the study conducted by Attahdaniel et al. (2020). The released HCN was also trapped in a 3.6 mol/L NaOH absorbing solution. They reported a NaCN yield ranging from 3.92 % to 5.86 %, and 9.46 % to 10.08 % using direct and acid hydrolysis, respectively, after drying the NaCN solution at 100 °C. Interestingly, The HCN released in both studies was collected by direct contact between the cassava extracts and the absorbing solution.

2.2.4 Application Areas of Hydrogen cyanide

Hydrogen cyanide (HCN) is a commercial commodity, widely used in many products such as nylon-66, cosmetic products, adhesives, computer electronics, dyes and pharmaceuticals (Yu, 2014). It is also used to prepare synthetic rubber, plastics and acrylic fibre (Omotayo et al., 2015). This highly volatile compound can also be used in several processes, including electroplating, ores concentration (Yu, 2014, Omotayo et al., 2015), fumigation and case hardening of iron and steel (Omotayo et al., 2015).

2.3 CASSAVA

2.3.1 Introduction

Cassava (*Manihot esculenta* Crantz), also called *yuca*, *manioc* or *mandioca* (Montagnac et al., 2009, Shackelford et al., 2018), is a domesticated plant amongst some 100 species belonging to the genus *Manihot* (Otekunrin and Sawicka, 2019, Ubwa et al., 2015) from the Euphorbiaceae family (Ubwa et al., 2015, Omomowo et al., 2015). This perennial crop is believed to have originated from Latin America (Figure 2.6) then introduced in the western

part of Africa in the 16th century by Portuguese merchants (Otekunrin and Sawicka, 2019, Spencer and Ezedinma, 2017). Before being cultivated in Madagascar and the eastern part of Africa, Cassava was first cultivated in the Congo basin and the Gulf of Guinea (Otekunrin and Sawicka, 2019). Cassava cultivation has been well established in the Congo basin since the early 1650s (Mabasa, 2007).

Cassava was introduced in South Africa (SA) during the significant tribal movements of Tsonga tribe members in the 1830s and 1860s. Tsonga tribe members adopted cassava as a food crop after being introduced into Mozambique by the Portuguese in the 17th century. They migrated towards the west into Mpumalanga province (old Eastern Transvaal) and Swaziland southward into the Northern part of KwaZulu-Natal province (Mabasa, 2007, Mudombi, 2010, Makwarela and Rey, 2006). Currently, it is mainly cultivated in KwaZulu-Natal, Mpumalanga and Limpopo (Mabasa, 2007, Govender, 2015, Britz, 2019) as a secondary food crop (Mabasa, 2007, Mudombi, 2010, Govender, 2015, Britz, 2019) by small scale farmers (Mabasa, 2007, Mudombi, 2010, Britz, 2019). Large scale cassava production in SA only regained interest in the late 1970s. Prior to this period, its production was negatively affected by a preference for maise (Makwarela and Rey, 2006).

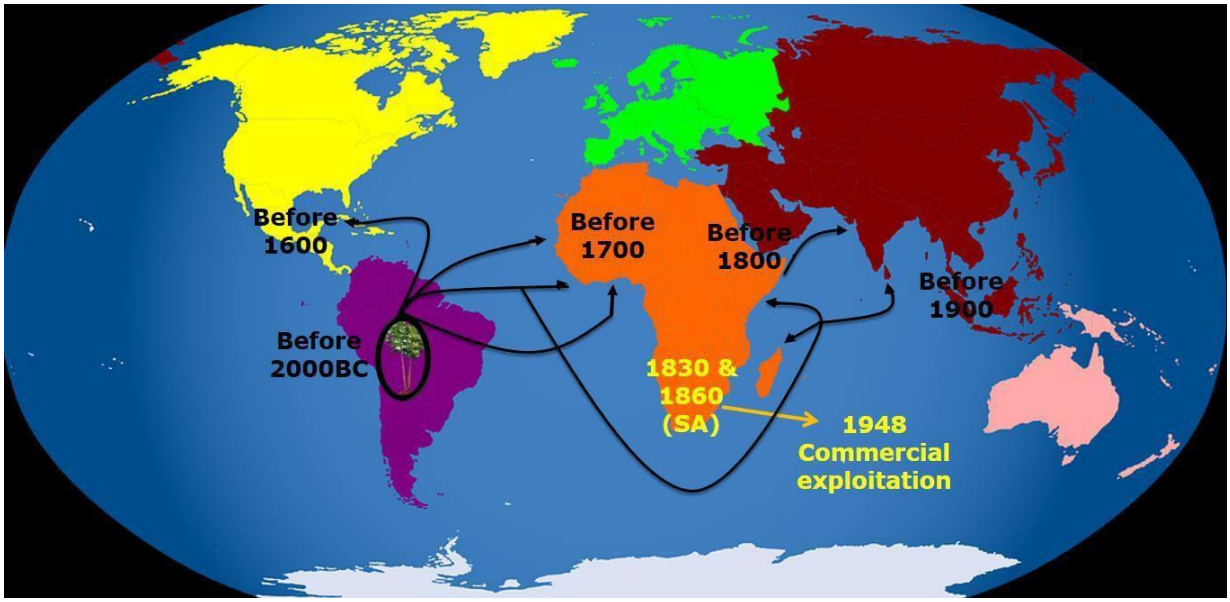

(Source: Adapted from (NHM, 2017)).

Figure 2.6: Worldwide spread of cassava

Cassava only became a staple food widely cultivated in Africa in the middle of the 19th century (Otekunrin and Sawicka, 2019). Cassava is known as "the drought, war and famine crop" since

it can grow under marginal conditions and be harvested throughout the year. Hence, supplying food during war and famine (Otekunrin and Sawicka, 2019, Shackelford et al., 2018). Cassava is considered as a crop contributing toward food security because of the ability of the roots to stay in the ground for about three years (Otekunrin and Sawicka, 2019, Ifeabunike et al., 2017), allowing it to be left unattended without deterioration during periods of unrest (Burns et al., 2010).

The tuberous roots and leaves are essential for humans and animals' usage (Bayitse et al., 2017, Pereira et al., 2016, Abdullahi et al., 2014, Guédé et al., 2013). Cassava has also found wide applications in many industries (Omomowo et al., 2015, Abdullahi et al., 2014, Eletta et al., 2016). Despite all the usefulness of Cassava, its use is limited by:

- The presence of natural toxins, namely Linamarin and lotaustralin (Ubwa et al., 2015, Ifeabunike et al., 2017, Guédé et al., 2013, Tivana et al., 2014, Cuvaca et al., 2015, Wilberforce and Ngele, 2016),
- The perishability of the roots (Bayitse et al., 2017, Ubwa et al., 2015, Guédé et al., 2013, Kouakou et al., 2016),
- The low protein content of the roots (Guédé et al., 2013, Wilberforce and Ngele, 2016).

2.3.2 Cassava Production

Cassava is a staple food for more than 500 million people (Bayitse et al., 2017, Omotayo et al., 2015, Diallo et al., 2014). It is cultivated mainly in the tropic and sub-tropic regions of Africa, Asia and Latin America (Abdullahi et al., 2014, Ding et al., 2016, Chikezie and Ojiako, 2013, Itoba-Tombo et al., 2019, Shackelford et al., 2018) for its roots and leaves (Ndam et al., 2019). Although seeds are also used to propagate cassava (Abdullahi et al., 2014), it is usually done by stem cuttings (Kouakou et al., 2016, Polthanee and Wongpichet, 2017). The cassava cuttings can be planted in horizontal, vertical or lean positions (Figure 2.7) (Abass et al., 2014, Abdullahi et al., 2014, Buasaengchan et al., 2019). Vertical planting is the principal method representing 93 % of all the propagation styles, while the lean and horizontal methods only represent 5 % and 2 %, respectively (Buasaengchan et al., 2019). The horizontal planting method is recommended in dry areas, while the vertical and lean plantation methods are preferable in areas of high rainfall (Abass et al., 2014). The horizontal method is preferred for leaf harvesting purposes (Buasaengchan et al., 2019). When planting the cassava cutting either

in a vertical or lean position, the knobs must be pointing upwards instead of downwards to avoid yield reduction (Kouakou et al., 2016).

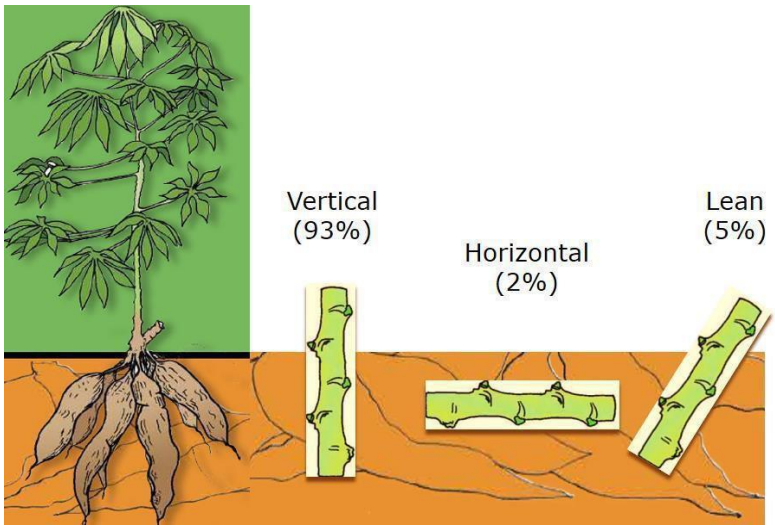

(Source: Adapted from Abass et al. (2014), Buasaengchan et al. (2019)).

Figure 2.7: Propagation methods of cassava

Figure 2.8 shows the cassava world production (Figure 2.8a), the primary producers (Figure 2.8b), importers (Figure 2.8c) and exporters (Figure 2.8d) for 2017. The world cassava production stood at more than 291 million tonnes in 2017, with Sub-Saharan Africa (SSA) accounting for 60.9 % of the production, and Nigeria remains the major cassava producing nation with more than 59 million tonnes or 20.4 % of the global production. Globally, Thailand was the significant exporter of cassava flour, starch/chips and pellets in 2017 though it ranks third in cassava production. China was the major importer of cassava products, such as flour, pellets, starch and chips (Otekunrin and Sawicka, 2019).

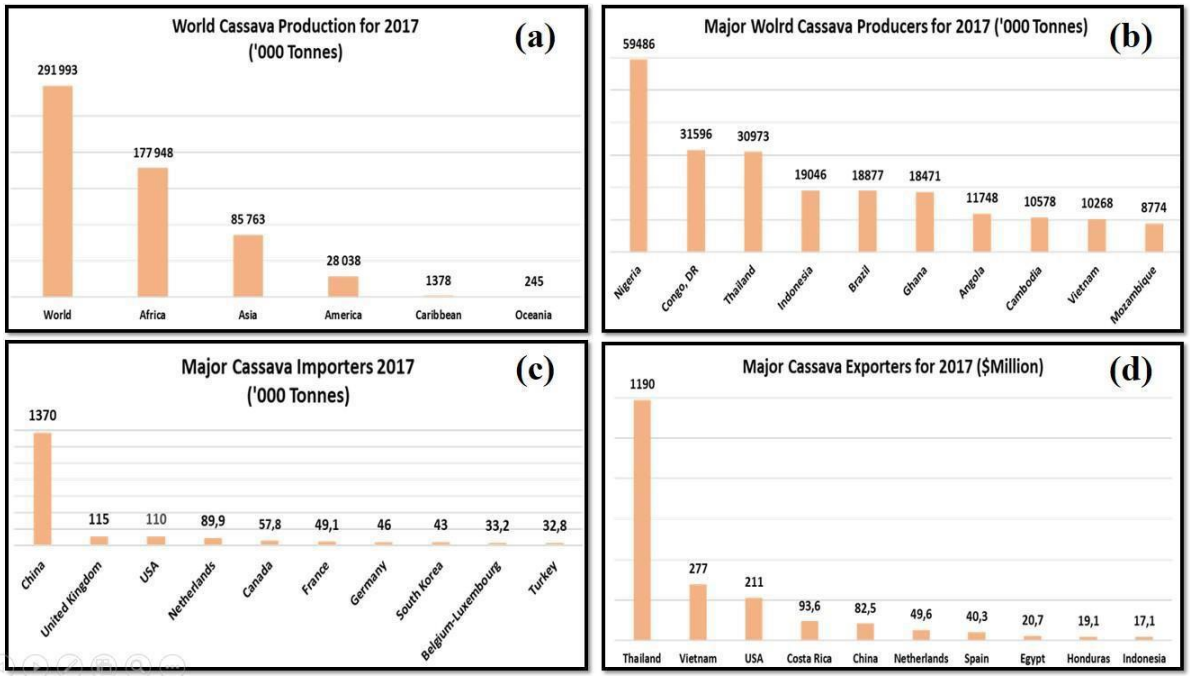

(Source: Adapted from Otekunrin and Sawicka (2019))

Figure 2.8: World cassava production (a), major producers (b), major importers (c) and major exporters (d) for 2017

Although SSA was the single largest cassava producing zone in 2017, none of the nations was among the leading exporting countries. This discrepancy can be explained because most cassava produced in SSA is locally consumed within each producing country (Spencer and Ezedinma, 2017, Chuasuwan, 2017).

2.3.3 Cyanogenic nature of cassava

The major limitation associated with the use of cassava is the presence of toxic cyanogenic glucosides in all parts of the plant (Ubwa et al., 2015, Ndubuisi and Chidiebere, 2018, Bolarinwa et al., 2016, Omotayo et al., 2015, Pereira et al., 2016). The ß-glucosidase enzyme, or linamarase, which hydrolyses the cyanogenic glucosides, is not located in the same compartments as the cyanogens. It is found in the cell and laticifers walls, while the cyanogens are inside the vacuoles (Figure 2.9) (Zidenga et al., 2017).

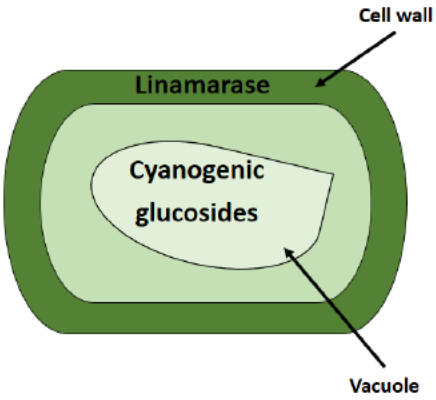

(Source: Adapted from Tivana (2012))

Figure 2.9: Location of cyanogenic glucosides and linamarase enzyme in plant cell

Free cyanide is liberated from cyanogenic glucosides when there is tissue disruption, such as during mechanical damages (Zidenga et al., 2017). The hydrolysis of these toxins is called cyanogenesis (Ndubuisi and Chidiebere, 2018). The main cyanogenic glucoside found in cassava is Linamarin (Ndubuisi and Chidiebere, 2018, Cuvaca et al., 2015, Srihawong et al., 2015). Cassava also contains a small amount of lotaustralin (Cuvaca et al., 2015, Srihawong et al., 2015). Figure 2.10 shows the chemical structure of the two cyanogenic glucosides found in cassava.

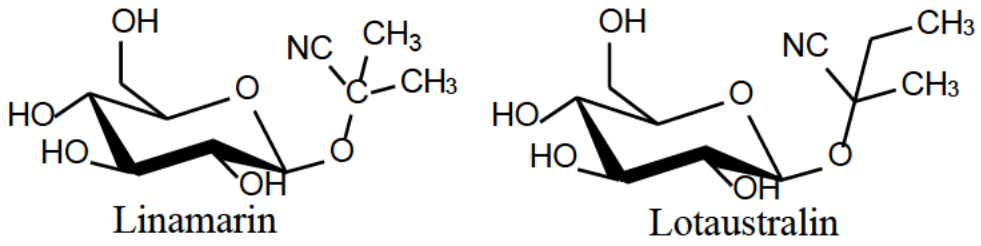

Figure 2.10: Chemical structures of cyanogenic glucosides found in cassava

The enzymatic degradation of cyanogenic glucosides initiates the cyanogenesis process arising from tissue disruption by the linamarase. This results in the liberation of the carbohydrate, which in this case is glucose, and α-hydroxynitrile (Srihawong et al., 2015, Abraham et al., 2016, Zidenga et al., 2017). The α-hydroxynitrile can either spontaneously decompose at pH > 5.0, and temperature > 35 °C or be enzymatically cleaved by hydroxynitrile lyase enzyme to give hydrogen cyanide (HCN) and ketone (Figure 2.11) (Abraham et al., 2016, Zidenga et al., 2017). In cassava, the hydroxynitrile lyase enzyme is only found in the leaves and stems but not in the roots (Zidenga et al., 2017).

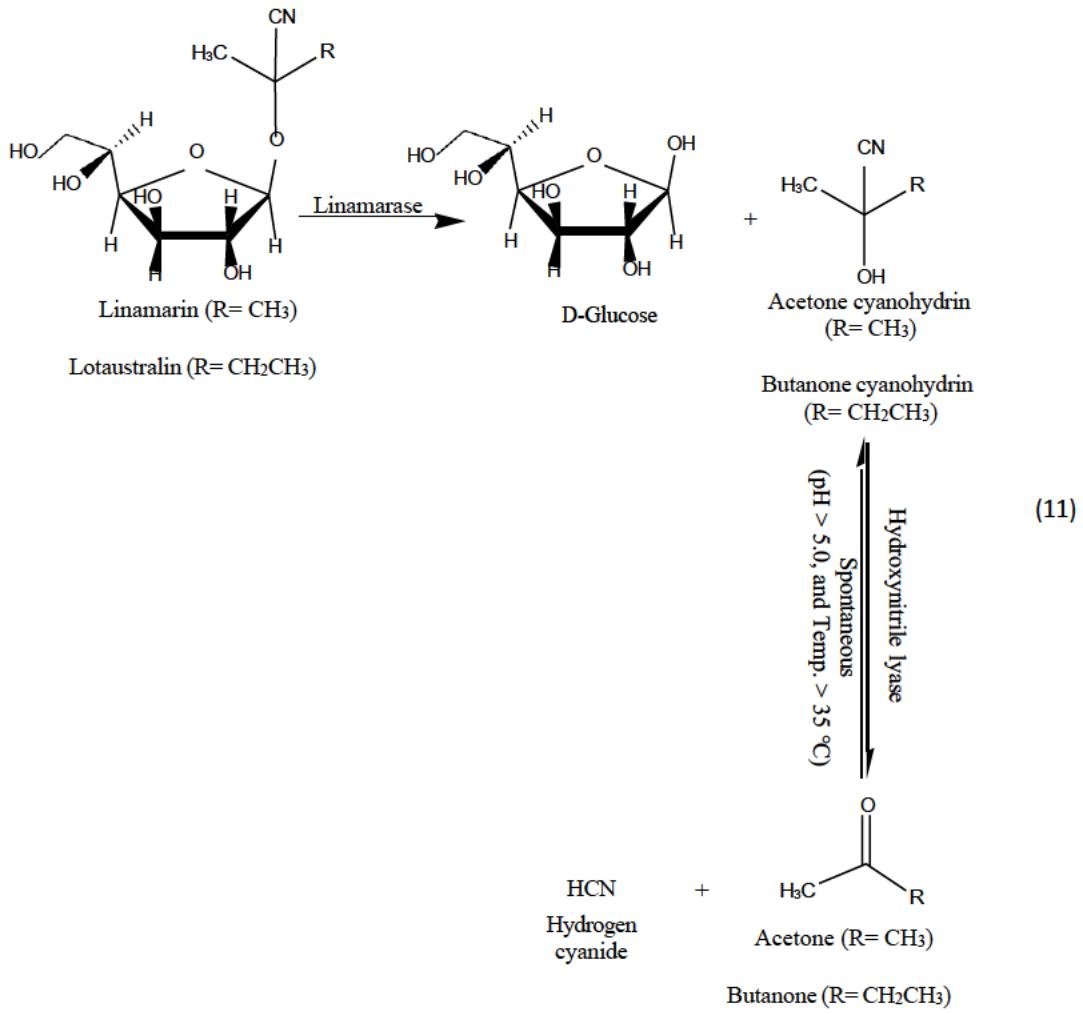

(11)

Figure 2.11: Hydrolysis of cyanogenic glucosides

The role of cyanogenic glucosides in cassava plant are:

- Nitrogen transporters (Abraham et al., 2016)
- Defence mechanism against the attack of herbivores (Ndubuisi and Chidiebere, 2018, Abraham et al., 2016, Rawat et al., 2015)
- Enhancement of plant elasticity, i.e. establishment, robustness and viability with response to environmental challenges (Rawat et al., 2015)

These natural toxins also impart a bitter taste to some cassava cultivars. They are synthesised in the leaves through n-hydroxylation of valine and isoleucine before being carried to the roots (Figure 2.12) (Nyirenda, 2021, Ndam et al., 2019), where they accumulate to a concentration of up to 2000 mg/Kg (Nyirenda, 2021).

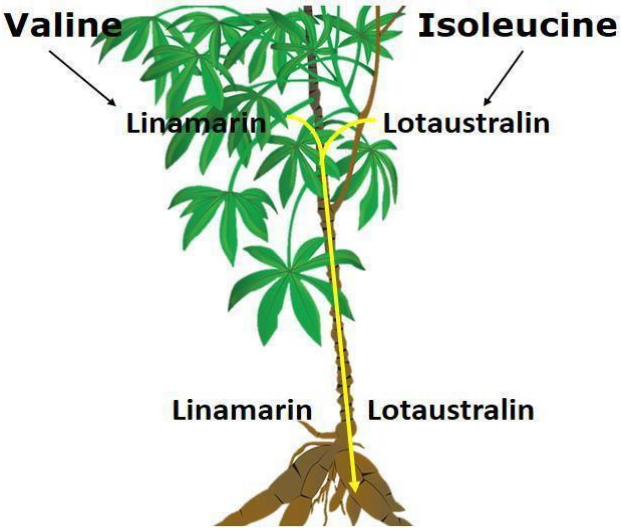

(Source: Adapted from Burns et al. (2010)).

Figure 2.12: Synthesis of cyanogenic glucosides in cassava

The cyanogens content depends on many factors, such as the genotype of the cultivar, age of the plant, soil type, seasonal conditions and geographic location (Nyirenda, 2021, Ndam et al., 2019).

The highest concentration of cyanogenic glucosides is found in cassava leaves and peels of the tubers (900-2000 mg HCN/Kg dry matter), while the pulp of the tubers has approximately 20 times less toxins levels (Nyirenda, 2021, Ndubuisi and Chidiebere, 2018). Based on the concentration of cyanogenic glucosides or HCN released during hydrolysis, cassava cultivars are classified as either bitter or sweet (Ndubuisi and Chidiebere, 2018). Bitter cassava is ideal for the natural production of HCN since they have a higher cyanogenic glucosides content.

The consumption of unprocessed or poorly processed cassava is linked to health issues that can either be classified as acute intoxication, chronic toxicity or neurological disorders, growth retardation, and goitre and cretinism (Nyirenda, 2021, Bolarinwa et al., 2016, Ndam et al., 2019). These health issues are exacerbated when short cut is taken during cassava processing methods, especially during periods of war, famine (Nyirenda, 2021) and drought (Burns et al., 2010).

2.3.4 Factors affecting the cyanide content of cassava

The variation in cyanide concentration observed within the same cassava plant or among different plants (Ndubuisi and Chidiebere, 2018) is dependent on different factors, such as seasonal conditions, soil type. Cultivar, altitude and age.

2.3.4.1 Seasonal conditions

The cyanide level in cassava has been shown to increase during drought periods or prolonged dry weather due to water stress on the plant (Ndubuisi and Chidiebere, 2018, Ndam et al., 2019, Mushumbusi, 2018).

2.3.4.2 Soil type

The cyanide level of cassava is high when planted on sandy soils as they poorly retain water compared to soils with high water retention. Furthermore, the cyanide level is known to increase when cassava is grown on soils rich in cyanide as a result of natural processes (wildfire, volcanos and microbial activities), human activities (gold mining, electroplating, textiles and plastics productions) or both since they act as cyanide reservoir (Mushumbusi, 2018).

2.3.4.3 Cassava cultivar

Several cassava cultivars have varying cyanogens concentrations, ranging from 1 to 2000mg HCN/Kg (Ndubuisi and Chidiebere, 2018, Mushumbusi, 2018). There are two general types of cassava, sweet (table cassava) and bitter (cassava for industry). This classification is linked to the capacity of HCN release if consumed. The variety containing less than 100mg/Kg of cyanogens per fresh root is sweet, while the one containing more than 100 mg/Kg of cyanogens is bitter (Araújo et al., 2019). However, since cassava is propagated using stem cutting, there is minimal variation in cyanide content between individuals from the same cultivar when grown under the same environmental conditions (Ndubuisi and Chidiebere, 2018).

2.3.4.4 Altitude

Cassava plants grown in low altitude regions have been found to have a higher cyanogens content compared to those grown in high altitudes (Bolarinwa et al., 2016, Mushumbusi et al., 2020).

2.3.4.5 Age of cassava crop

The cyanide level is dependent on the age of cassava. The younger the cassava crop, the higher the cyanogenic glucosides content (Mushumbusi et al., 2020).

2.3.5 Analysis of cyanogenic glucosides

Cyanogenic glucosides can be directly or indirectly determined (Bolarinwa et al., 2016, Barthet and Bacala, 2010, (CONTAM) et al., 2019).

2.3.5.1 Direct determination of cyanogenic glucosides

Direct determination of cyanogenic glucosides is based on instrumental techniques (Bolarinwa, 2013). The intact cyanogen glucosides are analysed after extraction using one of the following techniques:

- Thin-layer chromatography (TLC) (Bolarinwa et al., 2016, Barthet and Bacala, 2010).
- Reversed-phase liquid chromatography (RPLC) (Bolarinwa et al., 2016, Barthet and Bacala, 2010).
- Gas chromatography (Barthet and Bacala, 2010).
- High-performance liquid chromatography with UV-VIS detection (HPLC-UV), diode array detection (HPLC-DAD) ((CONTAM) et al., 2019) or refractive index detector (HPLC-RI) (Barthet and Bacala, 2010).
- Solid-phase extraction (SPE) together with liquid chromatography-tandem mass spectrometry (LC-MS/MS) for improved sensitivity and selectivity ((CONTAM) et al., 2019).
- Gas chromatography-mass spectrometry (GC-MS) (Bolarinwa et al., 2016, (CONTAM) et al., 2019).

2.3.5.2 Indirect determination of cyanogenic glucosides

Various methods have been developed to indirectly quantify cyanogenic glucosides as endogenous hydrogen cyanide (HCN) released upon cyanogenesis. The majority of the different methods available for the quantitative determination of HCN involve three main steps (Cho et al., 2013, Tivana et al., 2014, Ngugi et al., 2015):

2.3.5.2.1 Extraction of cyanogens from plant materials

It is usually carried out in dilute acid, such as 0.1 mol/L of phosphoric acid (Tivana et al., 2014, Ndam et al., 2019), to stop endogenous linamarase activity and to stabilise the cyanohydrins (Tivana et al., 2014, Ngugi et al., 2015).

The extraction can also be carried out in water (aqueous extraction) (Attahdaniel et al., 2020, Omotayo et al., 2015, Wilberforce and Ngele, 2016, Mushumbusi et al., 2020), preferably kept at a temperature lower than the HCN boiling point (25.7 °C) to prevent its loss.

2.3.5.2.2 Hydrolysis of cyanogenic glucosides to cyanide

The degradation of cyanogenic glucoside to cyanohydrin and glucose, then HCN in the prepared extract can be achieved using one of the following hydrolysis methods:

1. **Acid hydrolysis**

   Dilute acid solutions, such as 2 mol/L of sulphuric acid (H_2SO_4) at 100 °C for 50 minutes (Tivana et al., 2014), 0.8 mol/L of orthophosphoric acid (H_3PO4) at room temperature for 12 hours (Anhwange et al., 2011) or 4 mol/L of H_2SO_4 at 100 °C for 50 minutes (Cho et al., 2013) or 55 minutes (Attahdaniel et al., 2013, Attahdaniel et al., 2020), are used to release all the bonded cyanide.

2. **Enzymatic hydrolysis**

   Bonded cyanide is released by the action of exogenous linamarase on cyanogens (Tivana et al., 2014, Ngugi et al., 2015). The linamarase enzyme is added to the acid-extracted sample after adjusting the pH to 5-6. This hydrolysis process is fast at temperatures closer to 30°C and can be completed in under 15 minutes depending on the enzymatic activity (Tivana et al., 2014).

3. **Alkaline hydrolysis**

   The release of HCN from cyanogens is achieved by adding sodium hydroxide (Ngugi et al., 2015).

4. **Autolysis hydrolysis**

   The cyanogens are degraded by an endogenous enzyme, called linamarase, a naturally occurring enzyme found in cassava (Tivana et al., 2014, Diallo et al., 2014,

Mushumbusi et al., 2020, Attahdaniel et al., 2020, Ngugi et al., 2015). This hydrolysis method is suitable mainly for fresh cassava products (Tivana et al., 2014).

The main disadvantages associated with autolysis hydrolysis are:

- The long reaction time of up to 24 hours for some samples such as sun-dried cassava products (Tivana et al., 2014),
- Inability to be applied to cooked or roasted products because of the permanent inactivation of the endogenous linamarase enzyme (Tivana et al., 2014).

However, regardless of which method is used, total hydrolysis must be achieved to allow the complete release of bonded cyanide. In order to avoid loss of HCN released, hydrolysis must be performed in sealed containers.

2.3.5.2.3 Analysis of endogenous cyanide

Several methods have been developed to quantify endogenous HCN released from cyanogenic glucosides.

1. **Titration method**

   This quantification technique can be divided into two groups based on the detection technique of the endpoint. The detection technique can either be visual in the case of colour change or instrumental in the case of a potential change in the electrode (Mousavi, 2018).

   The titration method can be used after steam distillation of hydrogen cyanide (HCN) from autolysed cassava samples (Tivana et al., 2014, Mushumbusi et al., 2020). The main disadvantage of the titration method is the loss of HCN during the distillation process (Tivana et al., 2014). This method is suitable for determining cyanide levels equal to and above 1 mg/L (Diallo et al., 2014, Mousavi, 2018).

2. **Colorimetric methods**

   These various methods used to quantify hydrogen cyanide (HCN) rely on forming a coloured compound.

a. The alkaline picrate method

There are two distinct methods under the alkaline picrate method. Sodium isopurpurate (sodium 3,5-dicyano-6-hydroxylamino-2,4-dinitrophenolate) is the coloured compound formed in this method.

- **Semi-quantitative method**

This method relies on the reaction of HCN with alkaline picrate paper (paper impregnated with alkaline picrate solution, then dried for later use). The colour change is matched against a colour chart (Tivana et al., 2014).

- **Quantitative method**

The HCN is analysed using a spectrophotometer either after dissolving the resulting chromophore from alkaline picrate paper (Tivana et al., 2014, Ndam et al., 2019) or by directly adding the alkaline picrate solution to the sample (Tivana et al., 2014). The amount of HCN is estimated against a standard curve.

b. König reaction

The released HCN is oxidised to a cyanogen halide by reaction with chloramine T. The halide formed reacts with either pyridine or a related compound to form a dialdehyde. The dialdehyde combines with primary amines or compounds with active methylene groups, such as pyrazolone or barbituric acid, to produce a coloured complex (Tivana et al., 2014).

The cyanogen complex can also be reacted with sensor complexes of isonicotinic acid/1,3 – dimethylbarbituric acid or isonicotinic acid/barbituric acid to produce a coloured complex (Tivana et al., 2014). This method has a lower detection limit of 1 mg/L (Fukushima et al., 2016).

c. Resorcinol and picric acid method

Cyanide is reacted with picric acid and resorcinol in the presence of sodium carbonate. This method has been shown to detect cyanide levels below 0.01 µg CN^-/mL in environmental samples (Drochioiu et al., 2003).

3. **Flow injection analysis (FIA)**

This automatic or semi-automatic analytical method emerged in 1975 uses a fixed sample volume or zone injected into the carrier stream continuously flowing towards the detector. The changes of absorbance monitored by the potential electrode are constantly recorded by the detector. Any physical parameter change caused by the passage of the sample can be used to determine cyanide (Mousavi, 2018).

The detection techniques used in cyanide determination by flow injection method can be amperometry (Mousavi, 2018), flame atomic absorption spectrometry (Lopez Gomez and Martinez Calatayud, 1998, Dadfarnia et al., 2006) or fluorimetry (Recalde-Ruiz et al., 2000).

Sulphide, which interferes with the cyanide analysis, can be eliminated by adding lead salt to the sample before introducing it into the analyser (Mousavi, 2018). Carbonate and chlorine are also known to interfere with cyanide determination. The former can be eliminated by adding hydrated lime to the sample, while the latter can be eliminated by adding sodium arsenite or ascorbic acid to the sample prior to the analysis (Mousavi, 2018).

4. **Fluorescent probe**

This detection technique has many advantages over the other cyanide detection techniques, such as

- Rapid response time (Yahaya and Seferoglu, 2018, La et al., 2016, Long et al., 2019),
- Great sensitivity (Yu et al., 2017, Yahaya and Seferoglu, 2018, La et al., 2016, Long et al., 2019)
- Good selectivity (Yu et al., 2017, La et al., 2016), and
- Easy to use (Yu et al., 2017, Yahaya and Seferoglu, 2018, La et al., 2016, Long et al., 2019).

The development of chemo-sensors for the selective detection of cyanide has attracted much attention. Four principles mainly govern the strategies designed and developed for cyanide detection:

- Coordination to electron-deficient centre (La et al., 2016, Saha et al., 2010).
- Nucleophilic addition to the electron-deficient π-system (La et al., 2016).
- Hydrogen-bonding interaction (Yahaya and Seferoglu, 2018, La et al., 2016, Saha et al., 2010, Das et al., 2014).
- Metal-CN^- affinity (Displacement approach) (Yahaya and Seferoglu, 2018, La et al., 2016, Saha et al., 2010, Das et al., 2014).

The principle that has gotten the greatest attention is the displacement method (La et al., 2016). This strategy works on the idea that cyanide ion (CN^-) can extract copper ion (Cu^{2+}) from the metal receptor complex to form stable $Cu(CN)_x$ which produces detectable optical signal attention (La et al., 2016). The special attention attributed to this strategy arises from the recovery of the fluorescence of the copper (II) complexes chromophores, normally nonfluorescent due to the paramagnetic quenching effect, upon addition of CN^- (La et al., 2016).

The detection signal or the fluorescence intensity at a single wavelength can be affected by many factors, like environmental conditions, probes concentration, and the instrument's efficiency (Yu et al., 2017, Long et al., 2019). These limitations observed in most fluorescent cyanide sensors are caused by fluorescence quenching or enhancement. However, they can be overcome by using ratiometric fluorescent probes (Yu et al., 2017, Long et al., 2019). These ratiometric probes use the ratio of two different wavelengths, thus providing a built-in correction irrespective of the instrumental effects, receptor concentration and environmental conditions (Yu et al., 2017).

Furthermore, almost all fluorescent probes for cyanide detection can be operated in organic solvents (Yu et al., 2017, Saha et al., 2010, Das et al., 2014) or mixed aqueous solvents (Das et al., 2014), but not suited for detection in an aqueous medium (Yu et al., 2017, Das et al., 2014). Nevertheless, most fluorescent probes used for cyanide determination in water samples only exhibit fluorescence turn-on response. This specific type of response suffers from the same limitations as the one observed with fluorescence intensity at a single wavelength, and they are also overcome by using a ratiometric fluorescent probe (Long et al., 2019).

5. Ion selective electrode (ISE)

The electrochemical cell can also be used for cyanide determination. This cell comprises an ion-selective electrode (ISE), a reference electrode and a potentiometer. The ISE is mostly a membrane-based apparatus with an inner filling solution containing the ion of interest at the constant activity. The transportation of ions is triggered by the immersion of the electrode in the sample solution. The ions move from high ions concentrations to low ions concentration areas (Mousavi, 2018).

The cyanide concentration is directly proportional to the potential difference created by the selective binding of ions with the specific sites on the membrane. This technique is suitable for analysing samples with 0.5 to 10 mg/L cyanide (Mousavi, 2018). Some of the advantages observed with ISE (Mousavi, 2018) are

- fast response,
- wide linear range,
- economic aspects, and
- immunity to turbidity.

The reduction of the electrode life-span caused by heavy metals, such as mercury and lead, is the principal shortcoming associated with ISE (Mousavi, 2018).

6. Amperometric method

Another electrochemical technique that is used for cyanide determination is the Amperometric method. The cell used in this method consists of (Mousavi, 2018):

- A working electrode

  This electrode can either be gold, glassy carbon or silver. Amongst these electrode materials, silver is commonly used because of its properties, including a wide linear working range of 0.5 µg/L to 1g/L, low cost, long stability and excellent reproducibility.

- A reference electrode or Ag/AgCl electrode

- A counter electrode or steel electrode

The cyanide concentration is proportional to the current produced during an anodic reaction (Mousavi, 2018).

The eventual expiration of the electrode surfaces is the main shortcoming associated with the amperometric method. The formation of numerous products due to the reactions of other compounds besides cyanide with the working electrode and their adhesion to the electrode surface hinders other reactions. Thus, suppressing the generated current and the height of the recorded peaks. Other drawbacks observed with the coated or poisoned electrode surface are increased noise and drift in the cell. These limitations can be overcome by adding the appropriate standard, polishing or replacing the working electrode (Mousavi, 2018). Thiosulphate, metal-cyanide compounds, sulphide, and oxidants have also been known to cause analysis errors.

Regardless of the analytical method used for direct or indirect cyanogenic glucosides determination, care must be taken during the sample handling to limit analyte loss.

2.3.6Uses of cassava, impact of cyanide in cassava processing effluent and cyanide remediation

Cassava is an important food crop for more than 500 million people worldwide (Bayitse et al., 2017). It is widely cultivated in many tropical countries (Itoba-Tombo et al., 2019, Shackelford et al., 2018, Ndam et al., 2019, Lansche et al., 2020), with an approximate annual production of more than 291 million tonnes in 2017 (Otekunrin and Sawicka, 2019, Lansche et al., 2020). The crop carbohydrates production is about 40 % higher than rice and 25 % greater than maise (Waisundara, 2018). Hence, making it the most important source of carbohydrates in producing countries (Lansche et al., 2020). As reported by Ndubuisi and Chidiebere (2018), Pereira et al. (2016), and Bolarinwa et al. (2016), cyanogenic glucosides are found in all parts of the cassava plant (roots, leaves and stems) in varying concentrations because of different factors, such as the age of the plant and plant cultivar (Ndubuisi and Chidiebere, 2018, Mushumbusi, 2018).

Owing to the suitability of cassava for different applications, it is a valuable feedstock in various industries. The detoxification of cassava produces cyanide-rich wastes. If improperly discharged, this waste will negatively affect the environment.

2.3.6.1 Cassava uses

The importance of cassava has grown over the years because of its applicability in many sectors of the economy.

2.3.6.1.1 Cassava roots

Cassava is mainly cultivated for its swollen root (Mombo et al., 2017). The tuber has found many applications in different industries where it is used for:

- Human nutrition (Omomowo et al., 2015, Lansche et al., 2020, Mombo et al., 2017, Obueh and Odesiri-Eruteyan, 2016),
- Livestock feed (Omomowo et al., 2015, Lansche et al., 2020, Izah, 2018),
- Starch (Omomowo et al., 2015, Mombo et al., 2017, Watthier et al., 2019, Izah, 2018, Shittu et al., 2016),
- Pharmaceuticals (Watthier et al., 2019, Okudoh et al., 2014),
- Chemicals and paper (Omomowo et al., 2015, Watthier et al., 2019),
- Biodegradable plastics, glues, biofuels, adhesives, sweeteners and plywood (Mombo et al., 2017).

2.3.6.1.2 Cassava leaves

Cassava leaves are used for:

- Human consumption (Omomowo et al., 2015, Lansche et al., 2020, Mombo et al., 2017),
- Animal feeding (Lansche et al., 2020, Buasaengchan et al., 2019) and
- Natural fertilisation (Sharif et al., 2015).

The hydrophobic waxy surface of the cassava leaves is exploited in the pulp and paper industries to make water repellent food packaging (Sharif et al., 2014). Other application areas of cassava leaves are in the manufacturing of biocomposite sheets (Sharif et al., 2015), in the pharmaceutical industries (Mustarichie et al., 2020), and in the steel industries, where they can be used for pack cyaniding of mild steel (Akinluwade et al., 2018, Adetunji et al., 2015).

2.3.6.1.3 Cassava stems

Cassava stems are used for:

- Plant propagation (Itoba-Tombo et al., 2019, de Oliveira et al., 2020, Martín et al., 2017),
- Animal feeding (Adetunji et al., 2015, Martín et al., 2017), and
- Starch production (Mombo et al., 2017).

The stems can also be used as:

- Natural fertiliser (Nuwamanya et al., 2012, Zhu et al., 2015),
- Fuel for cooking (Zhu et al., 2015),
- Feedstock in biofuels production (Okudoh et al., 2014, Martín et al., 2017, Zhu et al., 2015),
- Feedstock in biochemical and biogas production (Zhu et al., 2015).

2.3.6.2 Impact of cyanide in cassava processing effluent

Cyanide contained in all parts of the plant, except the seeds (Gustafson, 2015), is generally removed as waste during processing for food and sometimes feed (Lansche et al., 2020, Akinluwade et al., 2018). Cyanide, which is one of the significant components of liquid residues (Trevisan et al., 2019, Lawal et al., 2019, Olaoye et al., 2018), produced during cassava processing, is hazardous for:

- The environment (Omomowo et al., 2015, Obueh and Odesiri-Eruteyan, 2016, Izah, 2018, Lawal et al., 2020, Achi et al., 2020),
- Human (Omomowo et al., 2015, Lawal et al., 2020, Chibueze Izah et al., 2018),
- Animals (Omomowo et al., 2015, Obueh and Odesiri-Eruteyan, 2016, Izah, 2018, Chibueze Izah et al., 2018) and
- Plants (Izah, 2018, Chibueze Izah et al., 2018, Afuye and MogajI, 2015).

The liquid residues produced during cassava processing originate from squeezed juice (Lawal et al., 2019, Jideofor, 2015) and water from extraction procedures (Oghenejoboh, 2015,

Howeler and Oates, 2000). The negative impacts observed with these cyanide-rich wastewaters are due to their unregulated disposal into:

- The nearest available watercourse (Omomowo et al., 2015, Izah, 2018, Lawal et al., 2020, Chibueze Izah et al., 2018) and
- Soils (Omomowo et al., 2015, Obueh and Odesiri-Eruteyan, 2016, Chibueze Izah et al., 2018)

Hence, it is crucial to treat the cassava processing effluents before disposal to reduce the cyanide concentration.

2.3.6.3 Cyanide remediation

During the production of cassava-based goods, unwanted wastewaters containing cyanide as one of the major components (Trevisan et al., 2019, Lawal et al., 2019, Olaoye et al., 2018) are generated as a result of cassava processing methods. Depending on cyanide concentration in the cassava wastewaters, they might represent a risk to the environments, humans, animals and plants (Izah, 2018). Therefore, they must be treated prior to being discharged.

The cyanide level of the cassava processing effluents can be reduced through natural, physical, chemical and biological processes. All these processes aim to attain a safe waste quality for the environments, humans, flora and fauna (Arévalo, 2019).

Whichever cyanide treatment process is used, the aim is to degrade the most toxic cyanide species at once or degrade free cyanide in the presence of interferences such as metals (Arévalo, 2019). Besides being cheap, easy and fast, the treatment method must also be capable of meeting local requirements for each industry and location, without producing unwanted by-products during the remediation process (Arévalo, 2019).

CHAPTER 3: MATERIALS AND METHODS

3.1 Materials

3.1.1 Sample collection

Fresh cassava leaves were purchased from local vendors in Durban and Johannesburg, South Africa. The leaves were first cleaned with tap water to remove dirt, then rinsed with Milli-Q water before being stored in a refrigerator at 4 °C awaiting analysis.

3.1.2 Chemicals and Preparation of reagents

All chemicals were Analytical grade

3.1.2.1 Absorbing solutions

a) **0.625 mol/L sodium hydroxide (NaOH) solution (2.5 % w/v)**

   12.5 g of NaOH was dissolved in approximately 250 mL of Milli-Q water. The solution was made up to 500 mL after cooling.

b) **5 mol/L NaOH solution (20 % w/v)**

   102.128 g of NaOH were dissolved in approximately 300 mL of Milli-Q water. The solution was made up to 500 mL after cooling.

c) **10 mol/L NaOH solution (40 % w/v)**

   200 g of NaOH were dissolved in approximately 300 mL of Milli-Q water. The solution was made up to 500 mL after cooling.

3.1.2.2 Sodium cyanide standard solutions

Caution: Sodium cyanide and all other cyanides are deadly poisons, and extreme care must be taken in their use.

a) **Sodium cyanide (NaCN) stock solution (1000 CN^- µg/mL)**

   1.98 g of NaCN were accurately weighed and dissolved in 1000 mL of Milli-Q water.

b) **Working standard solutions for methods comparison and cyanide recovery studies**

   These standards cyanide solutions were prepared by diluting suitable volumes of the stock NaCN solution (see Table 3.1) to 1000 mL with 0.01 mol/L sulphuric acid (H_2SO_4) solution.

Table 3.1: Preparation of test solutions for method comparison and cyanide recovery studies

Flask (1000 mL)	Volume of stock solution (mL)	Final HCN concentration (µg/mL)
1	10	10
2	40	40
3	100	100
4	400	400

c) Working standards for the spectrophotometric method

These standards solutions were prepared by diluting appropriate volumes of 100 µg HCN/mL (see Table 3.2) to 25 mL with 0.01 mol/L H_2SO_4.

Table 3.2: Preparation of standards for the spectrophotometric method

Flask (25 mL)	Volume of cyanide standard (mL)	Final HCN concentration (µg/mL)
0	0	Blank
1	0.250	1
2	1.25	5
3	2.50	10
4	3.75	15
5	5.00	20
6	6.25	25

3.1.2.3 Reagents for the alkaline titration method

a) 0.02 mol/L silver nitrate ($AgNO_3$) solution

3.4317 g of $AgNO_3$ was accurately weighed and dissolved in 1000 mL of Milli-Q water. This solution was standardised with 0.02 mol/L sodium chloride (NaCl) solution (see section 3.2.2.1 for standardization method).

b) 0.02 mol/L NaCl solution

0.3015 g of NaCl was accurately weighed and dissolved in 250 mL of Milli-Q water.

c) 5 % w/v potassium iodide (KI) solution

12.5 g of KI was dissolved in 250 mL of Milli-Q water.

d) 5 % w/v potassium chromate (K_2CrO_4) solution

5.05 g of K_2CrO_4 was dissolved in 100 mL of Milli-Q water.

e) 6 mol/L ammonia solution (NH_4OH)

448 mL of 25 % ammonia solution were mixed with Milli-Q water to make 1000 mL solution.

3.1.2.4 Reagent for the spectrophotometric method (alkaline picrate method)

a) Alkaline picrate solution

This solution was prepared by mixing equal volumes of 2.56 % w/v picric acid solution obtained by dissolving 1.31g of moist picric acid in a minimal amount of warm Milli-Q water, then made up to 50 mL mark and 5 % w/v sodium carbonate (Na_2CO_3) solution obtained by dissolving 2.51 g of Na_2CO_3 in 50 mL of Milli-Q water before the cyanide determination.

Caution: Moist picric acid (2,4,6-Trinitrophenol) - Dangerously explosive if allowed to dry out.

b) 0.01 mol/L sulphuric acid (H_2SO_4) solution

5.16 g of 95 % H_2SO_4 was added to 5000 mL of Milli-Q water.

d) Concentrated sulphuric acid (H_2SO_4)

3.1.2.5 Reagents for the determination of sodium carbonate and sodium hydroxide in sodium cyanide solution

a) 0.05 mol/L sodium carbonate (Na_2CO_3) solution

1.35-1.40 g of Na_2CO_3 was accurately weighed and dissolved in 250 mL of Milli-Q water.

b) 0.1 mol/L hydrochloric acid (HCl) solution

10 mL of 32 % HCl were mixed with Milli-Q water to make 1000 mL solution. This solution was standardised with 0.05 mol/L Na_2CO_3 solution (see section 3.2.3 for standardization method).

c) Phenolphthalein indicator solution

1 g of the reagent was dissolved in 50 mL of 96 % ethanol, then made to 100 mL mark with Milli-Q water.

d) Methyl orange indicator solution

0.5 g of the reagent was dissolved in 100 mL of Milli-Q water.

3.1.2.6 Reagents for racemic lactic acid synthesis

a) Reference materials

DL-lactonitrile, racemic lactic acid (DL-LA) and methyl-DL-lactate purchased from Sigma-Aldrich were used to confirm the identity of the compounds synthesised in each step.

b) 8 mol/L hydrochloric acid (HCl) solution

170 mL of 37 % HCl were added to Milli-Q to make a 250 mL solution.

e) Methanol (≥99.9 %, HPLC gradient grade)

f) Concentrated sulphuric acid (95.0-97.0 % H_2SO_4, ACS reagent grade)

3.2 Methods

3.2.1 Extraction of hydrogen cyanide from cassava leaves

3.2.1.1 Optimization of maceration time and temperature, and recovery time

Selecting the optimum extraction parameters was vital in developing the extraction methodology. Cassava samples (20 g of washed leaves grounded in 200 mL of cold Milli-Q water) were subjected to different maceration times and temperatures to determine the optimum conditions for autolysis, hydrolysis of cyanogenic glucosides by endogenous enzyme, producing the maximum amount of hydrogen cyanide (HCN). Cold Milli-Q water was used to maintain the temperature of the homogenate below 25 ℃ to avoid losing HCN gas. The liberated HCN was collected in a 2.5 % sodium hydroxide (NaOH) solution. Samples were macerated at 18 ℃ (room temperature), 30 ℃ and 37 ℃. At each maceration temperature, samples were left to stand for 60, 120, 180 and 240 minutes. The recovery of released HCN done under vacuum at 35 ℃ – 40 ℃ was evaluated after 30, 45 and 60 minutes.

3.2.1.2 Release of hydrogen cyanide from plant material

Figure 3.1 illustrates the release of hydrogen cyanide gas (HCN) from cassava leaves. 250 g of washed cassava leaves were grounded with 1000 mL of cold Milli-Q water in a blender for 3 minutes. The homogenate was immediately transferred to a stoppered distillation flask and macerated for 120 minutes at 30 ℃.

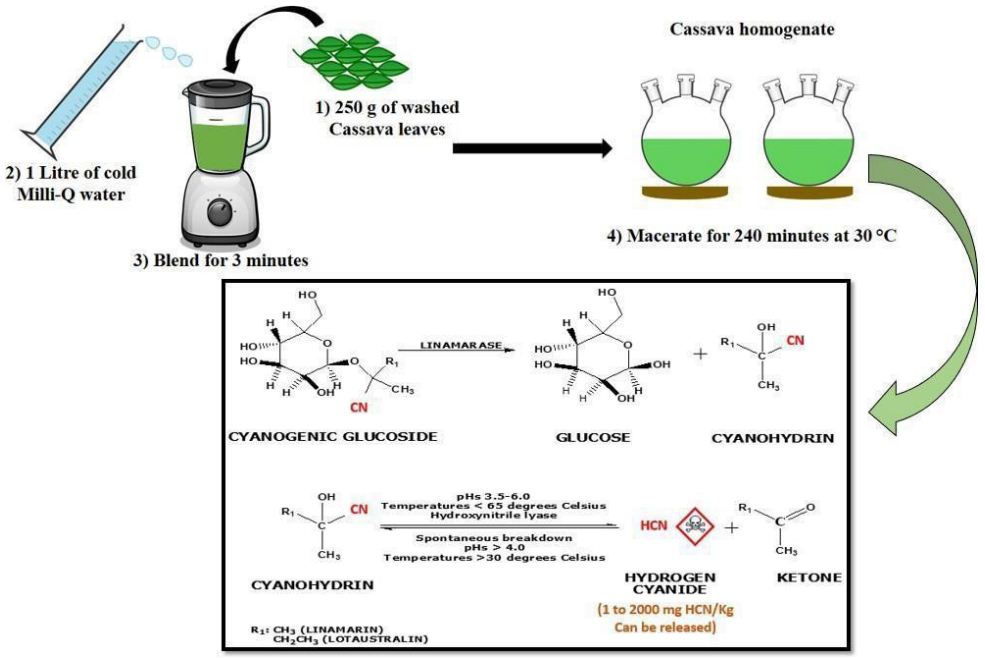

Figure 3.1: Release of hydrogen cyanide gas (cyanogenesis) from cassava leaves

3.2.1.3 Recovery of released hydrogen cyanide

The distillation flask containing the homogenate was quickly connected to a gas-tight system as shown in Figure 3.2 to recover the released HCN under vacuum at 35 °C – 40 °C. The flasks were connected using Teflon tubing through which atmospheric air was passed to agitate the homogenate and carry the liberated HCN. The latter was trapped in 5.0 mol/L NaOH solution (HCN absorbing solution) to form sodium cyanide (NaCN) solution. Before reaching the homogenate flask, atmospheric air was passed through a carbon dioxide (CO_2) remover system. The CO_2 remover system was built with five absorption vessels connected in series containing 10 mol/L NaOH (CO_2 absorbing solution). The flow was allowed to continue for 45 minutes.

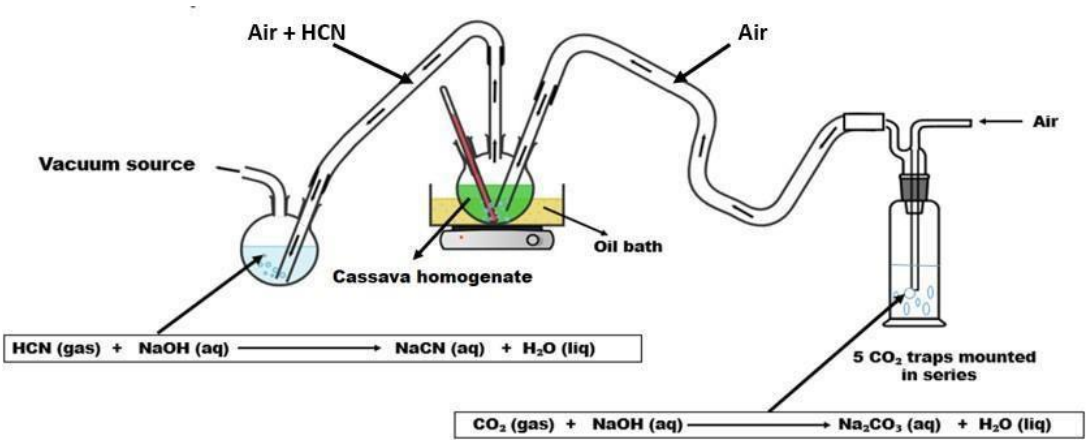

Figure 3.2: Hydrogen cyanide recovery under vacuum at 35 °C–40 °C

3.2.2 Quantification of extracted hydrogen cyanide

A comparative study between titrimetric (alkaline titration) and spectrophotometric (alkaline picrate solution) methods was conducted in order to determine the most effective method for cyanide determination. Four standard solutions of 10, 40, 100 and 400 µg HCN/mL (see Table 3.1) were considered.

3.2.2.1 Alkaline titration method (Titrimetric method)

20 mL of each standard test solution were titrated with standardised 0.02 mol/L silver nitrate ($AgNO_3$). The latter was standardised using Mohr's method adapted from Korkmaz (2001). 25 mL of the $AgNO_3$ solution were titrated against the 0.02 mol/L sodium chloride (NaCl) solution using a few drops of 5 % potassium chromate (K_2CrO_4) solution as an indicator. The endpoint was signalled when the colour changed from lemon-yellow to faint red-brown. A blank titration was also carried.

The cyanide concentration was determined using the alkaline titration method described by Anhwange et al. (2011). 20 mL of test sample were added into a conical flask containing 40 mL of Milli-Q water, 8 mL of 6 mol/L ammonia solution and 2 mL of 5 % w/v potassium iodide (KI) solution, used as an indicator (Figure 3.3). The resulting solution was slowly titrated with standardised 0.02 mol/L $AgNO_3$ to faint but permanent turbidity.

The cyanide concentration was calculated according to the formula given bellow:

$$1\ \text{mL of } 0.02\ \text{mol/L } AgNO_3 = 1.08\ \text{mg HCN}$$

$$\text{Or}$$

$$\text{HCN (mg/L)} = \text{Conc.} \times 54 \times V \times (\text{dilution/aliquot}) \quad (12)$$

Where: *Conc.* is the concentration of standardised 0.02 mol/L $AgNO_3$ and *V* is the volume of 0.02 mol/L $AgNO_3$ used in L

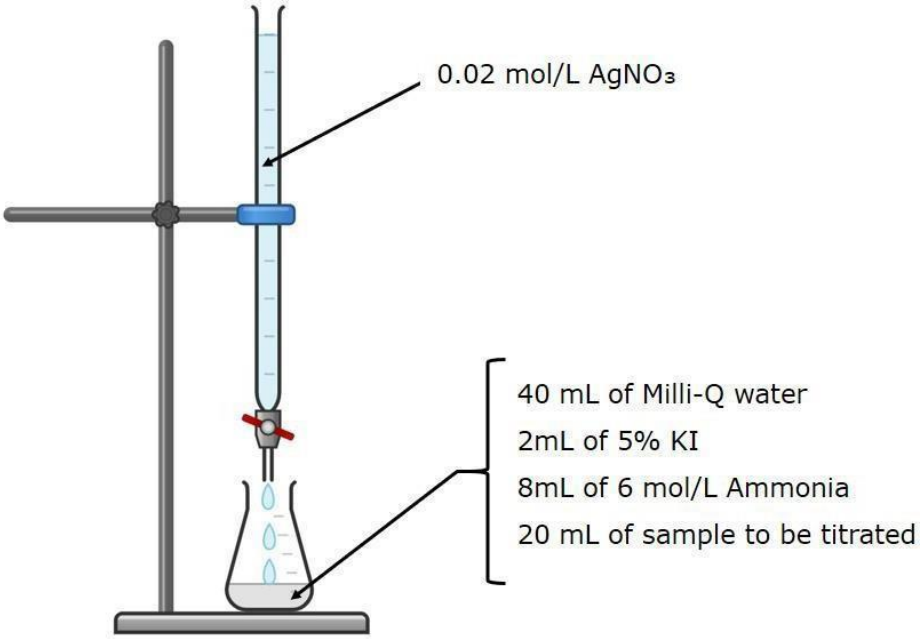

Figure 3.3: Titration set up

3.2.2.2 Alkaline picrate method (Spectrophotometric method)

The alkaline picrate method is based on the reaction between released hydrogen cyanide (HCN) and alkaline picrate solution (see section 3.2.2.4), producing sodium 3,5-dicyano-6-hydroxylamino-2,4-dinitrophenolate (Figure 3.4) (Oshima et al., 2003). The latter is commonly called sodium isopurpurate, and it is responsible for inducing the observed colour change. The colour intensity is directly proportional to the amount of cyanide present in the test samples. The HCN content of test samples was determined from a standard calibration curve.

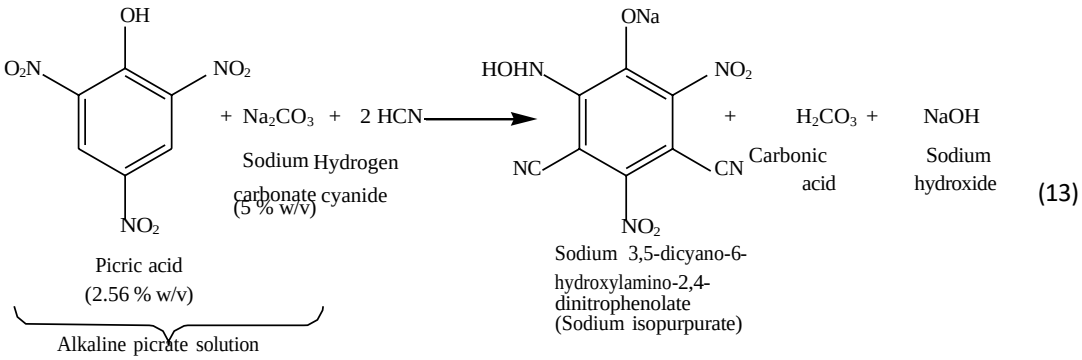

Figure 3.4: Formation of sodium isopurpurate

Standard solutions prepared in Table 3.1 were diluted with 0.01 mol/L sulphuric acid (H_2SO_4) (see Table 3.3). Appropriate volumes of these dilute standard solutions and standard solutions

prepared in Table 3.2 were transferred into vials and further diluted with alkaline picrate solution (See Table 3.4). The method used to treat the test samples (Figure 3.5) was adapted from Brito et al. (2009). For colour development, the vials were incubated for 15 minutes in a water bath at 37 °C. 15 µL of concentrated H_2SO_4 were added afterwards to stop the reaction and increase the stability of the readings. The absorbance of the resulting coloured solutions was measured using a UV-1800 Shimadzu UV-Visible spectrophotometer at 485 nm. The blank prepared with 0.01 mol/L H_2SO_4 was used to adjust the absorbance reading to zero.

Table 3.3: Dilution of standard test solutions

Concentration of cyanide standard (µg/mL)	Volume of cyanide standard (mL)	Volume of 0.01 mol/L H_2SO_4 (mL)	Final volume (mL)	Final HCN concentration (µg/mL)
10	2	0	2.00	10
40	1	1.00	2.00	20
100	0.400	1.60	2.00	20
400	0.100	1.90	2.00	20

Table 3.4: Preparation of cyanide solutions for UV analysis

	Standard solutions for the calibration curve			
Vial	Concentration of cyanide standard (µg/mL)	Volume of cyanide standard (ml)	Volume of alkaline picrate solution (mL)	Final HCN concentration (µg/mL)
1	1	2	2	0.5
2	5	2	2	2.5
3	10	2	2	5.0
4	15	2	2	7.5
5	20	2	2	10.0
6	25	2	2	12.5

Table 3.4: Preparation of cyanide solutions for UV analysis (cont'd)

	Test standard solutions			
Vial	**Concentration of cyanide standard (µg/mL)**	**Volume of cyanide standard (ml)**	**Volume of alkaline picrate solution (mL)**	**Final HCN concentration (µg/mL)**
7	10	2	2	5.0
8	20	2	2	10.0
9	20	2	2	10.0
10	20	2	2	10.0

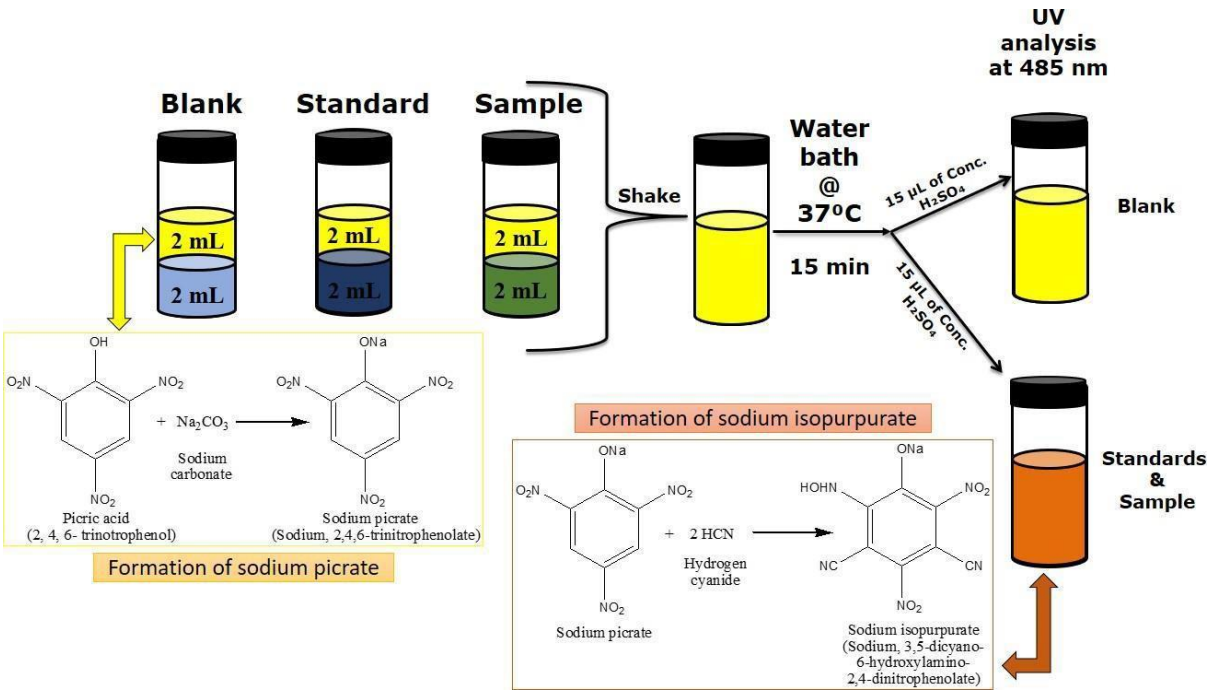

Figure 3.5: Samples preparation for UV analysis

3.2.3 Determination of sodium carbonate and sodium hydroxide in sodium cyanide Solutions

The amount of sodium carbonate (Na_2CO_3), formed by the reaction between atmospheric carbon dioxide (CO_2) and NaOH absorbing solution, need to be quantified and removed before drying the sodium cyanide (NaCN) solution since it will affect the yield of the starting material needed to synthesise racemic lactic acid (DL-LA) if present in a significant amount. Na_2CO_3 was removed by the freezing out carbonates method described by Asterion (2016). The NaCN solution (distillate) was cooled to a temperature close to zero (1 °C – 4 °C) to remove Na_2CO_3

by precipitation. The carbonate thus removed could be used in the alkaline picrate method (see section 3.2.2.2). Residual sodium hydroxide (NaOH) was also determined since it influences the amount of Na_2CO_3 formed during the drying process.

Na_2CO_3 and residual NaOH content in the NaCN solution was determined by the indicator method against standardised 0.1 mol/L hydrochloric acid (HCl) solution (eGyanKosh, 2017). The latter was standardised by titrating 25 mL against a primary solution of 0.05 mol/L Na_2CO_3 using methyl orange indicator. The endpoint was signalled when the colour changed from yellow to orange. The concentration of HCl solution was calculated based on the following equation:

$$M_{HCl} = \frac{2\, M_{Na_2CO_3} \times V_{Na_2CO_3}}{V_{HCl}} \tag{14}$$

There were two equivalence points associated with the determination of Na_2CO_3 and NaOH in the NaCN solution. The first equivalence point, which indicates complete neutralisation of NaOH and half neutralisation of Na_2CO_3 or its conversion to the bicarbonate, was detected with phenolphthalein. 25 mL of sample was titrated against standardised 0.1 mol/L hydrochloric acid (HCl) solution until the indicator colour changed from pink to colourless. The second equivalence point indicating neutralisation of the bicarbonate was detected with methyl orange. Two drops of the latter were added to the above sample, and the titration was continued till the colour changed from yellow to orange. The corresponding chemical reactions associated with this method are summarised as:

$$\begin{aligned} &OH^- + H^+ \longrightarrow H_2O \quad (NaOH)\ (HCl) \\ &CO_3^{2-} + H^+ \longrightarrow HCO_3^- \quad (Na_2CO_3)\ (HCl) \end{aligned} \quad \left.\right\} \text{Equivalence point detected with phenolphthalein} \tag{15}$$

$$HCO_3^- + H^+ \longrightarrow H_2CO_3 \quad (HCl) \quad \left.\right\} \text{Equivalence point detected with methyl orange}$$

The concentration and strength of Na_2CO_3 and NaOH in the NaCN solution were calculated based on the equations shown below and displayed in Table 3.5:

a) Estimation of the concentration of Na_2CO_3 in the NaCN solution in mol/L

$$M_{Na_2CO_3} = \frac{M_{HCl} \times V_{HCl}}{2V_{Na_2CO_3}} \quad (16)$$

b) Estimation of the strength of $NaCO_3$ in the NaCN solution in g/L

$$M_{Na_2CO_3} \times Molar\ mass_{Na_2CO_3} \quad (17)$$

c) Estimation of the concentration of NaOH in the NaCN solution in mol/L

$$M_{NaOH} = \frac{M_{HCl} \times V_{HCl}}{V_{NaOH}} \quad (18)$$

d) Estimation of the strength of NaOH in the NaCN solution in g/L

$$M_{NaOH} \times Molar\ mass_{NaOH} \quad (19)$$

Table 3.5: Volumes of HCl solution used to titrate Na_2CO_3 and NaOH in the NaCN solution

Sample Aliquot (mL)	**Burette reading (mL)**			**Titrant used for NaOH and half of Na_2CO_3 (mL)**	**Titrant used for NaOH and Na_2CO_3 (mL)**	**Titrant used for HCO_3^- (mL)**	**Titrant used for Na_2CO_3 (mL)**	**Titrant used for NaOH (mL)**
	Initial volume	**1st endpoint**	**2nd endpoint**					
25	V_1	V_2	V_3	$V_4 = (V_2-V_1)$	$V_5 = (V_3-V_1)$	$V_6 = (V_5-V_4)$	$V_a=2V_6$	$V_b= (V_5-2V_6)$

(Source: adapted from eGyanKosh (2017)).

3.2.4 Drying of sodium cyanide solution

Figure 3.6 illustrates the drying process. The volume of the sodium cyanide solution (NaCN) prepared using hydrogen cyanide (HCN) extracted from cassava leaves was reduced on a hotplate prior to drying. The concentrated solution was then tested for residual sodium hydroxide (NaOH) and sodium carbonate (Na_2CO_3) according to the method described in section 3.2.3. The purified cyanide concentrate was further dried on a rotary evaporator before being placed in the oven at 100 °C to obtain the NaCN salt (green NaCN). The yield of NaCN produced was calculated based on the following formula:

$$\%\ yield\ NaCN\ = \frac{mass\ of\ NaCN\ produced}{Mass\ of\ cassava\ leaves} \times 100\ \% \qquad (20)$$

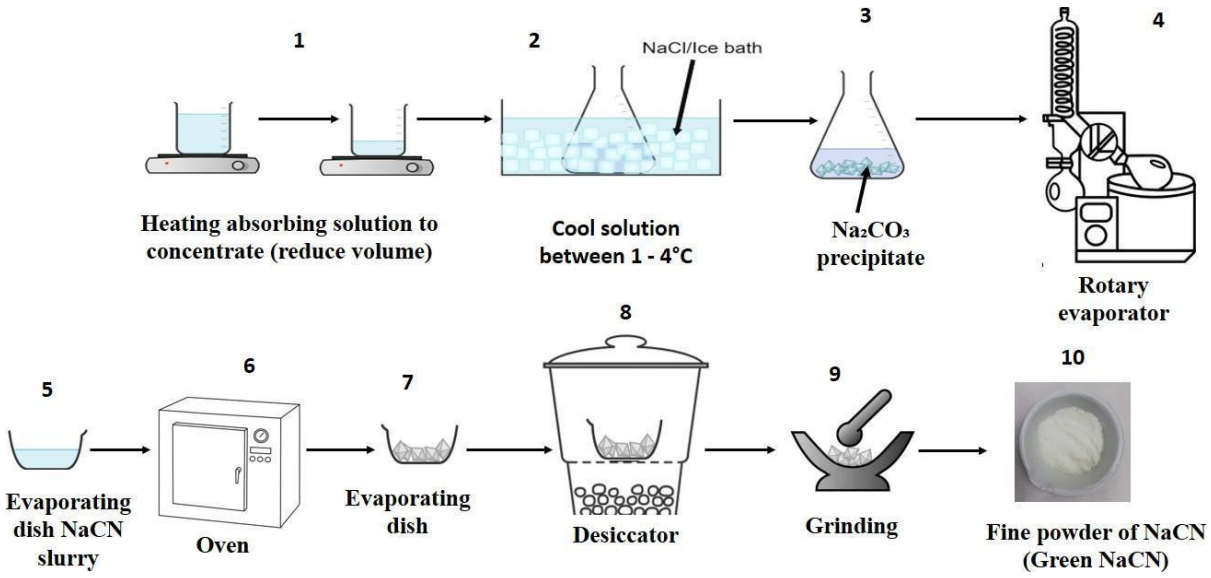

Figure 3.6: Steps of drying process

3.2.5 Synthesis of racemic lactic acid

The chemical synthesis process used to prepare racemic lactic acid (DL-LA) is a four-step process (Ghaffar et al., 2014, Komesu et al., 2017b). The yield of product synthesised at each step was calculated using the following formula:

$$\%\ yield\ of\ product\ = \frac{actual\ yield}{theoretical\ yield} \times 100\ \% \qquad (21)$$

3.2.5.1 Addition of hydrogen cyanide/Preparation of DL-lactonitrile

DL-lactonitrile (2-hydroxypropanenitrile) was prepared by the addition of hydrogen cyanide (HCN), generated in situ from synthesised sodium cyanide (NaCN) salt (see section 3.2.4), to acetaldehyde according to the method adapted from Chan (1985).

a) 58 mL (1.03 mole) of acetaldehyde was slowly added to a stirred aqueous sodium cyanide solution (48 g or 0.98 mole in 116 mL of Milli-Q water) for 1 hour at a temperature kept at 0 °C – 5 °C. The reaction mixture was stirred at the same temperature for an additional hour after completing the addition step.

b) 80 mL (0.98 mole) of 37 % hydrochloric acid (HCl) was then fed into the reaction vessel at 0 °C – 5 °C temperature for two and a half hours. The reaction mixture was

stirred for an additional 30 minutes at the same temperature before being extracted with 3 x 50 mL of diethyl ether.

c) The ethereal extracts were dried with magnesium sulphate, then concentrated by rotary evaporation to give DL-lactonitrile. The chemical reaction associated with this step can be summarised as:

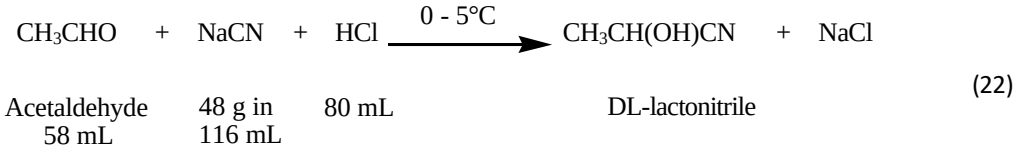

(22)

3.2.5.2 Hydrolysis by hydrochloric acid

DL-lactonitrile was hydrolysed with dilute HCl to produce DL-LA (2-hydroxypropanoic acid) based on the following method:

The reaction mixture prepared by adding 8 M HCL to DL-lactonitrile was refluxed for six hours at 100 °C. The chemical reaction associated with the hydrolysis step can be summarised as:

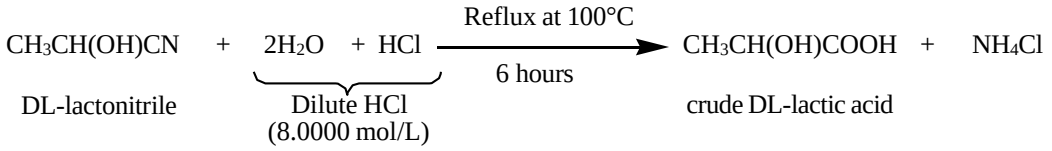

(23)

3.2.5.3 Esterification (Fischer esterification)

Crude DL-LA was isolated and purified by esterification with methanol to produce methyl-DL-lactate (methyl (±)-2-hydroxypropanoate) according to the following method:

2.5 moles of methanol and 5 mL of concentrated sulphuric acid (H_2SO_4) were added to crude DL-LA. The reaction mixture was then refluxed for six hours at 100 °C. Methyl-DL-lactate was isolated and purified from the reaction mixture by rotary evaporation. The chemical reaction associated with this step can be summarised as:

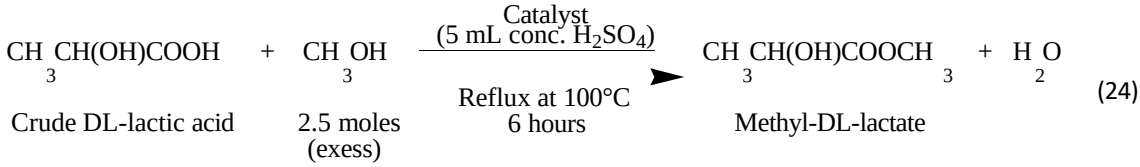

(24)

3.2.5.4 Hydrolysis by acidified water

Methyl-DL-lactate was hydrolysed with acidified Milli-Q water to produce pure DL-LA. The methanol produced was removed and recycled back in the synthesis process. The method used to prepare purified DL-LA is as follow:

2.5 moles of Milli-Q water and 5 mL of concentrated H_2SO_4 were added to methyl-DL-lactate. The reaction mixture was refluxed for six hours at 100 °C. The chemical reaction associated with this hydrolysis step can be summarised as:

$$\underset{\text{Methyl-DL-lactate}}{CH_3CH(OH)COOCH_3} + \underset{\substack{\text{2.5 moles}\\\text{(exess)}}}{H_2O} \xrightarrow[\substack{\text{Reflux at 100°C}\\\text{6 hours}}]{\substack{\text{Catalyst}\\\text{(5 mL conc. } H_2SO_4\text{)}}} \underset{\text{Pure DL-lactic acid}}{CH_3CH(OH)COOH} + CH_3OH \quad (25)$$

The overall yield of this multistep synthesis process was calculated using the partial yields (yield from each synthesis step) expressed to decimals:

$$Overall\ \%\ yield = (yield\ 1\ \times yield\ 2\ \times yield\ 3\ \times yield\ 4) \times 100\% \quad (26)$$

3.2.6 Structural confirmation of synthesised products

ATR-FTIR, XRD, and SEM-EDS were used to determine the identity, crystal structure, and purity of the green NaCN, obtained as described in section 3.2.4 against a control NaCN sample. On the other hand, the products isolated during the synthesis process of racemic lactic acid (see section 3.2.5) were identified by ATR-FTIR and ^{1}H-QNMR. The latter technique was also used to evaluate the purity of products.

3.2.6.1 Attenuated Total Reflectance - Fourier Transform Infrared Spectroscopy (ATR-FTIR)

On a Shimadzu QART-S single reflectance ATR accessory linked to an IR Spirit Shimadzu Spectrophotometer, the ATR-FTIR spectra of both control and green NaCN were recorded in the wavenumber range of 4000–400 cm-1. The same settings were used to investigate control and precipitated Na_2CO_3.

3.2.6.2 X-ray diffraction analysis (XRD)

The crystal structure and phase purity of finely crushed and homogenous green NaCN and precipitated Na_2CO_3 were investigated using this technique. The XRD patterns were obtained on a PANalytical X'Pert PRO X-Ray Diffractometer at 25 °C and an angle of 2θ using CuKα

radiation (wavelength (λ) = 1.5406 Armstrong (Å)). All the samples were analysed using the PANalytical program X'Pert Highscore in a range of 4.0124 to 89.9814°2θ using a step size of 0.0170°/step.

3.2.6.3 Scanning Electron Microscopy with Energy Dispersive X-Ray spectroscopy (SEM-EDS)

This technique was utilised to analyse the morphology and determine the elemental composition of finely crushed green NaCN and precipitated Na_2CO_3. SEM-EDS spectra were recorded on JEOL 7800F Field Emission Scanning Electron Microscope (FE-SEM). Control NaCN and Na_2CO_3 were studied on the same instrument

3.2.6.4 ^{1}H Quantitative nuclear magnetic resonance (^{1}H QNMR)

The acquisition was carried out using a Bruker Avance III HD spectrometer, operating at a proton frequency equal to 500 MHz. This technique was chosen for quantitative analysis since the NMR peak area (integral) is proportional to the number of nuclei (Choi et al., 2021). This relation will be used to determine the concentration or purity of the isolated products by comparing peak areas. Control and synthesised DL-lactonitrile were prepared in dimethyl sulfoxide-d6 (DMSO-*d6*, ≥ 99.9 %), while the other samples were prepared in deuterium oxide (D_2O, 99.95 %). Dimethylformamide (DMF, ≥ 99.8 %) was used as an internal standard (IS) to evaluate the purity of the isolated products. The NMR samples were prepared by transferring 50 µL of the analyte and 5 µL of DMF to 500 µL of solvent. The resulting solutions were vigorously shaken then transferred to the NMR tubes for analysis. The number of scans was 32. All NMR spectra were processed using the MestReNova software. The first step in using the information provided by the NMR spectrum was to identify the chemical shift signal(s) arising from the target analyte. In this study, the signal(s) identification was achieved by comparing the target analyte spectrum to that of the control sample. The chemical shifts were referenced to δ2.50 ppm for DMSO-*d6* and δ4.65 ppm for D_2O. The next step was to determine the integral of the signal peak. When dealing with a target analyte giving rise to one chemical shift signal, its integral and the number of protons causing the signal must be used to determine the purity of the target analyte. However, when dealing with multiple chemical shift signals, the integral of the target analyte is the average of its normalised integrals. The number of protons taken as one was used to determine the purity (Pauli et al., 2014). The integral of a target analyte giving rise to multiple signals was calculated as follows:

$$Integral = \left(\frac{^{1}}{n_1} + \frac{^{2}}{n_2} + \cdots \frac{^{x}}{n_x}\right) \div N \quad (27)$$

Where *Int* is the integral, *n* is the number of protons giving rise to the signal and *N* is the number of signal within the target analyte.

The purity of the target analyte was determined using the following equation:

$$P_t = \frac{A_t}{A_{std}} \times \frac{n_{std}}{n_t} \times \frac{Mw_t}{Mw_{std}} \times \frac{W_{std}}{W_t} \times P_{std} \quad (28)$$

Where *P* is the purity, *A* is the NMR peak area, *n* is the number of ^{1}H atoms contributing to the signal, *Mw* is the molecular weight, *W* is the weight, and subscripts "*t*" and "*std*" refer to target analyte and the internal standard, respectively.

The weight of the target analyte was determined from the measured density as follows:

$$Weight = measured\ density \times volume\ used \quad (29)$$

3.2.7 Statistical analysis

Four replicates were performed in all analyses, except where otherwise specified. Statistical analyses were performed in excel (Microsoft office 2016). Results were expressed as the mean ± standard error of the mean ($SEM_{stat.}$), except for optimization of maceration time and temperature.

CHAPTER 4: RESULTS AND DISCUSSION

4.1 Comparative study using two different analytical methods

In order to determine the most effective method to quantify hydrogen cyanide (HCN), the alkaline picrate method (spectrophotometric method) and alkaline titration method (titrimetric method) were compared. Four standard test solutions of 10, 40, 100 and 400 µg HCN/mL were considered (see Table 3.1). The results of the analysis are summarised in Table 4.1.

Table 4.1: Hydrogen cyanide concentration in standard solutions as determined by two different methods

		Concentration (µg/mL)		
Method	**n**	**Expected**	**Determined±SEM**	**$t_{calculated}$**
Alkaline picrate method	4	10	9.79±0.07	-3.184
Alkaline titration method	4	10	12.81±0.52	5.380
		Concentration (µg/mL)		
Method	**n**	**Expected**	**Determined±SEM**	**$t_{calculated}$**
Alkaline picrate method	4	40	40.40±0.22	1.796
Alkaline titration method	4	40	43.60±0.44	8.090

$t_{critical\ (95\ \%\ CL,\ 3\ degrees\ of\ freedom)} = 3.182$

Table 4.1: Hydrogen cyanide concentration in standard solutions as determined by two different method (cont'd)

Method	n	Concentration (µg/mL)		$t_{calculated}$
		Expected	Determined±SEM	
Alkaline picrate method	4	100	100.85±0.30	2.786
Alkaline titration method	4	100	103.82±0.52	7.326
Method	**n**	**Concentration (µg/mL)**		**$t_{calculated}$**
		Expected	**Determined±SEM**	
Alkaline picrate method	4	400	400.95±0.38	2.479
Alkaline titration method	4	400	404.94±0.70	7.014

$t_{critical\ (95\ \%\ CL,\ 3\ degrees\ of\ freedom)} = 3.182$

The expected and determined HCN concentrations were significantly different ($t_{calculated} > t_{critical}$ at 95 % confidence level) with the titrimetric method. This discrepancy in HCN concentration could be attributed to the analyst's arbitrary determination of the endpoint signalled by faint but permanent turbidity. Hence, the visual endpoint detection technique was replaced with the instrumental technique for an accurate endpoint determination (Mousavi, 2018).

The HCN concentrations determined by the spectrophotometric method (see Table 4.1), interpolated from the standard calibration curve shown in Figure 4.1, were found to be not significantly different from the standards ($t_{calculated} < t_{critical}$ at 95 % confidence level).

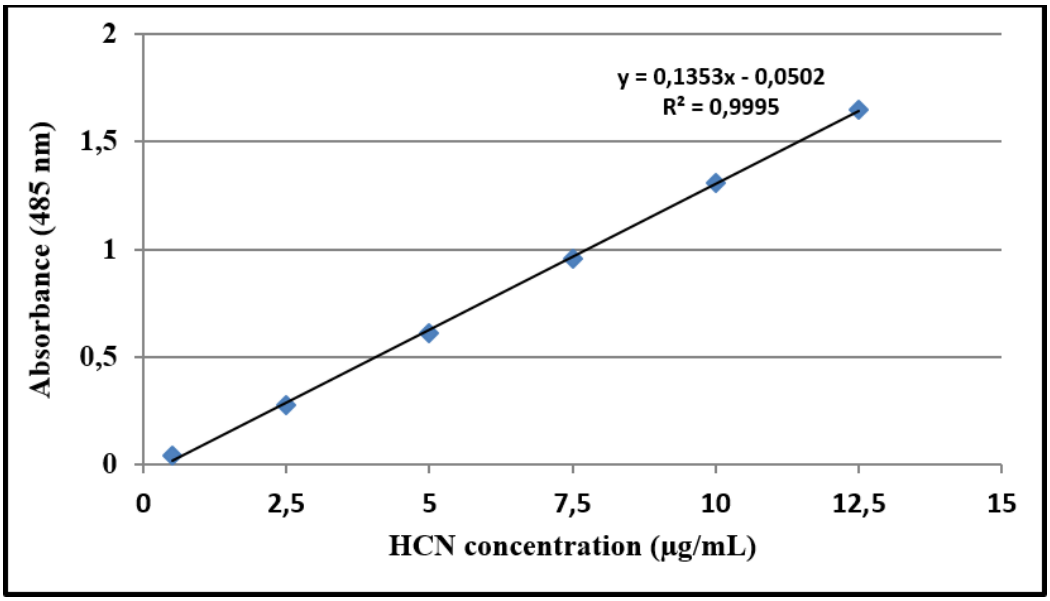

Figure 4.1: Typical standard calibration curve for the spectrophotometric determination of HCN

The above curve was generated using absorbance values given in Table 4.2. Although this method's determination of higher concentrations relied on dilution (see Table 3.3), the measured absorbance values (see Table 4.2) were close to the expected values. These results show the high reproducibility and reliability of the spectrophotometric method. A new calibration curve was generated for each cyanide determination since the analysis was done overtime during the saturation process (see section 4.3).

Table 4.2: Absorbance values

Standard solutions for the calibration curve

Vials	HCN concentration (µg/mL)	Absorbance
1	0.5	0.038
2	2.5	0.278
3	5.0	0.609
4	7.5	0.958
5	10.0	1.308
6	12.5	1.648

Table 4.2: Absorbance values (cont'd)

Test standard solutions

Vials	HCN concentration (µg/mL)	Absorbance	
		Expected	Measured
7	5.0	0.609	0.612
8	10.0	1.308	1.316
9	10.0	1.308	1.314
10	10.0	1.308	1.306

4.2 Optimization of hydrogen cyanide extraction from cassava leaves

An attempt was made to find the optimum conditions (maceration time, maceration temperature and recovery time of liberated hydrogen cyanide gas) for maximum hydrogen cyanide (HCN) generation from cassava leaves via autolysis of the main cyanogenic glucoside Linamarin and the small amount of lotaustralin.

Identifying these conditions was helpful in the processing of cassava leaves to ensure complete hydrolysis of cyanogenic glucosides for the complete release and volatilisation of HCN gas.

4.2.1 Optimization of maceration time

Figure 4.2 shows the hydrogen cyanide (HCN) concentration from cassava leaves macerated for 60, 120, 180 and 240 minutes. HCN concentrations increased from 60 to 240 minutes for all the replicate analyses. However, while minimal from 120 to 240 minutes, it was rather abrupt from 60 to 120 minutes.

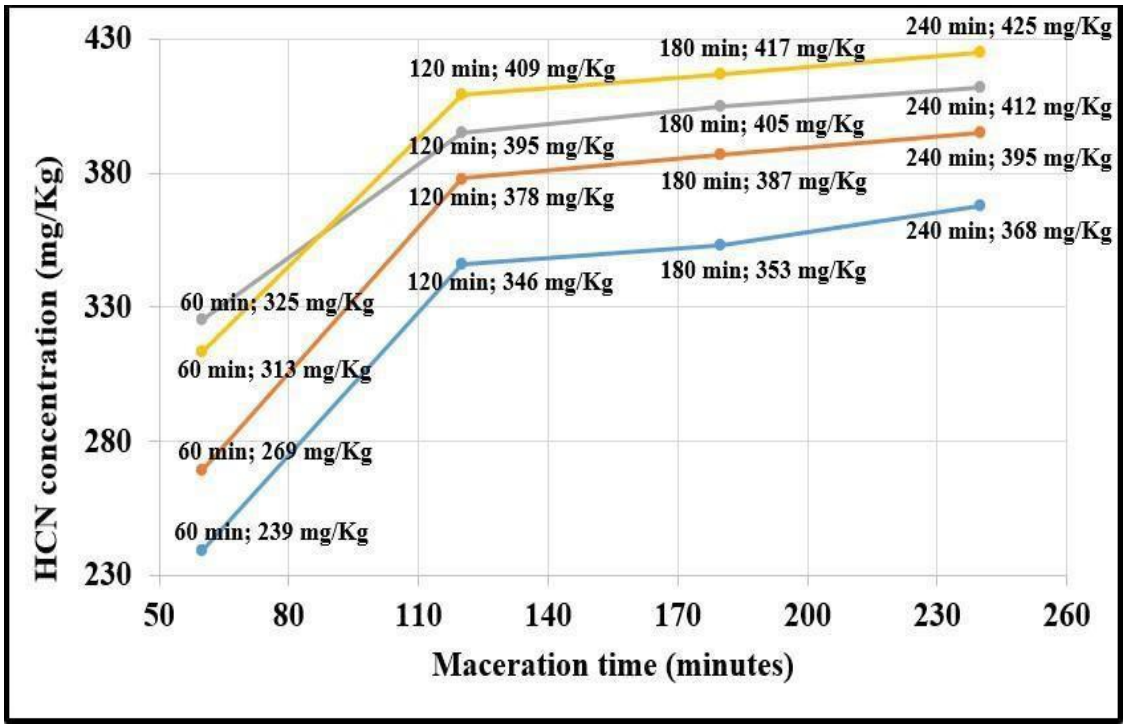

Figure 4.2: HCN concentration (mg/Kg) at different maceration times

Therefore, based on these results, it is safe to say that autolysis can be carried out for 120 to 240 minutes. This finding corroborates the earlier reports by Dusica et al. (2012), who macerated linseed for 120 to 240 minutes, while Omotayo et al. (2015); Gervason A et al. (2017) and Wangari (2013) left the cassava samples to stand for 180 minutes before trapping the liberated HCN gas in an absorption solution. Thus, 120 minutes of maceration time was used throughout this work to generate HCN gas from cassava leaves.

4.2.2 Optimization of maceration temperature

Figure 4.3 shows the HCN concentrations extracted from cassava leaves macerated at 18 °C (room temperature), 30 °C, 37 °C for 120 minutes. The concentration of extracted HCN increased from 18 to 30 °C and decreased beyond 30 °C. These results suggest that the optimum temperature for the enzymatic activity of linamarase and α-hydroxynitrile lyase enzymes, both found in cassava leaves, is 30 °C. The decrease in HCN concentrations beyond 30 °C could be caused by the decrease in enzymatic activity (Castada et al., 2020, Adeleke et al., 2017) or enzymes inactivation (Castada et al., 2020). From these results, the optimum maceration temperature was 30 °C. This temperature was used in further HCN extraction.

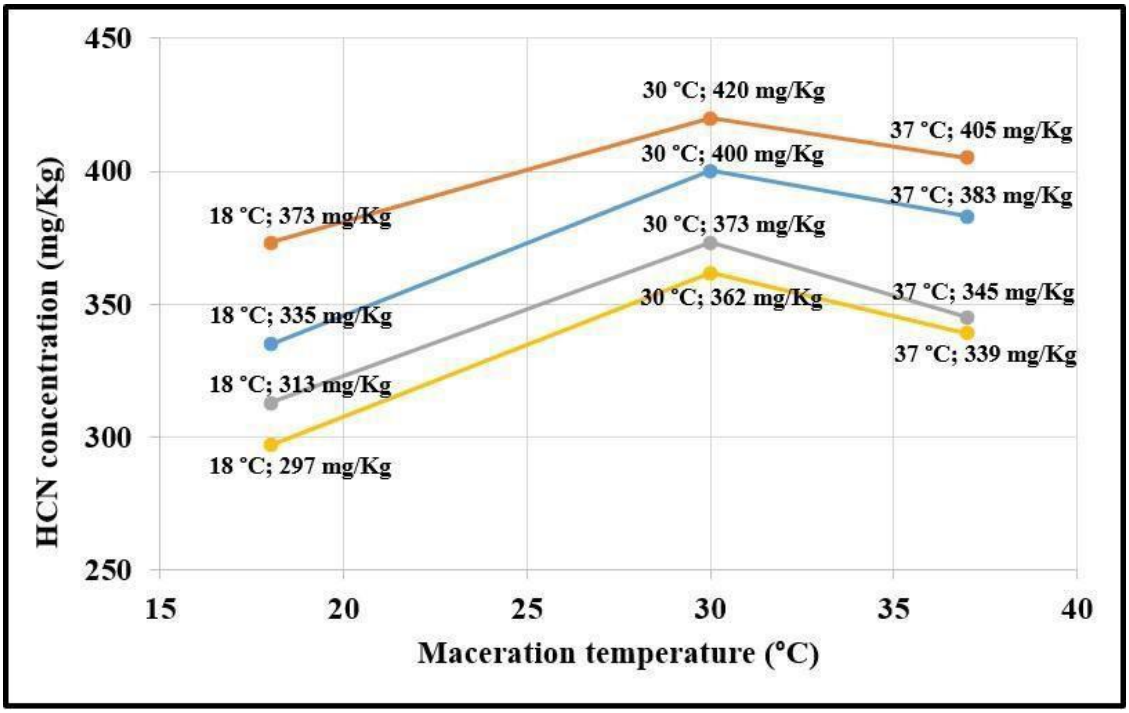

Figure 4.3: HCN concentration (mg/Kg) at different maceration temperatures

4.2.3 Optimization of recovery time

Figure 4.4 shows that the percentage of HCN gas recovered at different times, from cassava leaves macerated at 30°C for 120 minutes and extracted under vacuum at 35 °C – 40 °C, were 97.68±0.51 %; 98.28±0.52 % and 96.55±0.53 % after 30, 45 and 60 minutes of extraction, respectively. Although all the % HCN recovered at different times fall within the accepted range of 95 % - 105 %, we can see from these results that the highest recovery was achieved after 45 minutes of extraction.

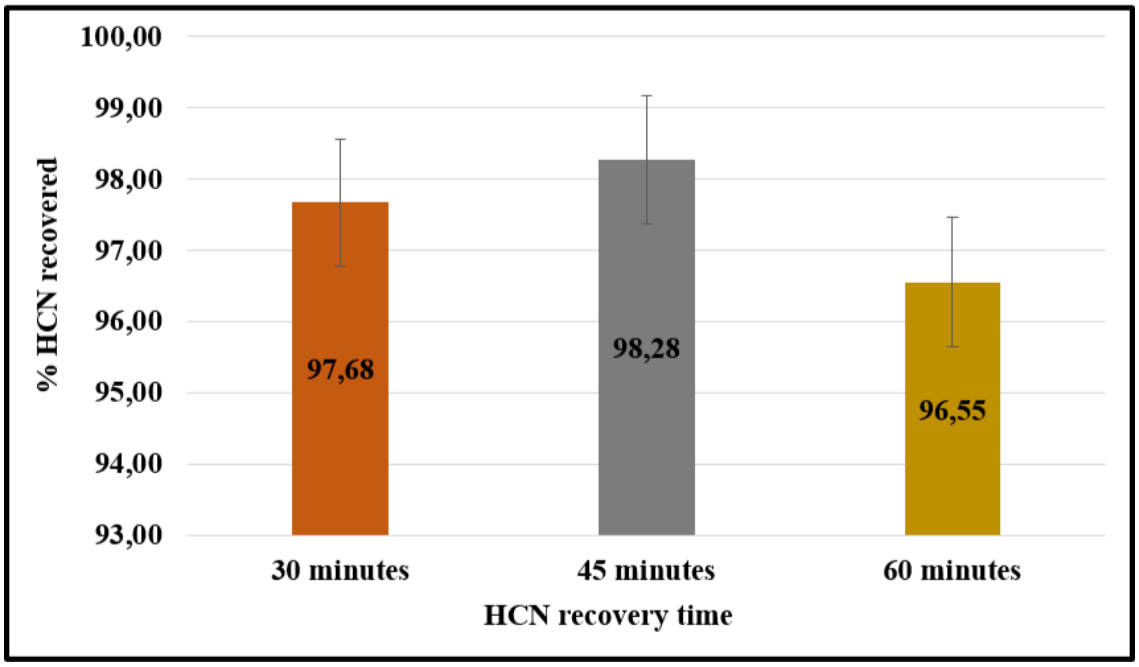

Figure 4.4: % HCN recovered at different times under vacuum at 35 °C – 40 °C

From the obtained results, the optimum conditions for maximum generation of HCN gas from cassava leaves via autolysis were determined to be maceration at 30 °C for 120 minutes with an extraction time of 45 minutes under vacuum at 35 °C – 40 °C.

4.3 Saturation of absorbing solution with naturally produced hydrogen cyanide

The saturation of the absorbing solutions with HCN gas extracted from cassava leaves was done using the optimum HCN extraction conditions described in section 4.2. Figure 4.5 shows the results for the saturation of the absorbing solution used in this study, which consisted of 400 ml of 5.1064 mol/L NaOH. According to the result, 42.75 Kg of fresh cassava leaves were needed to saturate the absorbing solution. Hence, the amount of cassava leaves required for the saturation process solely depends on their HCN content. The saturation process done using the optimum extraction conditions was continued until the concentration of the prepared NaCN solution, determined by the spectrophotometric method, plateaued.

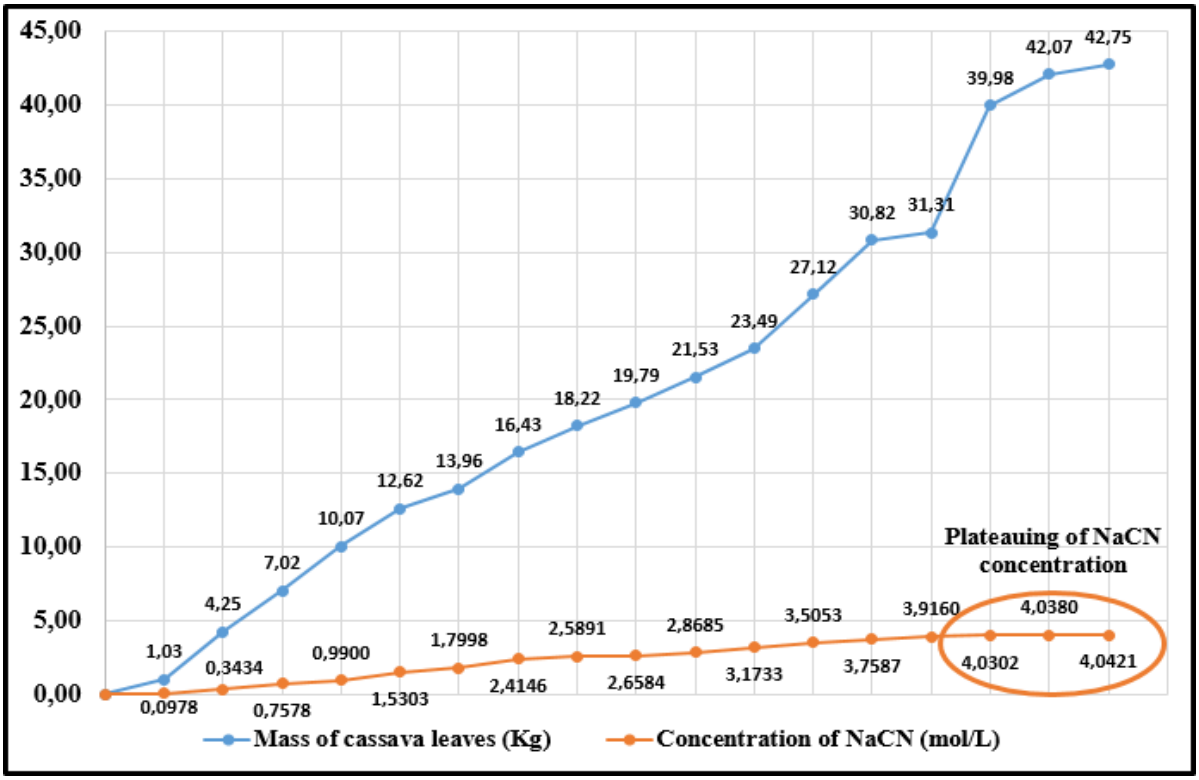

Figure 4.5: Saturation of 5.1064 mol/L NaOH absorbing solution over time with HCN gas extracted from cassava leaves

In addition, the NaCN concentration at the end of the saturation process (4.0421 mol/L) was found to be lower than that of the original absorbing solution (5.1064 mol/L). Based on this result, the NaCN's final concentration is affected by the concentration of the absorbing solution, and the amount of CO_2 absorbed from the atmosphere. The reaction between CN^- ions and CO_2 with Na^+ ions forming NaCN and Na_2CO_3 causes the decrease in NaCN's concentration. Hence, the concentration of absorbing solution must always be higher than the intended NaCN concentration, and care must be taken to limit the exposure of absorbing solution to atmospheric air.

4.4 Determination of sodium carbonate and residual sodium hydroxide in sodium cyanide salt

Table 4.3 shows the titration results and the Na_2CO_3 and the residual NaOH contents in sodium cyanide salts as determined by the indicator method against standardised 0.1 mol/L HCl solution. Na_2CO_3 is formed by the reaction between atmospheric CO_2 and the NaOH absorbing solution.

Table 4.3: Estimation of Na_2CO_3 and residual NaOH in sodium cyanide

Sample Aliquot (mL)	Burette reading (mL)			Titrant used for NaOH and half of Na_2CO_3 (mL)	Titrant used for NaOH and Na_2CO_3 (mL)	Titrant used for HCO_3^- (mL)	Titrant used for Na_2CO_3 (mL)	Titrant used for NaOH (mL)
	Initial volume	1st endpoint	2nd endpoint					
	V_1	V_2	V_3	$V_4 = (V_2-V_1)$	$V_5 = (V_3-V_1)$	$V_6 = (V_5-V_4)$	$V_a = 2V_6$	$V_b = (V_5-2V_6)$
Titration of 4.0421 mol/L control NaCN solution								
25	0.00	6.94±0.01	7.59±0.01	6.94±0.01	7.59±0.01	0.66±0.02	1.31±0.04	6.28±0.03
Titration of 4.0421 mol/L green NaCN solution								
25	0.00	16.42±0.01	19.42±0.01	16.42±0.01	19.42±0.01	3.00±0.02	6.00±0.03	13.42±0.03

Estimation of Na_2CO_3 and residual NaOH

	Na_2CO_3		Residual NaOH	
	Control NaCN solution	Green NaCN solution	Control NaCN solution	Green NaCN solution
Molarity (mol/L)	0.06809	0.2345	0.6529	1.0488
Strength (g/L)	7.2169	24.8547	26.1160	41.9520
Percentage (%)	0.72	2.49	2.61	4.20

The amount of Na_2CO_3 and residual NaOH were 0.72 % and 2.49 % in control NaCN and 2.61 % and 4.20 % in green NaCN. The results from the green NaCN show that a substantial amount of NaOH was still present in the absorbing solution after observation of plateauing of

the NaCN concentration. This unreacted NaOH can react with atmospheric CO_2 to form more Na_2CO_3 impurities during the drying process. Therefore, it is preferable to carry on with the saturation process long after the onset of plateauing of NaCN concentration to reduce the amount of residual NaOH and dry the distillate concentrate in an inert oven. The reaction between atmospheric CO_2 and the absorbing solution during its preparation and handling also adds to the amount of Na_2CO_3.

4.5 Characterization of sodium cyanide prepared using HCN gas extracted from cassava leaves

The NaCN salt prepared according to the method described in section 4.3 (green NaCN) and dried as per the method described in section 3.2.4 was characterised against NaCN standard salt to confirm its identity and crystal structure and determine its purity. After drying the thus prepared NaCN solution, 79.241 g of NaCN salt were obtained, representing a percentage yield of 0.19 %. The latter was calculated using equation 20:

$$\%\,\text{yield NaCN} = \frac{79.241\text{g}}{42.75 \times 10^3\,\text{g}} \times 100\,\% = 0.19\,\%$$

This low yield further confirms that the cassava leaves used in this study had a low HCN content. Therefore, it can be improved by using cassava variety or different cyanogenic plants with a higher HCN content.

4.5.1 Attenuated total reflectance- Fourier transform infrared spectroscopy (ATR-FTIR)

Figure 4.6 shows the ATR-FTIR spectra of control and green NaCN. Due to water absorption, the small, sharp O-H stretching peak at 2970 cm^{-1}. They exhibited a characteristic sharp, high-intensity peak at 2090 cm^{-1} corresponding to C≡N stretching vibration, observed with inorganic cyanide (Nandiyanto et al., 2019). Next to this, an absorption band occurred at 1738 cm^{-1}, followed by another band at 1594 cm^{-1} (control NaCN) and 1607 cm^{-1} (green NaCN). These peaks appeared due to vapour phase water.

Since NaCN prepared from the neutralisation method is always known to contain Na_2CO_3 as its major impurity, the characteristic IR absorption bands known for the carbonate group were found in both the control and synthesised sample. The IR spectrum of control NaCN showed C-O stretching peak at 1449 cm^{-1} and C-O in-plane and out of plane bending peaks at 863 cm^{-}

[1] and 686 cm^{-1}, respectively. The spectrum of green NaCN showed an intense, broad band at 1438 cm^{-1} attributed to C-O stretching and narrow, sharp bands at 879 cm^{-1} and 702 cm^{-1} corresponding to C-O in-plane and out of plane bending, respectively. The high intensities of the carbonate group observed in green NaCN further confirm the titration findings shown in Table 4.3.

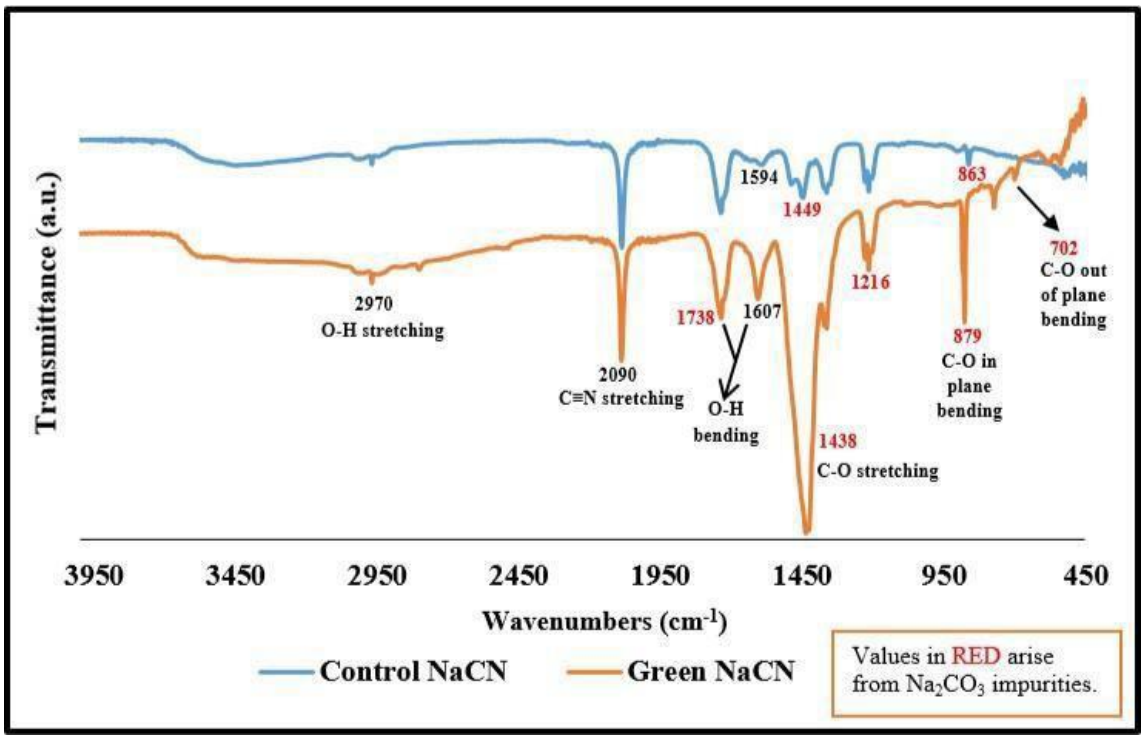

Figure 4.6: ATR-FTIR spectra of sodium cyanide

Figure 4.7 shows the ATR-FTIR spectra of control and precipitated Na_2CO_3. The spectrum of the control sample showed a small, broad peak at 1738 cm^{-1} resulting from vapour phase water. The intense, broad absorption band at 1421 cm^{-1} was attributed to C-O stretching. The narrow, sharp bands at 878 cm^{-1} and 702 cm^{-1} appeared due to C-O in-plane and out of plane bending, respectively. The spectrum of precipitated Na_2CO_3 showed similar peaks except for the small, broad peak at 3575 cm^{-1} caused by vapour phase water and the narrow peak at 2970 cm^{-1} caused by water absorption by the sample.

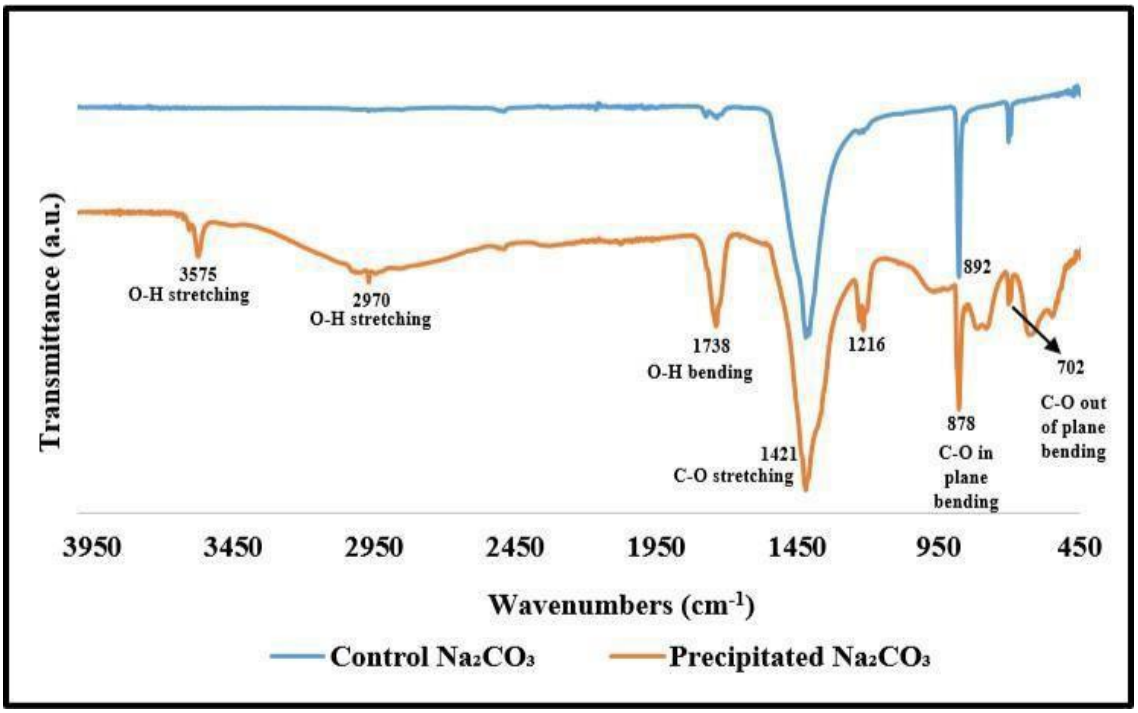

Figure 4.7: ATR-FTIR spectra of sodium carbonate

4.5.2 X-ray diffraction analysis (XRD)

Figure 4.8 shows the XRD pattern for control and green NaCN. From the patterns, the two samples showed similar XRD patterns at 2θ angles of (30.3622°, 30.4557°); (34.1697°, 34.3051°); (38.6422°, 38.5661°); (43.4601°, 43.5524°); (51.4398°, 51.5940°); (53.9323°, 54.0450°); (63.1456°, 63.2228°) and (71.6529°, 71.,7345°), respectively. The control NaCN phase was matched to sodium cyanide reference phase ICDD 00-030-1187, while the green NaCN phase was matched to sodium cyanide reference phase ICDD 00-037-1490. Further analysis of the XRD pattern of the synthesised sample revealed the presence of Na_2CO_3. The phase of the latter was matched to sodium carbonate reference phase ICDD 00-037-0451. These results are in accordance with NaCN ATR-FTIR and titration findings, as shown in Figure 4.6 and Table 4.3, respectively. Both techniques showed that green NaCN had a high Na_2CO_3 level (2.49 %) than control NaCN (0.72 %). The discrepancy in Na_2CO_3 level can be explained by the reaction between residual NaOH (4.20 % in green NaCN) and atmospheric CO_2 during the drying process, done in an air oven.

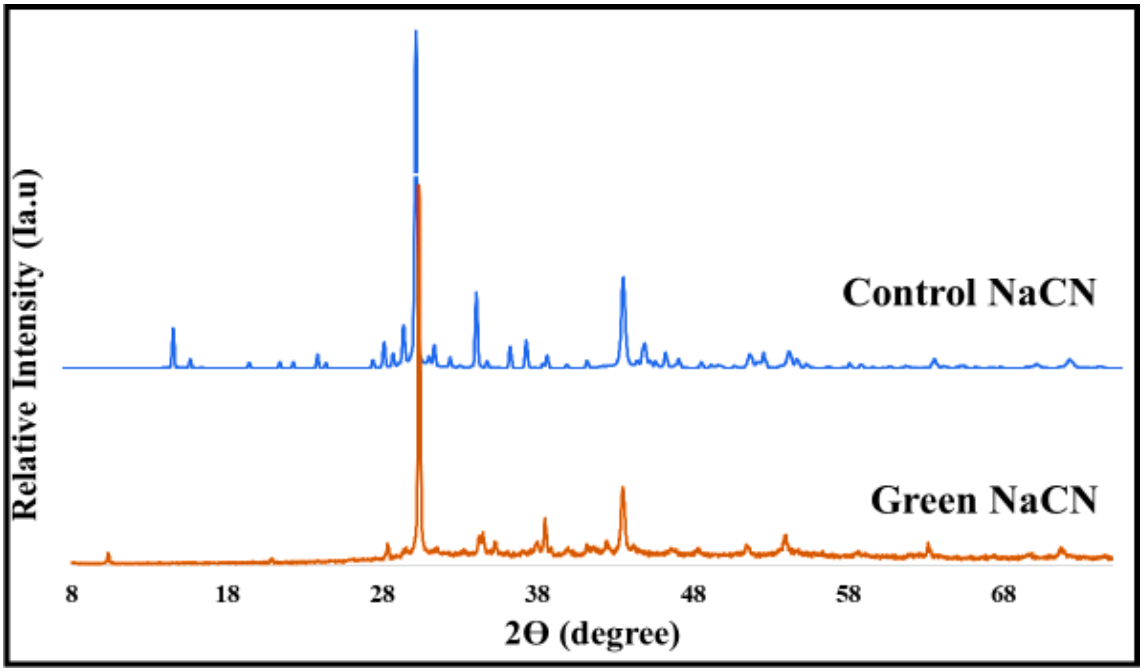

Figure 4.8: X-ray diffraction patterns of sodium cyanide

The XRD patterns of control and precipitated Na_2CO_3 as shown in Figure 4.9 had great similarities at 2θ angles, with the following peaks having noticeable intensities: (26.0488°, 26.1171°); (27.6403°, 27.6929°); (30.1267°, 30.2095°); (33.0273°, 33.1090°); (34.1899°, 34.2551°); (34.5083°, 34.5967°); (35.2238°, 35.2897°); (37.9650°, 38.0721°); (41.0923°, 41.1613°); (41.4807°, 41.5597°); (46.5246°, 46.6025°); (48.2568°, 48.3199°); (53.5670°, 53.6561°); (72.2691°, 72.0894°); (74.4908°, 74.5749°) and (80.3060°, 80.4246°), respectively. The control and green NaCN phases were strongly matched to the sodium carbonate reference phase ICDD 04-011-4108 and ICDD 05-001-0022.

Based on the results, green NaCN and precipitated Na_2CO_3 were crystalline. Green NaCN had a cubic crystal structure (experimental values: a=b=c=5.8894 Å and α=β=γ=90°) (Tesleva et al., 2016), while precipitated Na_2CO_3 had a monoclinic crystal structure (experimental values: a=8.9040 Å, b=5.2390 Å, c=6.0420 Å and α=γ=90°, β=101.35°).

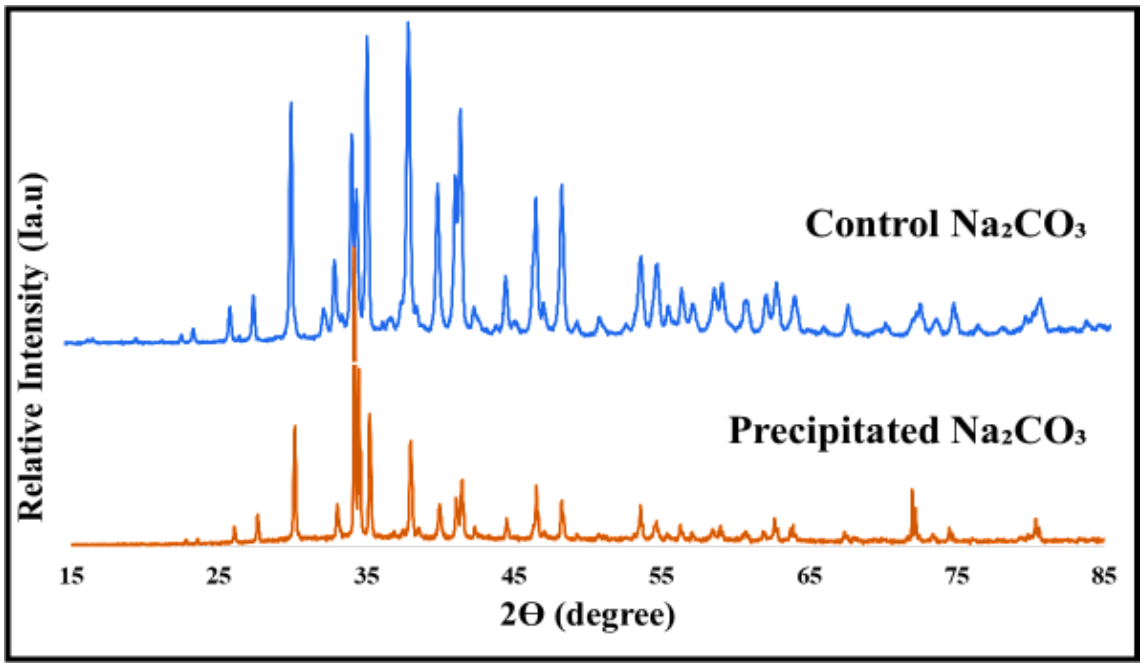

Figure 4.9: X-ray diffraction patterns of sodium carbonate

4.5.3 Scanning electron microscopy with energy dispersive x-ray spectroscopy (SEM/EDS)

The morphology of control samples (NaCN (a) and Na_2CO_3 (c)), green NaCN (b) and precipitated Na_2CO_3 (d) are shown in Figure 4.10. Based on the SEM images, the monoclinic shape of Na_2CO_3 was also observed in control NaCN sample, which appeared cubic in structure (Figure 4.10a). A similar observation was made with the synthesised sample (green NaCN) (Figure 4.10b). The SEM images of control Na_2CO_3 (Figure 4.10c) and precipitated Na_2CO_3 (Figure 4.10d) showed an identical monoclinic structure. These results agree with the ones obtained from ATR-FTIR and XRD analysis.

In order to confirm the formation of NaCN by the proposed method, EDS analysis was performed on the synthesised salt. From the EDS spectrum in Figure 4.10b, both NaCN and Na_2CO_3 can be seen in the synthesised sample. The same results were also observed in the control sample. The quantity of sodium (Na), carbon (C), nitrogen (N) and oxygen (O) were 25.8, 32.3, 7.2 and 34.7 in atomic %, respectively, in green NaCN. Their quantities were 12.2, 59.0, 16.3 and 12.5 in atomic %, respectively, in control NaCN (Figure 4.10a). The latter also contained a small amount of aluminium impurities (0.1 % in atomic %). EDS spectrum of precipitated Na_2CO_3 (Figure 4.10d) showed Na, C and O in 28.3, 31.9 and 39.8 atomic %, respectively. EDS spectrum of control Na_2CO_3 (Figure 4.10c) revealed 24.0, 37.5 and 38.5 in

atomic % for Na, C and O, respectively. Hence, the precipitated Na_2CO_3 can be used to prepare the alkaline picrate solution for cyanide determination (see section 3.1.2.4). These results further complement and confirm the XRD analysis findings.

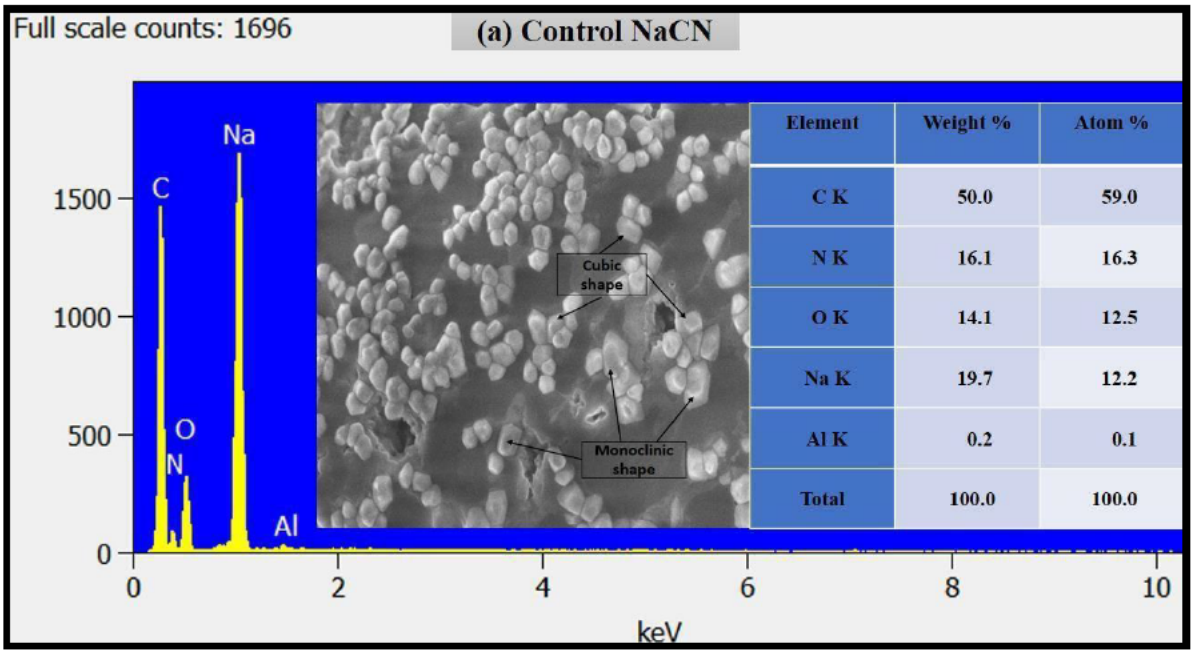

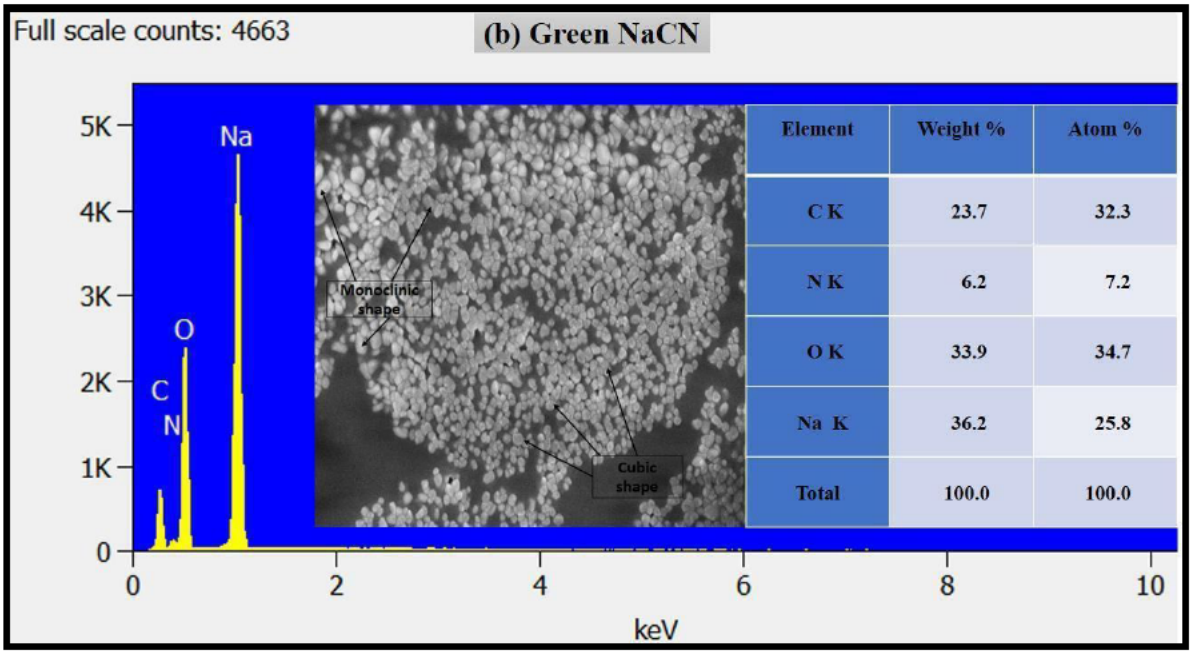

Figure 4.10: SEM images and EDS spectra of (a) control NaCN, (b) green NaCN, (c) control Na_2CO_3 and (d) precipitated Na_2CO_3

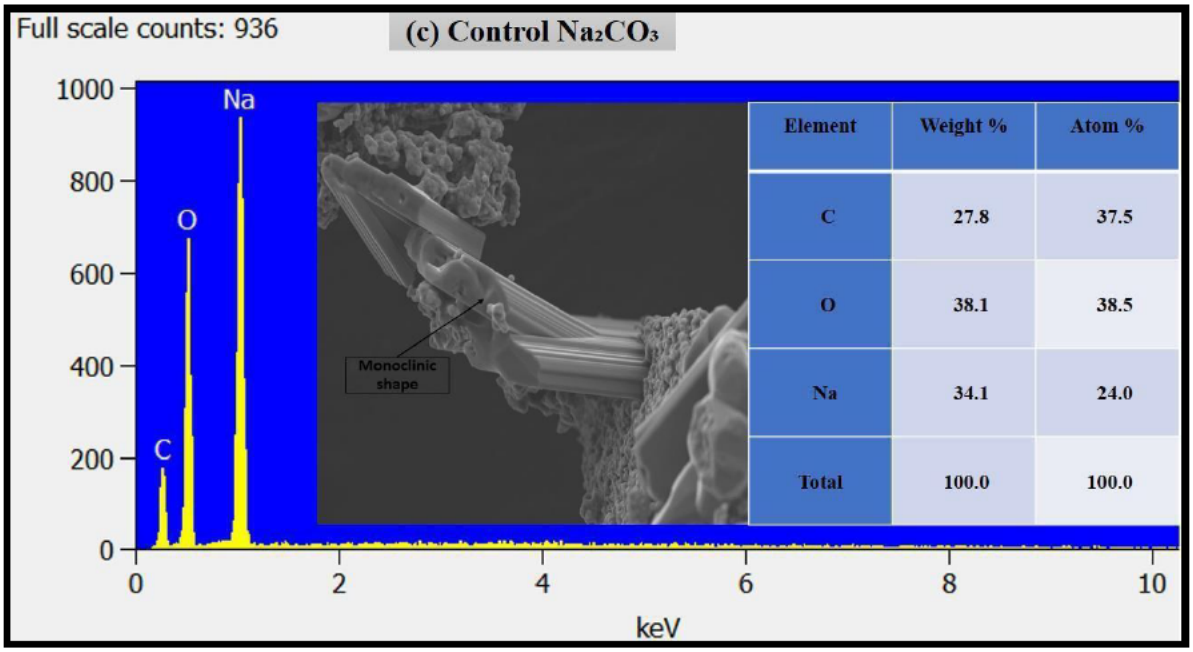

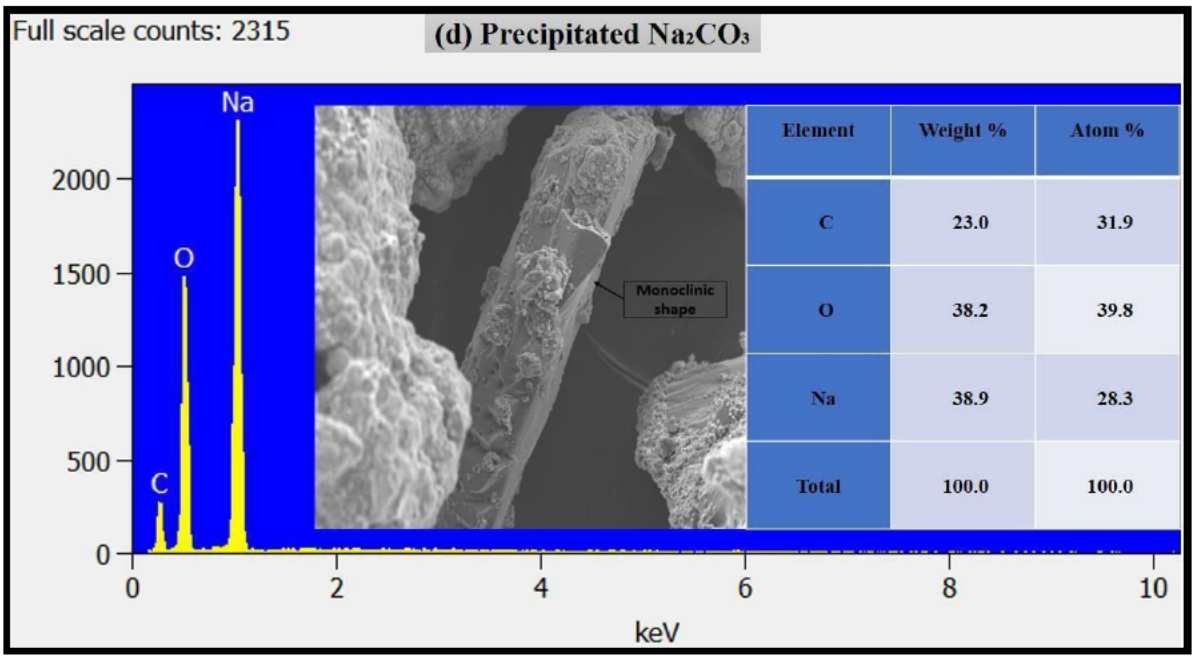

Figure 4.10: EDS spectra of (a) control NaCN, (b) green NaCN, (c) control Na_2CO_3 and (d) precipitated Na_2CO_3 (cont'd)

4.6 Synthesis of racemic lactic acid

Racemic lactic acid was synthesised through a four-step process. The detailed synthesis procedures used for its preparation are given in the following sections. Detailed identification processes are also explained in the following sections. The amount of synthesised compounds

(see Table 4.4) used in ^{1}H QNMR were calculated from the measured densities. These densities were close to the expected values.

Table 4.4: Density and weight of synthesised compounds

Analyte	Molecular weight (g/mol)	Expected density (g/mL)	Measured density (g/mL)	Volume used for ^{1}H QNMR (µL)	Weight (mg)
DMF (IS)	73.09	0.944	-	5	4.72
DL-lactonitrile	71.08	0.991	0.980	50	49.0
Crude DL-lactic acid	90.08	1.209	1.020	50	51.0
Purified DL-lactic acid			1.198	50	59.9
Impure Methyl-DL-lactate	104.10	1.093	1.123	50	56.1
Purified Methyl-DL-lactate			1.111	50	55.6

4.6.1 Addition of hydrogen cyanide/Preparation of DL-lactonitrile (Step 1)

Hydrogen cyanide (HCN) used to prepare DL-lactonitrile (2-hydroxypropanenitrile) was generated in situ from the synthesised NaCN (green NaCN). DL-lactonitrile was synthesised according to the method described in section 3.2.5.1 and Figure 4.11. The amount of reactants used and product obtained are shown below with equation 22:

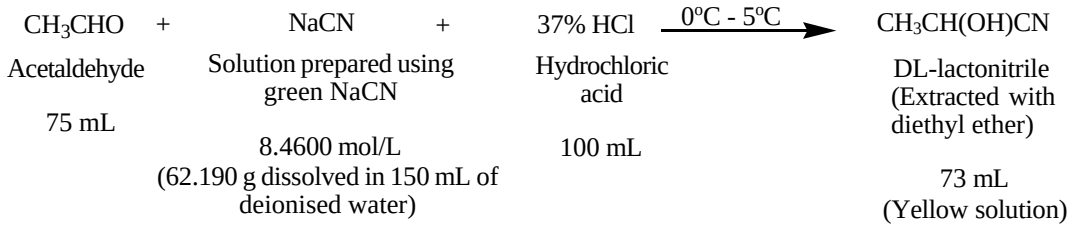

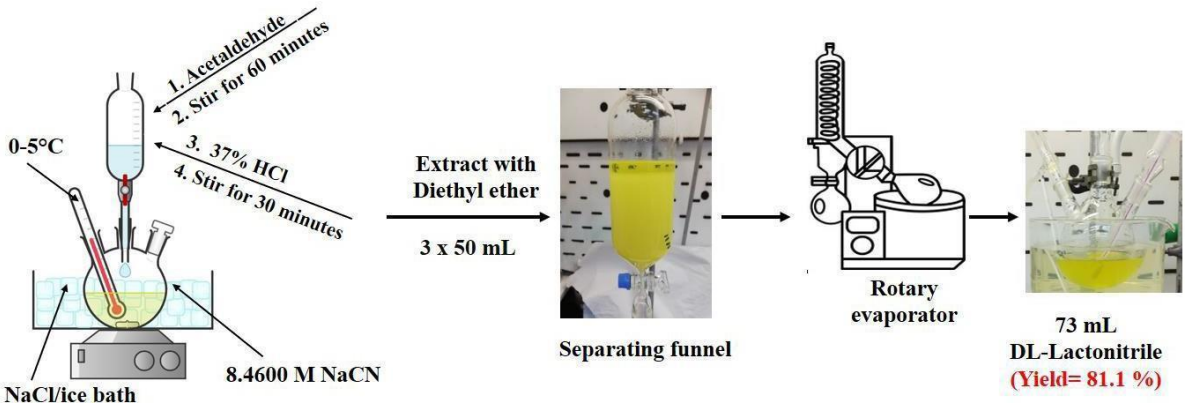

Figure 4.11: Synthesis of DL-lactonitrile

Based on the volume of the product obtained at the end of this first step, the percentage yield was calculated using equation 21:

$$\%\ yield\ of\ DL-lactonitrile\ = \frac{73\ mL}{90\ mL} \times 100\ \% \ = 81.1\ \%$$

The product was isolated in 81.1 % yield and identified as DL-lactonitrile against a control sample using the following spectral techniques:

4.6.1.1 Attenuated total reflectance- Fourier transform infrared spectroscopy (ATR-FTIR)

Figure 4.12 illustrates the ATR-FTIR spectra of control and DL-lactonitrile samples. The spectrum of the control sample showed characteristic bands at 3419, 2995, 2942 and 2251 cm^{-1} that were caused by OH, CH_3, C-H and C≡N stretching, respectively. The synthesised DL-lactonitrile spectrum showed similar bands, except for the OH stretch peaking at 3382 cm^{-1}. Further analysis of the spectra revealed extra peaks at (1744 cm^{-1}, 1763 cm^{-1}); (1660 cm^{-1}, 1654 cm^{-1}) and (1194 cm^{-1}, 1206 cm^{-1}) for control and synthesised sample, respectively. These peaks suggest that the NaCN salt used to synthesis of both DL-lactonitrile samples contained Na_2CO_3 impurities. Furthermore, based on the carbonate peak intensities, we can see that the green NaCN salt contained more Na_2CO_3 impurities than the NaCN salt used to synthesise the control DL-lactonitrile. These results further support the findings of the titration analysis and the other spectral analysis of NaCN salts.

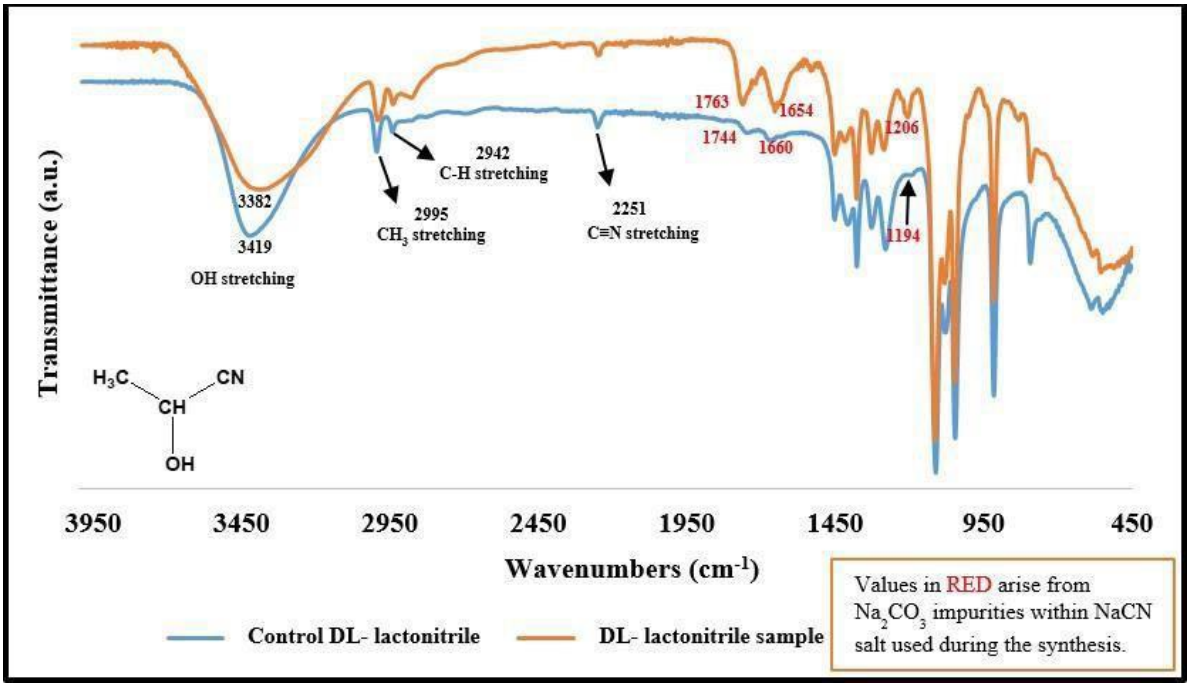

Figure 4.12: ATR-FTIR spectra of control and synthesised DL-lactonitrile

4.6.1.2 ^{1}H Quantitative nuclear magnetic resonance (^{1}H QNMR)

Figure 4.13a shows the ^{1}H QNMR spectrum of control DL-lactonitrile (Sigma-Aldrich, 69830), while Figure 4.13b shows the ^{1}H QNMR of synthesised DL-lactonitrile. Figure 13c shows the spectrum of the DMSO-*d6* only and Figure 13d shows the spectrum of 37 % HCl. From visual inspection, when comparing Figures 13a and 13b, we can confirm that the isolated product was DL-lactonitrile. The insets show the J-splitting within each of the two chemically shifted signals of DL-lactonitrile. The CH_3 protons appeared around δ1.38 ppm in both samples as a doublet after coupling with the adjacent CH proton. The quartet at about δ4.54 ppm observed in both samples results from the ^{1}H nucleus of the CH group after coupling with the CH_3 protons. The number of protons responsible for the chemical shift signals within the DL-lactonitrile sample was calculated using the peak areas in Figure 4.13b. The peak area ratios of the CH and CH_3 groups were 1:3, respectively. These ratios agreed with those from the control sample. Interestingly, we noticed singlets around δ3.5 ppm and δ6.3 ppm in both DL-lactonitrile samples. These signals arose from water and one of the reactants, 37 % HCl, respectively. They were identified against the DMSO-*d6* (Figure 13c) and 37% HCl (Figure 13d) spectra. The water peak is due to moisture absorbed by DMSO-*d6* during its handling. Based on the intensity of the water peak in Figure 13b, we can see that the synthesised DL-lactonitrile contained water, which can be removed by drying.

Equation 27 was used to calculate the integral of DMF and DL-lactonitrile.

$$Integral_{DMF} = [(1.00 \div 1) + (3.48 \div 3) + (3.39 \div 3)] \div 3 = 1.10$$

and

$$Integral_{DL-lactonitrile} = [(7.05 \div 1) + (20.95 \div 3)] \div 2 = 7.02$$

The purity of synthesised DL-lactonitrile was determined using data provided in Table 4.4 and equation 28:

$$P_{DL-lactonitrile} = \frac{7.02}{1.10} \times \frac{1}{1} \times \frac{71.08}{73.09} \times \frac{4.72}{49.0} \times 99.8\,\% = 59.7\,\%$$

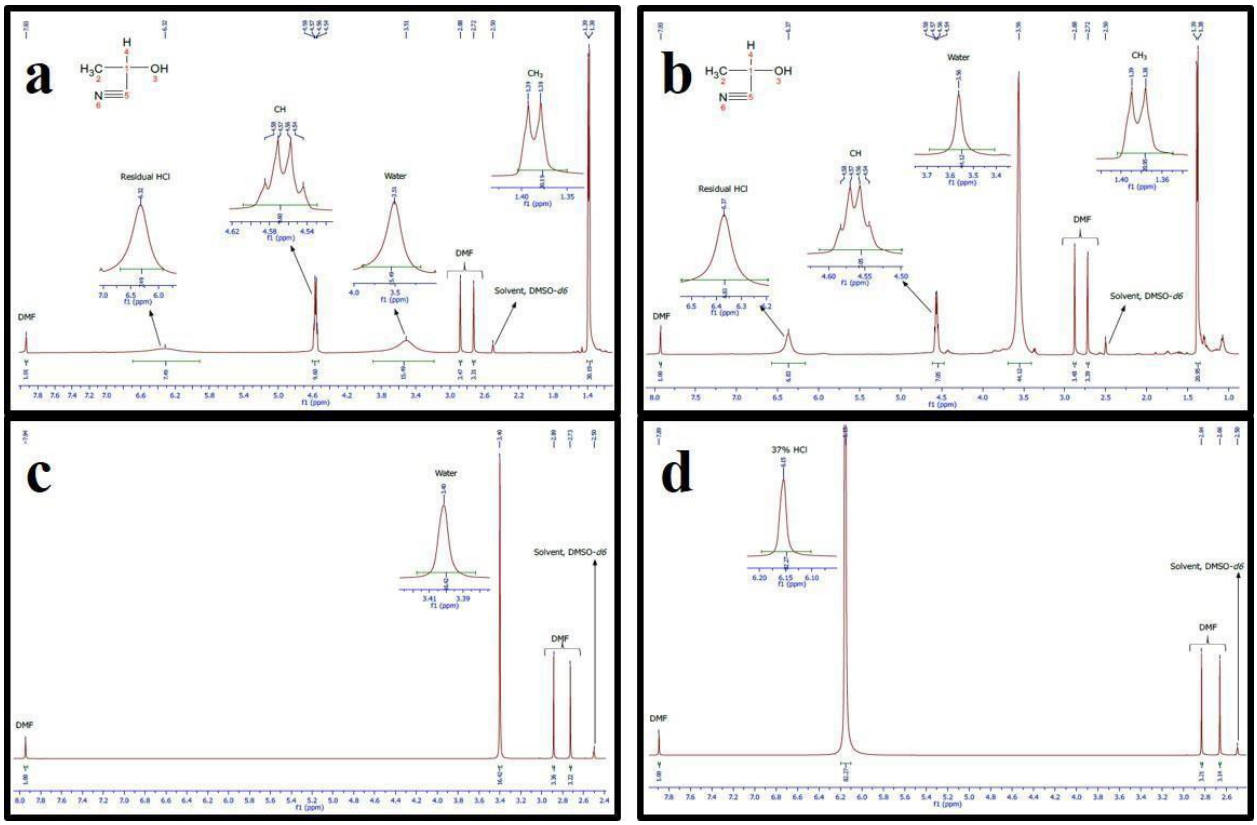

Figure 4.13: ^{1}H QNMR (500 MHz, DMSO-*d6*) spectra of (a) control DL-lactonitrile, (b) synthesised DL-lactonitrile, (c) solvent only and (d) 37% HCl

4.6.2 Hydrolysis by hydrochloric acid (Step 2)

DL-lactonitrile prepared in step 1 was hydrolysed with 8 mol/L of hydrochloric acid (HCl) to produce crude racemic lactic acid (crude DL-LA) according to the method described in section

3.2.5.2 and Figure 4.14. The amount of reactants used and product obtained are shown below in equation 23:

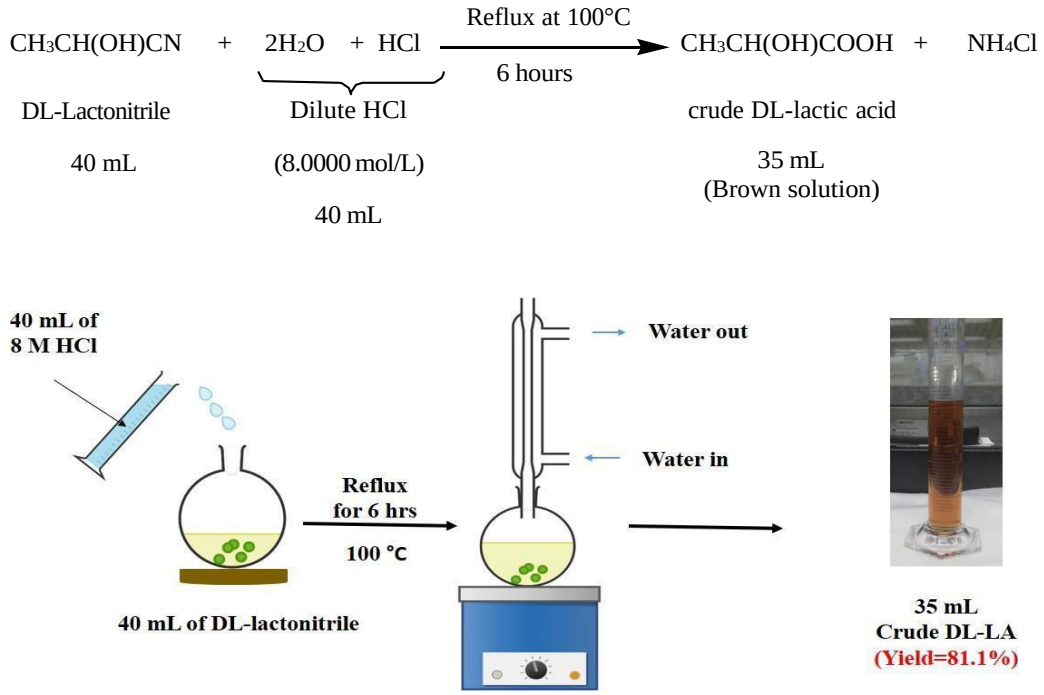

Figure 4.14: Hydrolysis of synthesised DL-lactonitrile

After cooling the resulting solution, crystallised ammonium chloride (NH_4Cl) was removed by decantation. 35 mL of DL-LA was collected, and the percentage yield was calculated using equation 21:

$$\%\ yield\ of\ DL-LA\ = \frac{35\ m\!l}{41.6\ m\!l} \times 100\ \% \ = 84.1\ \%$$

The product was isolated in 84.1 % yield and identified against a control sample bought from Sigma-Aldrich to confirm conversion of the nitrile group to the carboxylic group. The techniques used for structure confirmation were:

4.6.2.1 Attenuated total reflectance- Fourier transform infrared spectroscopy (ATR-FTIR)

The ATR-FTIR spectra of the control and crude DL-LA are shown in Figure 4.15. The control sample spectrum exhibits a single broad peak at 3385 cm^{-1}, while the synthesised sample shows two bands at 3385 and 3216 cm^{-1}. These broad bands can be attributed to OH stretching modes. In the region below 3000 cm^{-1}, both samples exhibit peaks at 2988, 2970 and 1717, 1209 and

912 cm^{-1}, respectively attributed to CH_3, CH, C=O and C-O stretches, and OH out-of-plane bend. However, some peaks were missing from the synthesised sample. Hence, it is called crude DL-LA.

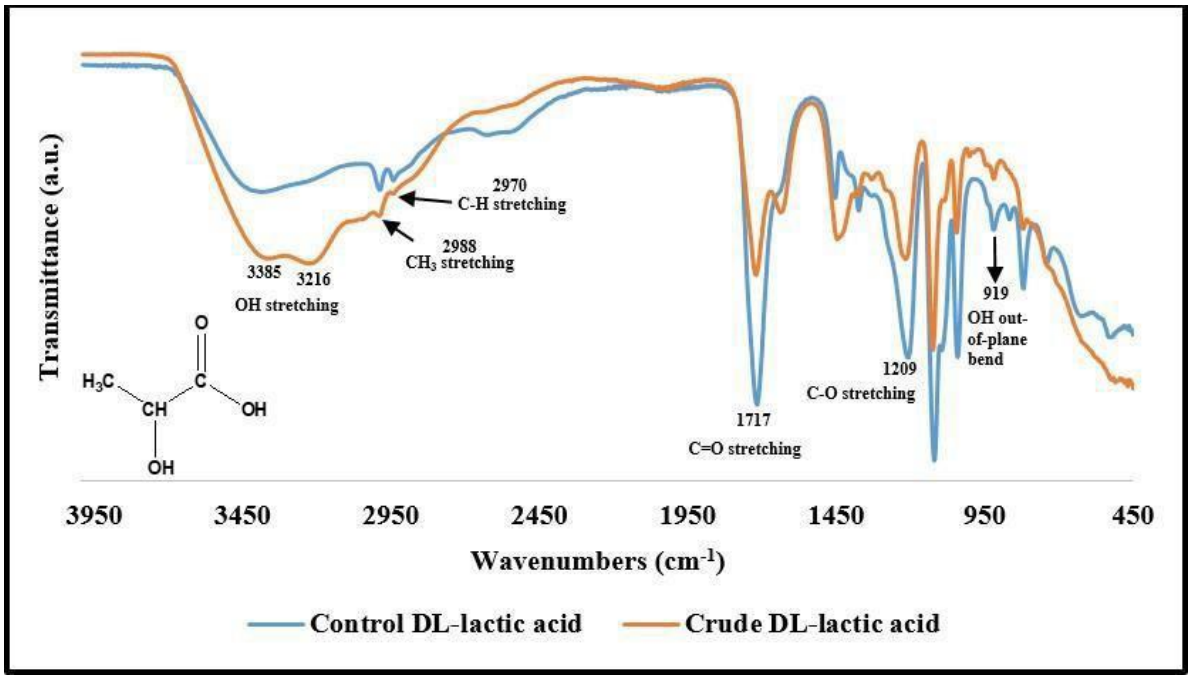

Figure 4.15: ATR-FTIR spectra of control and crude racemic lactic acid

4.6.2.2 ^{1}H Quantitative nuclear magnetic resonance (^{1}H QNMR)

Figures 4.16a and 4.16b illustrate the ^{1}H QNMR spectra of control racemic lactic acid (Sigma-Aldrich, 69785) and crude racemic lactic acid. We can say that the nitrile was successfully converted to carboxylic acid upon studying the spectra. The J-splitting of the two chemical shifts within both samples are shown in the insets. The doublet around δ1.2 ppm ensues from the CH_3 group, while the quartet around δ4.2 ppm arises from the CH group. The peak area ratios obtained from crude DL-lactic acid determined the number of protons giving rise to the chemical shift signals. These ratios were 1:3 for CH and CH_3 groups, respectively. These values were in agreement with the ratios from the control sample.

The integral of DMF and crude DL-lactic acid were determined using equation 27:

$$Integral_{crude\ DL-lactic\ acid} = [(1.31 \div 1) + (4.44 \div 3)] \div 2 = 1.40$$

and

$$Integral_{DMF} = [(1.00 \div 1) + (3.33 \div 3) + (3.28 \div 3)] \div 3 = 1.07$$

Using equation 28 and the values in Table 4.4, the purity of crude DL-lactic acid was determined as follows:

$$P_{crude\ lactic\ acid} = \frac{1.40}{1.07} \times \frac{1}{1} \times \frac{90.08}{73.09} \times \frac{4.72}{51.0} \times 99.8\,\% = 14.9\,\%$$

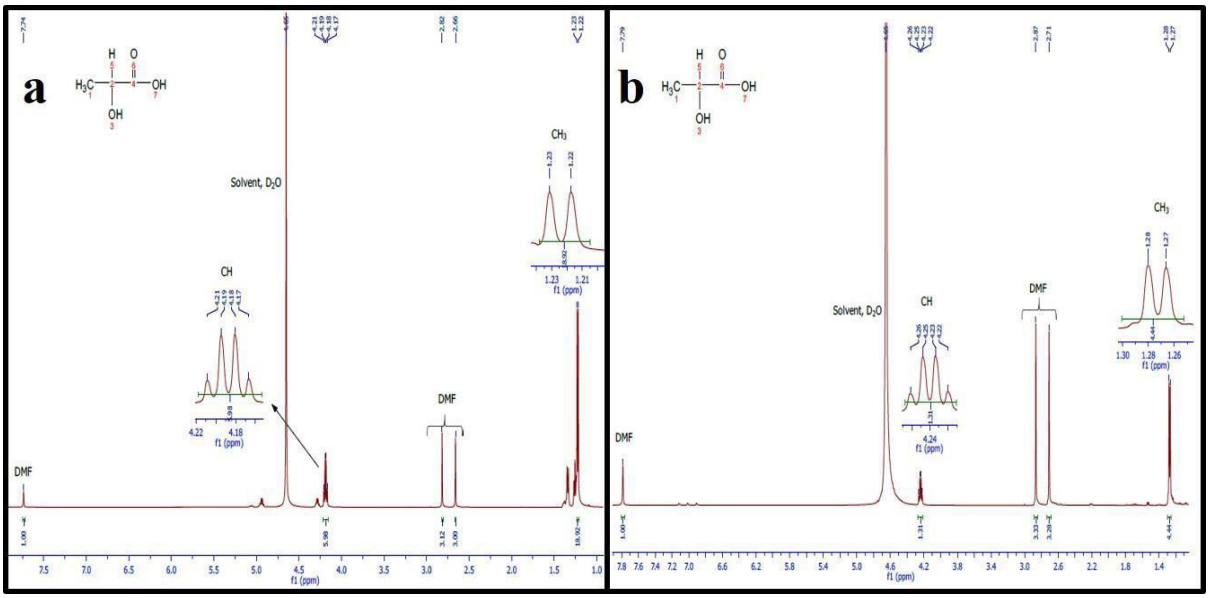

Figure 4.16: ^{1}H QNMR (500 MHz, D_2O) spectra of (a) control racemic lactic acid and (b) crude racemic lactic acid

4.6.3 Esterification (Step 3)

Crude DL-LA was purified by esterification to produce methyl-DL-lactate (methyl (±)-2-hydroxypropanoate) using the method described in section 3.2.5.3 and as shown in Figure 4.17. The amount of reactants used and product obtained are shown below in equation 24:

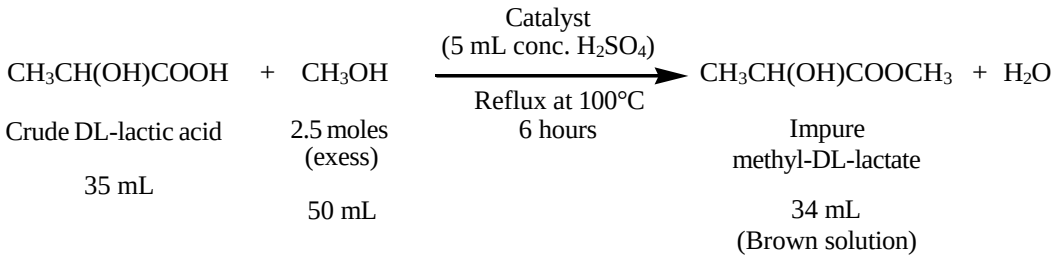

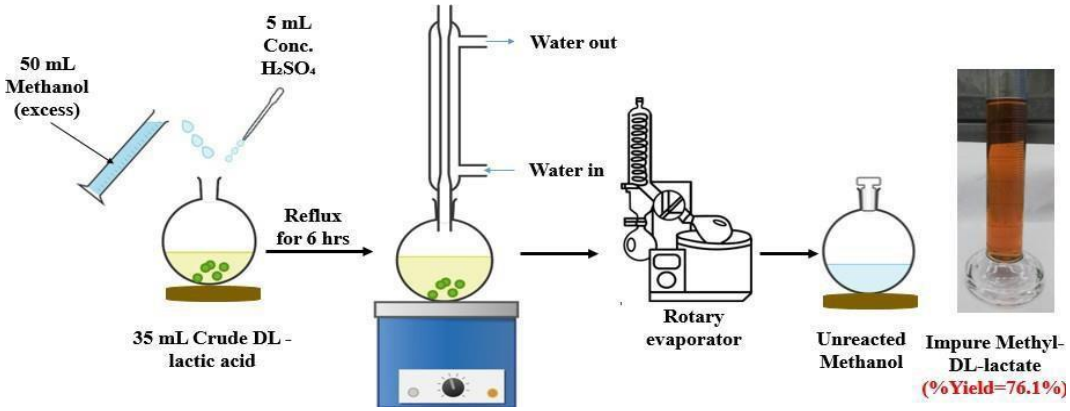

Figure 4.17: Esterification of crude racemic lactic acid

34 mL of sample was collected, representing a percentage yield of 76.1 %. The latter was calculated using equation 21:

$$\%\, yield\ of\ methyl - DL - lactate\ = \frac{34\ mL}{44.7\ mL} \times 100\ \% \ = 76.1\ \%$$

ATR-FTIR and ^{1}H QNMR were used to confirm the conversion of the carboxylic acid group to the ester group.

4.6.3.1 Attenuated total reflectance- Fourier transform infrared spectroscopy (ATR-FTIR)

Figure 4.18 displays the ATR-FTIR spectra of control and synthesised methyl-DL-lactate samples. The spectrum of the control sample shows a broad band at 3442 cm^{-1} and sharp peaks at 2985, 2955, 1732 (C=O), 1211 (OC=O) and 1124 (C-OH) cm^{-1}. The synthesised sample also had similar spectral features observed at the same wavenumbers, except for the broad band peaking at 3369 cm^{-1}. Besides these characteristic ester group peaks, the synthesised sample also exhibited small peaks at 1644, 1023 and 821 cm^{-1}.

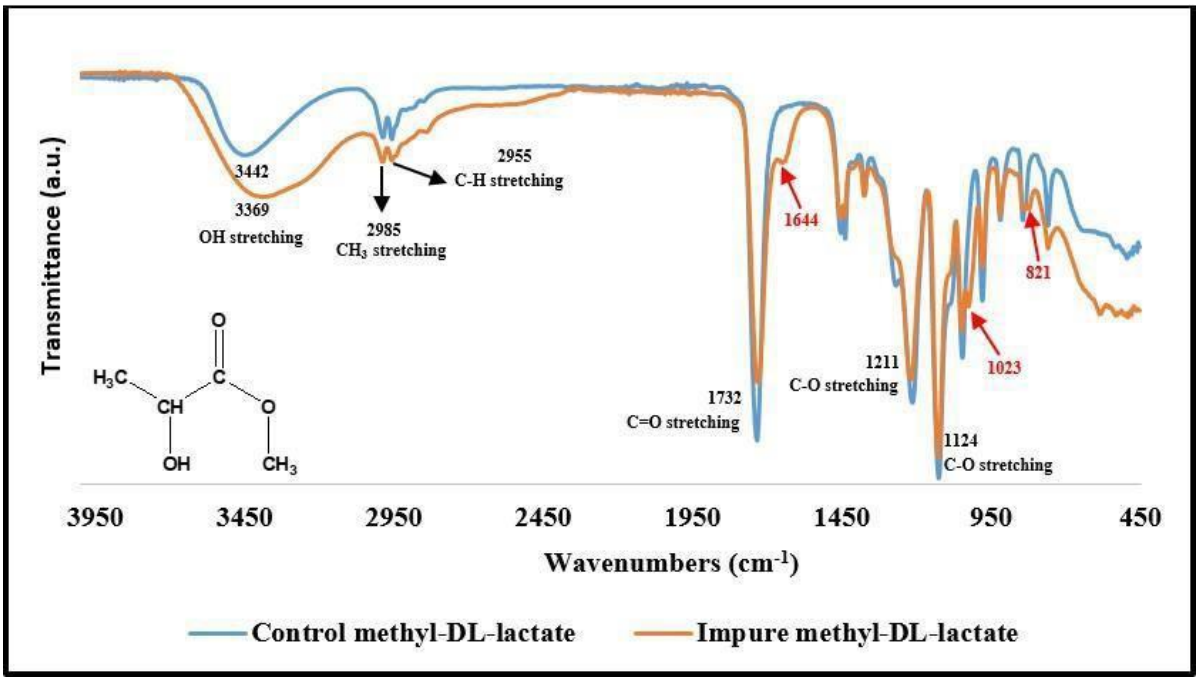

Figure 4.18: ATR-FTIR spectra of control and impure methyl-DL-lactate

This sample was purified by triple extraction with 50 mL of diethyl ether and 50 mL of Milli-Q water, followed by triple washing of the organic layer with 25 mL of saturated sodium bicarbonate solution ($NaHCO_3$) to neutralise the catalyst, sulphuric acid (H_2SO_4) (Figure 4.19).

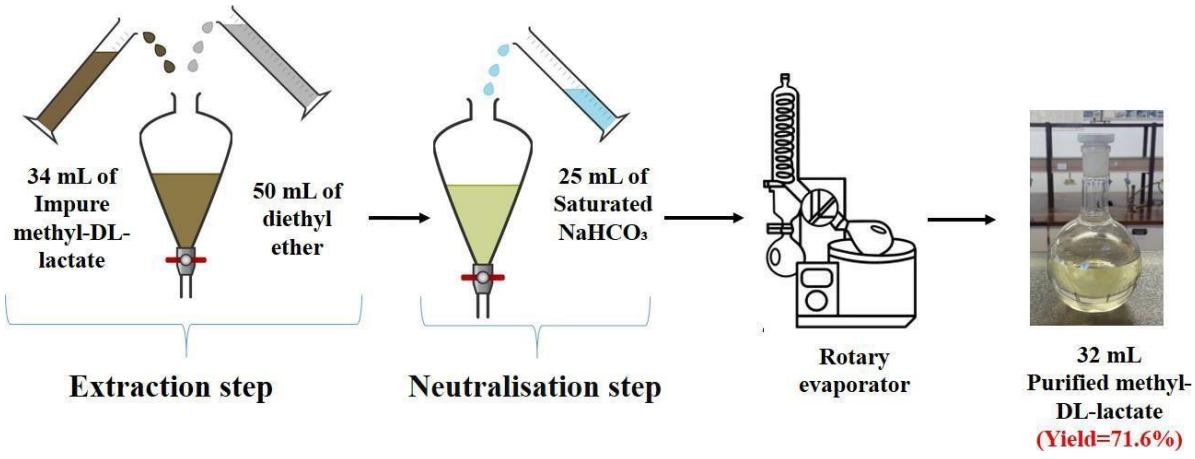

Figure 4.19: Purification of impure methyl-DL-lactate

The percentage yield of the purified methyl-DL-lactate sample, determined to be 71,6 %, was also calculated using equation 21:

$$\%\ yield\ of\ methyl-DL-lactate\ = \frac{32\ \cancel{m}}{44.7\ \cancel{m}} \times 100\ \% \ = 71.6\ \%$$

There was a 4.5 % decrease in the yield of the methyl-DL-lactate sample after its purification. This problem can be overcome by using an extraction solvent with a better distribution coefficient.

ATR-FTIR and ^{1}H QNMR verified the purity of the resulting solution against the control methyl-DL-lactate, and their spectra are shown in Figure 4.20 and Figure 4.21c, respectively. From the results observed in the former Figure, only the band peaking at 1638 cm^{-1} still appeared on the synthesised sample as opposed to the additional three peaks observed in Figure 4.18.

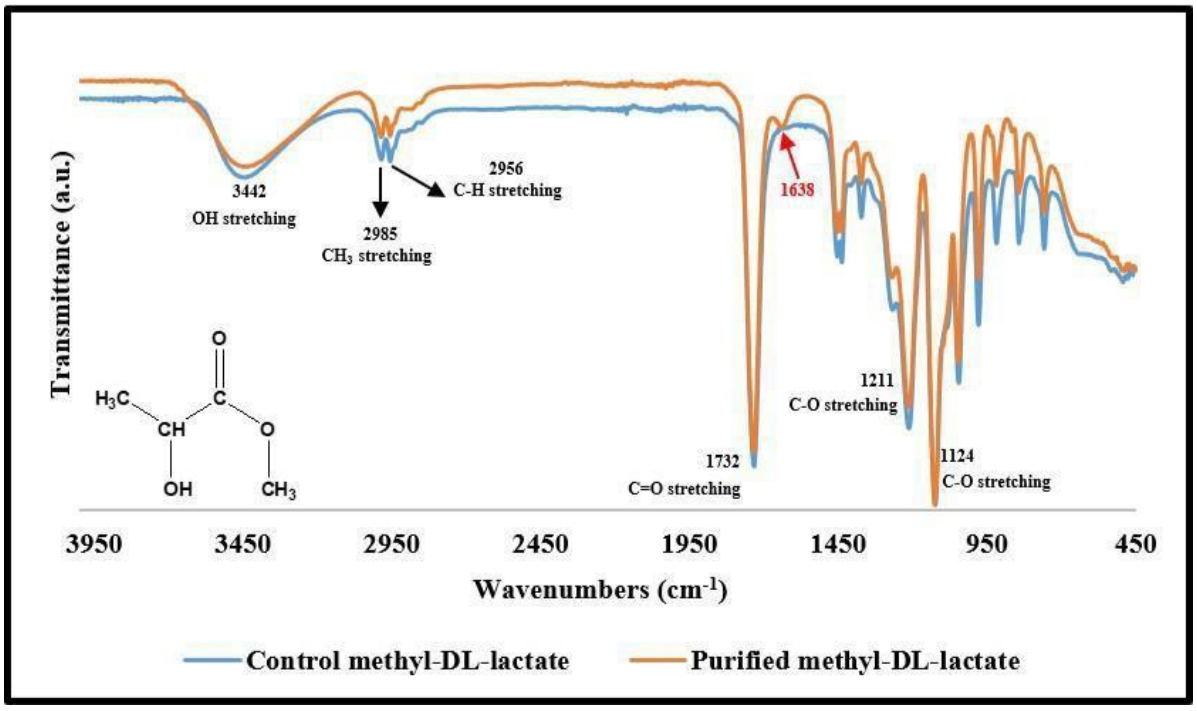

Figure 4.20: ATR-FTIR spectra of control and purified methyl-DL-lactate

4.6.3.2 ^{1}H Quantitative nuclear magnetic resonance (^{1}H QNMR)

The ^{1}H NMR spectra of control, impure and purified methyl-DL-lactate are shown in Figures 4.21a, 4.21b and 4.21c, respectively. Figure 4.21 clearly shows formation of a new signal around 3.6 ppm. This chemical shift confirms the conversion of the carboxylic group to ester. The doublet around δ1.2 ppm arises from the $CH_{3\ (1)}$ group adjacent to the CH group, while the singlet around δ3.6 ppm arises from the methoxy group (OCH_3) within the methyl-DL-lactate molecule. The quartet around δ4.2 ppm emanates from the CH group. This split was caused by the neighbouring $CH_{3\ (1)}$ group. However, the singlet around δ3.2 ppm arises from methanol,

one of the reactants in the synthesis process. This major impurity was observed in the NMR of all three methyl-DL-lactate samples. Its highest concentration was observed in the impure sample (5.1 %), followed by the purified sample (3.4 %), and the lowest content was in the control sample (1.6 %). The methanol content in the purified sample can be distilled off to reduce its concentration. The peak areas in Figures 4.21b and 4.21c were used to calculate the number of protons causing the chemical shift signals within the respective methyl-DL-lactate sample. The peak area ratios between CH, $CH_{3\ (1)}$ and $CH_{3\ (8)}$ groups from the impure sample were 1:3:2, respectively. These peak ratios do not agree with the expected ratio of 1:3:3. This discrepancy can be due to impurities. On the other hand, the peak area ratios between the groups from the purified sample agreed with the expected values.

The integral of DMF and purified methyl-DL-lactate were determined using equation 27:

$$Integral_{purified\ methyl-DL-lactate} = [(3.95 \div 1) + (10.87 \div 3) + (13.76 \div 3)] \div 3 = 4.05$$

and

$$Integral_{DMF} = [(1.00 \div 1) + (3.36 \div 3) + (3.18 \div 3)] \div 3 = 1.06$$

The purity of purified methyl-DL-lactate was calculated based on the data displayed in Table 4.4 using equation 28:

$$P_{purified\ methyl-DL-lactate} = \frac{4.05}{1.06} \times \frac{1}{1} \times \frac{104.10}{73.09} \times \frac{4.72}{55.6} \times 99.8\ \% = 46.1\ \%$$

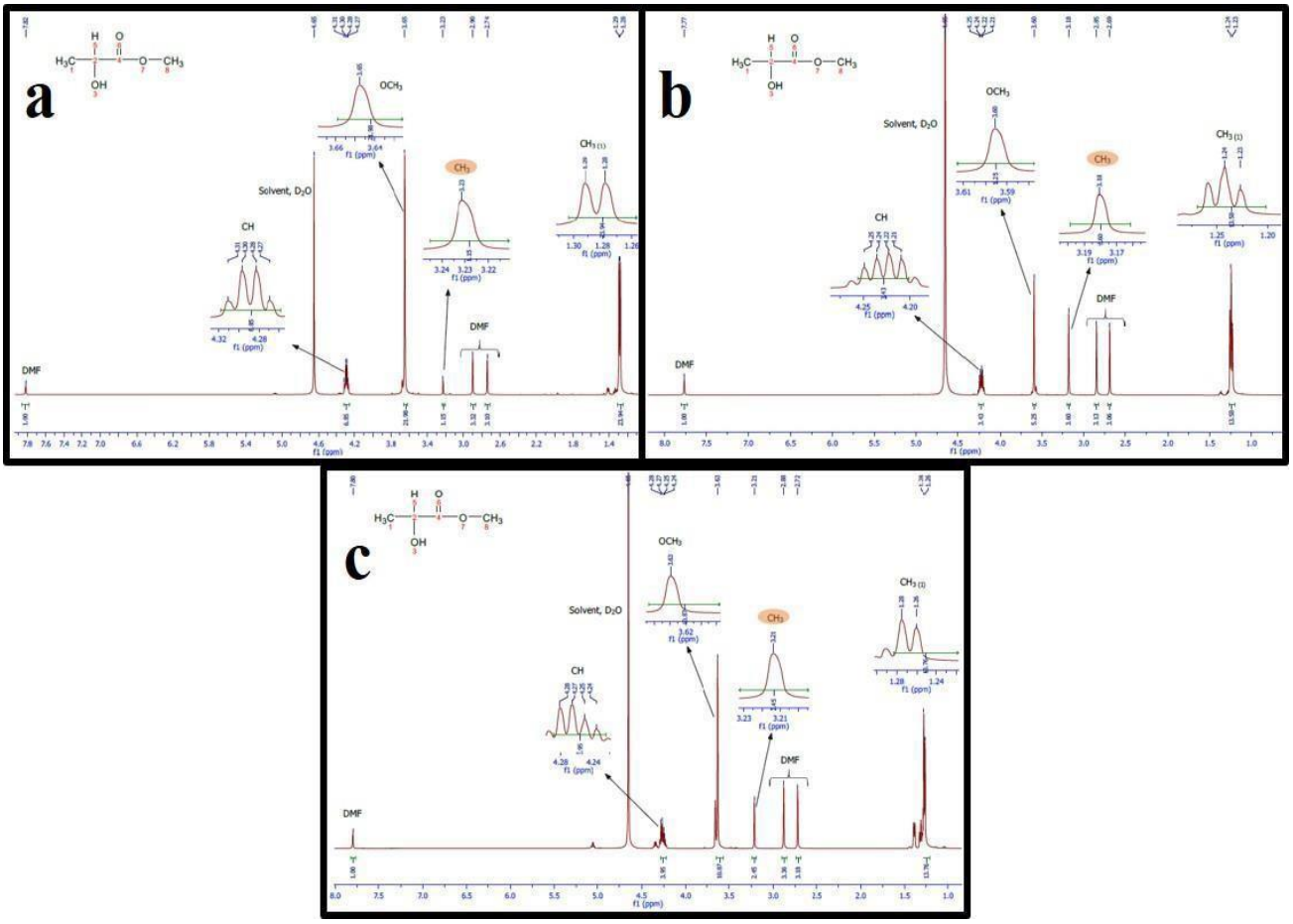

Figure 4.21: ^{1}H QNMR (500 MHz, D_2O) Spectra of (a) control methyl-DL-lactate, (b) impure methyl-DL-lactate and (c) purified methyl-DL-lactate

4.6.4 Hydrolysis by acidified water (Step 4)

The method described in section 3.5.2.4 and Figure 4.22 was used to hydrolyse the purified methyl-DL-lactate with acidified Milli-Q water to produce pure racemic lactic acid (pure DL-LA) and methanol. The latter was removed and recycled back in the synthesis process. The amount of reactants used and product obtained are shown below in equation 25:

$$\underset{\substack{\text{Purified}\\ \text{methyl-DL-lactate}\\ 32\text{ mL}}}{CH_3CH(OH)COOCH_3} + \underset{\substack{2.5\text{ moles}\\ \text{(exess)}\\ 20\text{ mL}}}{H_2O} \xrightarrow[\substack{\text{Reflux at 100°C}\\ \text{6 hours}}]{\substack{\text{Catalyst}\\ \text{(5 mL conc. } H_2SO_4\text{)}}} \underset{\substack{\text{Pure DL-lactic acid}\\ 22\text{ mL}\\ \text{(Light brown solution)}}}{CH_3CH(OH)COOH} + CH_3OH$$

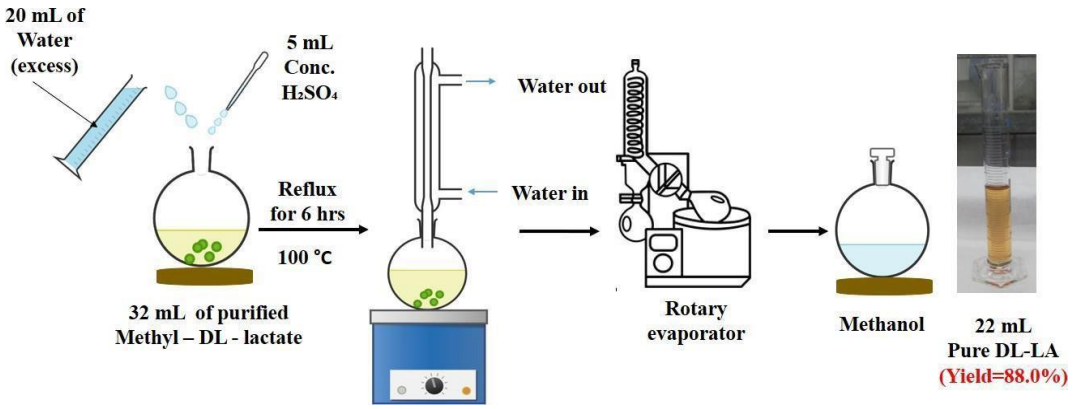

Figure 4.22: Hydrolysis of purified methyl-DL-lactate with acidified water

22 mL of pure racemic lactic acid, representing a percentage yield of 88.0 %, was collected. The latter was calculated from equation 21:

$$\%\ yield\ of\ synthesised\ racemic\ lactic\ acid\ = \frac{22\ \cancel{mL}}{25.0\ \cancel{mL}} \times 100\ \%\ = 88.0\ \%$$

The overall % yield associated with this four-step synthesis process was determined using equation 26:

$$overall\ \%\ yield = (0.811\ \times 0.841\ \times 0.716\ \times 0.880) \times 100\ \%\ = 43.0\ \%$$

4.6.4.1 Attenuated total reflectance- Fourier transform infrared spectroscopy (ATR-FTIR)

Figure 4.23 illustrates the ATR-FTIR spectra of control and purified DL-LA. The purified DL-LA spectrum displays similar spectral features as the control sample at 3385, 2986, 2970, 1717, 1216 and 916 cm^{-1} as opposed to the spectrum of crude DL-LA showed in Figure 4.17, which had an extra broad band above 3000 cm^{-1} and some missing peaks below 1450 cm^{-1}. Therefore, it can be concluded that the crude DL-LA sample was successfully purified after synthesis with sodium cyanide prepared using hydrogen cyanide extracted from cassava leaves.

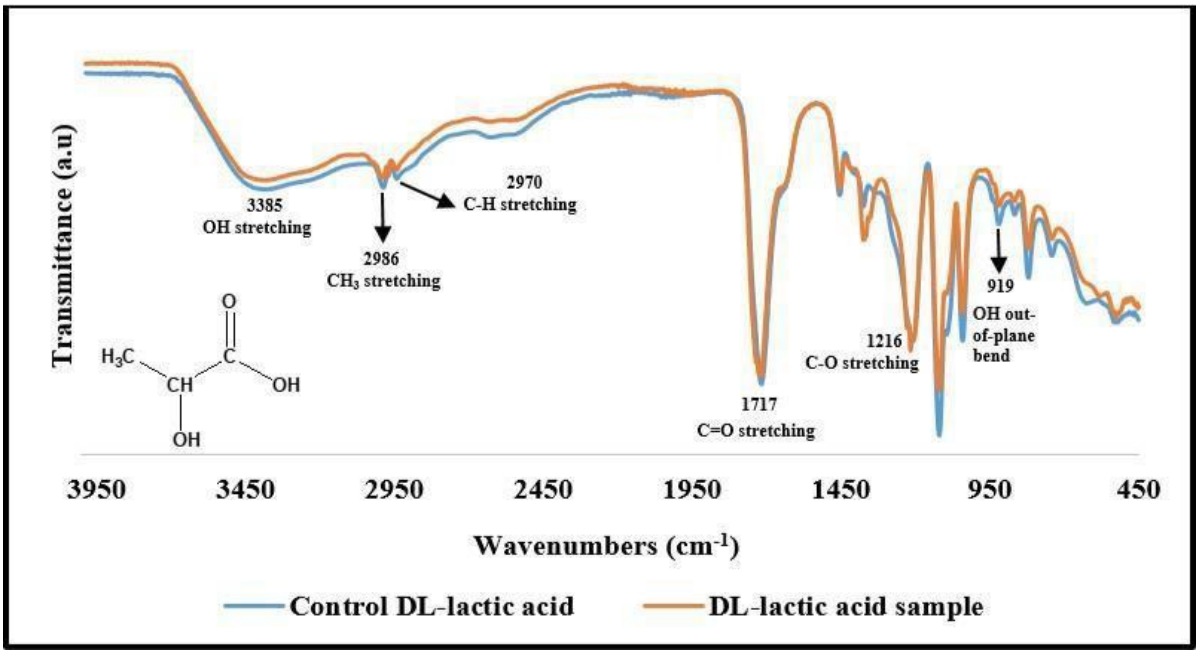

Figure 4.23: ATR-FTIR spectra of control and pure racemic lactic acid

The ATR-FTIR spectra of control and recovered methanol are shown in Figure 4.24. The spectrum of control methanol shows OH stretching and bending vibrations at 3309 and 625 cm^{-1}, respectively. It also displayed bands peaking at 2942 and 1022 cm^{-1}, attributed to CH_3 and C-O stretches. The recovered methanol exhibited similar spectral features, with the OH bend peaking at 613 cm^{-1}.

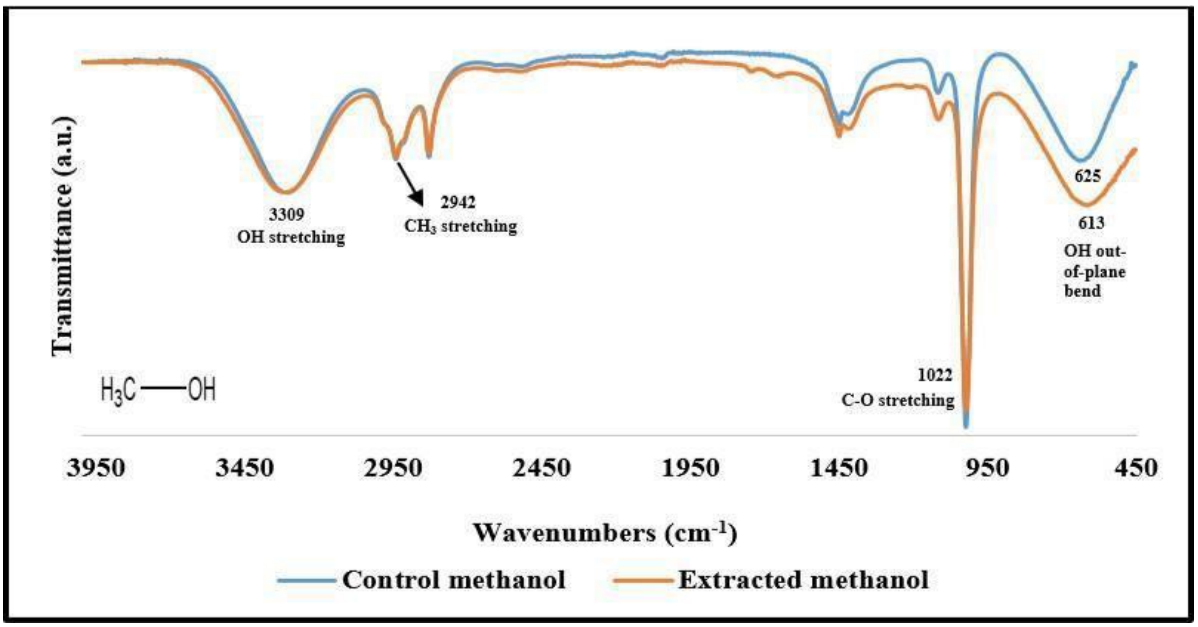

Figure 4.24: ATR-FTIR spectra of control and recovered methanol

4.6.4.2 ^{1}H Quantitative nuclear magnetic resonance (^{1}H QNMR)

Figure 4.25 shows the ^{1}H NMR spectrum of synthesised racemic lactic acid. The disappearance of the singlet observed around δ3.6 ppm in Figure 4.21 confirms the conversion of the ester group to carboxylic acid. However, the small amount of methyl-DL-lactate present in synthesised racemic lactic acid was identified by the small singlet observed at δ3.55 ppm arising from the methoxy group (OCH_3). The peak areas ratios of CH and CH_3 groups within the target analyte were 1:3, respectively.

The integral of DMF and synthesised DL-lactic acid were determined using equation 27:

$$Integral_{synthesised\ DL-lactic\ acid} = [(5.96 \div 1) + (18.91 \div 3)] \div 2 = 6.13$$

and

$$Integral_{DMF} = [(1.00 \div 1) + (3.30 \div 3) + (3.22 \div 3)] \div 3 = 1.06$$

Using equation 28 and the data in Table 4.4, the purity of synthesised DL-lactic acid was calculated:

$$P_{Synthesised\ racemic\ lactic\ acid} = \frac{6.13}{1.06} \times \frac{1}{1} \times \frac{90.08}{73.09} \times \frac{4.72}{59.9} \times 99.8\,\% = 56.0\,\%$$

From the calculated purity values from steps 2 and 4, we can see that we successfully purified the crude racemic lactic acid produced using the methods described in sections 3.5.2.3 and 3.5.2.4.

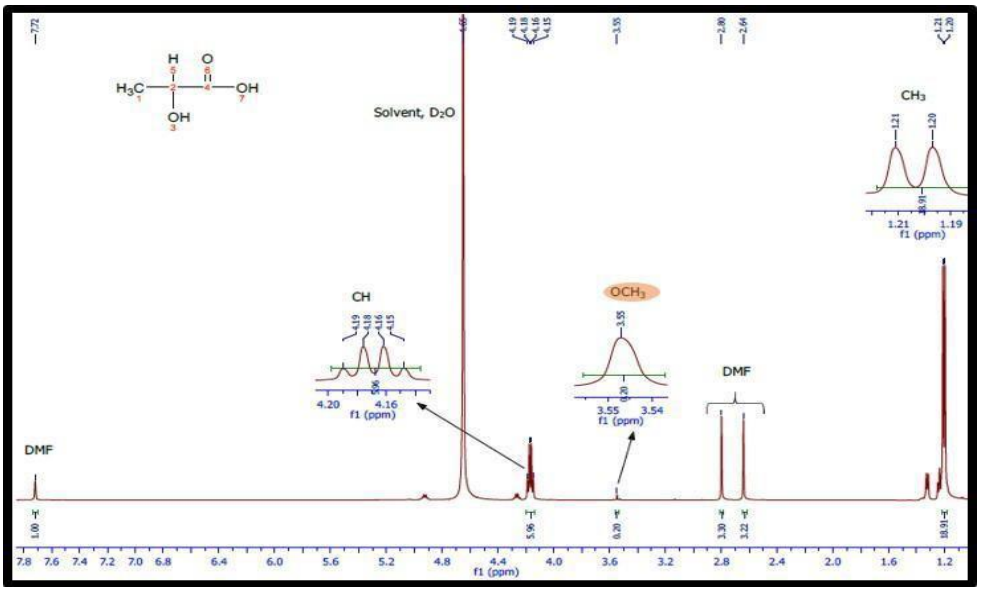

Figure 4.25: ^{1}H QNMR (500 MHz, D_2O) spectrum of synthesised racemic lactic acid

Methanol extracted from step 4 was also analysed by ^{1}H NMR (Figure 4.26b) to determine its suitability for reuse in the esterification process (step 3). We could see that it contained trace level of methyl-DL-lactate, identifiable from the doublet around δ1.2 ppm and the singlet around δ3.6 ppm. The chemical shift arising from the CH_3 group within extracted methanol was identified by comparing its spectrum to that of control methanol (Figure 4.26a). This group gave rise to a singlet around δ3.2 ppm.

The integral of DMF was determined using equation 27:

$$Integral_{DMF} = [(1.00 \div 1) + (3.43 \div 3) + (3.24 \div 3)] \div 3 = 1.07$$

The purity of extracted methanol was determined using equation 28:

$$P_{extracted\ methanol} = \frac{36.08}{1.07} \times \frac{1}{3} \times \frac{32.04}{73.09} \times \frac{4.72}{43.5} \times 99.8\% = 53.4\ \%$$

Therefore, based on the above information, we can say that extracted methanol can be safely reused in the racemic lactic acid synthesis process without worrying about cross-contamination.

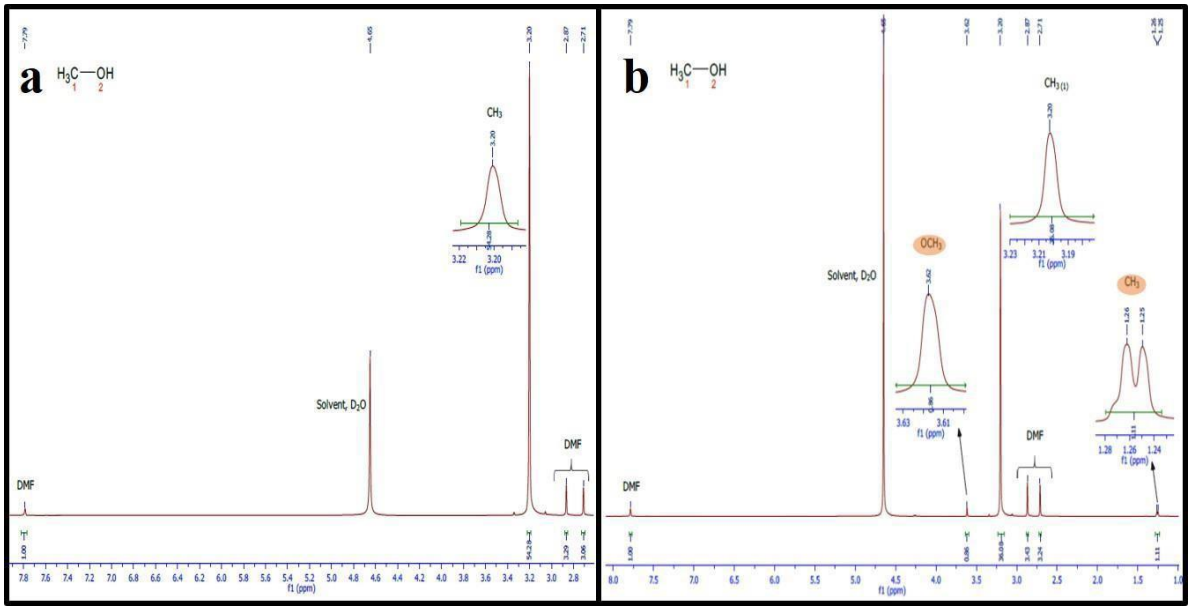

Figure 4.26: ^{1}H QNMR (500 MHz, D_2O) spectra of (a) control methanol and (b) extracted methanol

CHAPTER 5: CONCLUSIONS AND RECOMMENDATIONS

5.1 Conclusions

Hydrogen cyanide (HCN), a clear poisonous liquid or gas, can either be synthetically prepared or naturally produced. All the hydrogen cyanide used is synthetically manufactured and relies on diminishing fossil fuel resources for its preparation. Hence, this study aimed to produce HCN from a natural resource, such as cassava leaves and then use it to prepare racemic lactic acid through the chemical process.

Due to the importance of the extraction process, an attempt was made to identify the optimum extraction conditions for the complete release of HCN from cassava leaves. For this purpose, three parameters studied in quadruplicate were considered. For the first parameter, four maceration times (60, 120, 180 and 240 minutes) were studied. The second parameter to be investigated was maceration temperature, and three different temperatures (30 °C, 37 °C and 40 °C) were considered. The last parameter to be studied was the recovery time of the released hydrogen cyanide under a vacuum at 35 °C – 40 °C. Three different times (30, 45 and 60 minutes) were investigated. From the obtained results, the optimum conditions for achieving the complete release and volatilisation of HCN extracted from cassava leaves were maceration for 120 minutes at 30 °C, followed by 45 minutes of HCN recovery at 35 °C – 40 °C under vacuum. These optimum extraction parameters were used in this research to saturate the NaOH absorbing solution with released HCN and prepare a NaCN solution with a final concentration of 4.0421 mol/L.

The determination of HCN concentration during the saturation process necessitated this compound's precise detection and quantification. Among different analysis methods, alkaline titration and alkaline picrate methods were compared. Based on the reproducibility and reliability results of four standard samples (10, 40, 100 and 400 µg/mL) tested in quadruplicate, alkaline picrate method was selected to quantify HCN in the NaOH absorbing solution. The alkaline picrate method was chosen as the most effective method for the determination of HCN because its tcalculated values ($-3.184_{(10\mu g/mL)}$, $1.796_{(40\mu g/mL)}$, $2.786_{(100\mu g/mL)}$ and $2.479_{(400\mu g/mL)}$) were found to be smaller than tcritical value (3.182) at 95 % confidence level and 3 degrees of freedom. On the other hand, the alkaline titration method was rejected for cyanide

determination because its tcalculated values ($5.380_{(10\mu g/mL)}$, $8.090_{(40\mu g/mL)}$, $7.326_{(100\mu g/mL)}$ and $7.014_{(400\mu g/mL)}$) were found to be greater than tcritical value.

In addition, the amounts of sodium carbonate (Na_2CO_3) and residual sodium hydroxide (NaOH) present in control and green NaCN salt were determined by the indicator method against standardised 0.01 mol/L hydrochloric acid (HCl). Na_2CO_3 and residual NaOH concentrations were 0.72 % and 2.61 % in the control sample and 2.49 % and 4.20 % in the green NaCN sample. The reported amount of Na_2CO_3 in green NaCN solution (distillate solution) was determined after reducing its concentration by the freezing out carbonates method. This method involves cooling the sample to temperatures close to 0 °C (1 °C – 4 °C) to crystallise Na_2CO_3.

79.241 g of NaCN crystals (0.19 % yield, green NaCN) were obtained after drying the prepared NaCN solution at 100 °C. This amount was prepared from 42.750 Kg of fresh cassava leaves. A comparative study was done between green NaCN and control NaCN to confirm the identity, purity, and crystal structure of the synthesised sample. The purity and identity of green NaCN were verified using XRD, ATR-FTIR and EDS techniques, while its cubic crystal form was corroborated by SEM analysis. All four techniques revealed the presence of Na_2CO_3 as an impurity in both samples, as is the case with NaCN prepared by the neutralisation method. EDS of the standard sample also revealed the presence of aluminium as an impurity, while ATR-FTIR of green NaCN showed that it contained more Na_2CO_3 (2.49 %) than the control sample (0.72 %). The high residual NaOH content of green NaCN (4.20 %) could have favoured the formation of more carbonates by reacting with atmospheric air during the drying process, done in an air oven.

Green NaCN (62.190 g in 150 mL of Milli-Q water) was used to generate HCN in situ. The released HCN was reacted with acetaldehyde (75 mL) in the presence of 37 % HCl (100 mL) to give DL-lactonitrile (73 mL, 81.1 % yield, 59.7 % pure). Crude racemic lactic acid (35 mL, 84.1 % yield, 14.9 % pure) was obtained by hydrolysing DL-lactonitrile (40 mL) with 8 mol/L HCl (40 mL). Esterification of crude racemic lactic acid (35 mL) with excess methanol (50 mL) gave methyl-DL- lactate (32 mL, 71.6 % yield, 46.1 % pure). Concentrated sulphuric acid (5 mL) was used as a catalyst. The lactate (32 mL) was hydrolysed with excess water (20 mL) in the presence of concentrated sulphuric acid (5 mL) to give pure racemic lactic acid (22 mL, 88.0 % yield, 56.0 % pure). Hence, the overall yield of this multistep synthesis process was

43.0 %. ATR-FTIR and ^{1}H QNMR techniques were used to determine the product's identity obtained at each synthesis step. ^{1}H QNMR was also used to determine their purity with DMF as the internal standard.

In conclusion, albeit the poor yield associated with green NaCN production, HCN was successfully extracted from cassava leaves with minimal impurities using the extraction protocol established in this research. Hence, allowing its use in the chemical synthesis of racemic lactic acid.

5.2 Recommendations

In future work, it will be necessary to use cassava variety high in HCN (bitter cassava) or another cyanogenic plant with high HCN content, such as bamboo shoot (1000 to 8000 mg HCN/Kg), apricot kernel (49 to 4000 mg HCN/Kg) to improve NaCN yield. Furthermore, since NaCN was prepared by the neutralisation method, care must be taken to limit the contact time between the absorbing solution and atmospheric air to avoid the formation of more carbonate impurities. The formation of carbonate impurities can also be curbed by continuing the saturation process well past the first plateauing of the NaCN concentration, thus considerably reducing the amount of residual NaOH. This research also suggests that it is possible to transform the once fossil fuel-based chemical process into a cost-effective and environmentally friendly process if bioacetaldehyde, now produced at an industrial scale by Sekab, is used. This research will also provide an avenue to use naturally produced HCN as green NaCN to manufacture other valuable chemicals.

REFERENCES

(CONTAM), E. P. o. C. i. t. F. C., Schrenk, D., Bignami, M., Bodin, L., Chipman, J. K., Mazo, J. d., Grasl-Kraupp, B., Hogstrand, C., Hoogenboom, L. R., Leblanc, J.-C., Nebbia, C. S., Nielsen, E., Ntzani, E., Petersen, A., Sand, S., Vleminckx, C., Wallace, H., Benford, D., Brimer, L., Mancini, F. R., Metzler, M., Viviani, B., Altieri, A., Arcella, D., Steinkellner, H. and Schwerdtle, T. 2019. Evaluation of the health risks related to the presence of cyanogenic glycosides in foods other than raw apricot kernels. *EFSA JOURNAL,* 17**,** 5662.

(DAFF), D. P. P. 2010. Cassava - Production guideline *In:* Agriculture, F. a. F. (ed.). Pretoria, South Africa: Department of Agriculture, Forestry and Fisheries.

(EFSA), E. F. S. A. 2007. Opinion of the Scientific Panel on contaminants in the food chain [CONTAM] related to cyanogenic compounds as undesirable substances in animal feed. *EFSA Journal,* 434**,** 1-67.

(FAO), F. a. A. O. o. t. U. N. November 2018. Food Outlook-Biannual Report on Global Food Markets. Rome.

Abass, A. B., Towo, E., Mukuka, I., Okechukwu, R., Ranaivoson, R., Tarawali, G. and Kanju, E. 2014. Growing cassava : A training manual from production to postharvest. Ibadan, Nigeria: International Institute of Tropical Agriculture (IITA).

Abdel-Rahman, M. A. and Sonomoto, K. 2016. Opportunities to overcome the current limitations and challenges for efficient microbial production of optically pure lactic acid. *Journal of Biotechnology,* 236**,** 176-92.

Abdel-Rahman, M. A., Tashiro, Y. and Sonomoto, K. 2013. Recent advances in lactic acid production by microbial fermentation processes. *Biotechnology Advances,* 31**,** 877-902.

Abdullahi, N., Sidik, J. B., Ahmed, O. H. and Zakariah, M. H. 2014. Effect of planting methods on growth and yield of cassava (Manihot esculenta Crantz) grown with polythene-covering. *Journal of Experimental Biology and Agricultural Sciences,* 1**,** 480-487.

Abraham, K., Buhrke, T. and Lampen, A. 2016. Bioavailability of cyanide after consumption of a single meal of foods containing high levels of cyanogenic glycosides: a crossover study in humans. *Archives of Toxicology,* 90**,** 559-574.

Achi, C. G., Hassanein, A. and Lansing, S. 2020. Enhanced Biogas Production of Cassava Wastewater Using Zeolite and Biochar Additives and Manure Co-Digestion. *Energies,* 13**,** 491.

Acosta, H. L., Stelnicki, E. J., Rodriguez, L. and Slingbaum, L. A. 2005. Use of absorbable poly (d,l) lactic acid plates in cranial-vault remodeling: presentation of the first case and lessons learned about its use. *Cleft Palate–Craniofacial Journal,* 42**,** 333-339.

Adeleke, B. S., Olaniyi, O. O. and Akinyele, B. J. 2017. Isolation and screening of bacteria associated with fermented cassava peels for linamarase production. *International Journal of Applied Microbiology and Biotechnology Research,* 5**,** 20-26.

Adetunji, A., Isadare, D., Akinluwade, K. and Adewoye, O. 2015. Waste-to-Wealth Applications of Cassava–A Review Study of Industrial and Agricultural Applications. *Advances in Research,* 4**,** 212-229.

Afuye, G. G. and MogajI, K. O. 2015. Effect of cassava effluents on domestic consumption of 'shallow well' water in Owo Local Government Area, Ondo State. *Physical Sciences Research International,* 3**,** 37-43.

Akinluwade, K., Rominiyi, A., Isadare, D., Adetunji, A. and Adeoye, M. 2018. Pack-cyaniding: A Comparative Study of Low and High-Temperature Treatment. *Archives of Current Research International,* 12**,** 1-12.

Akoetey, W. 2015. *Direct Fermentation of Sweet Potato Starch into Lactic Acid by Lactobacillus amylovorus: The Prospect of an Adaptation Process.* Master of Science in Food science, University of Arkansas.

Ameen, S. M. and Caruso, G. 2017. The Importance of Lactic Acid in the Current Food Industry. An Introduction. *In:* Ameen, S. M. andCaruso, G. (eds.) *Lactic Acid in the Food Industry.* Italy: Springer.

Amelework, A. B., Bairu, M. W., Maema, O., Venter, S. L. and Laing, M. 2021. Adoption and Promotion of Resilient Crops for Climate Risk Mitigation and Import Substitution: A Case Analysis of Cassava for South African Agriculture. *Frontiers in Sustainable Food Systems,* 5**,** 1-14.

Anhwange, B. A., Asemave, K., Ikyenge, B. A. and Oklo, D. A. 2011. Hydrogen Cyanide Content of Manihort Utilissima, Colocasia Esculenta, Dioscorea Bulbifera and Dioscorea Domentorum Tubers Found in Benue State. *International Journal of Chemistry,* 3**,** 69-71.

Araújo, F. d. C. B. d., Moura, E. F., Cunha, R. L., Neto, J. T. d. F. and Silva1, R. d. S. 2019. Chemical root traits differentiate 'bitter' and 'sweet' cassava accessions from the Amazon. *Crop Breeding and Applied Biotechnology,* 19**,** 77-85.

Arévalo, A. T. V. 2019. *Biological degradation of cyanide using native bacteria isolated from a cassava-processing effluent.* Master in Science, Escola Politécnica da Universidade de São Paulo.

Asterion, A. 2016. Carbonates in the Plating Bath. Available from: https://asterionstc.com/2016/06/carbonates-plating-bath/ 2021].

Attahdaniel, E., Ebisike, K., Adeeyinwo, C. E., Adetunji, A. R. and Samuel Olugbenga O Olusunle Adewoye, O. O. 2013. Production of Sodium Cyanide from Cassava Wastes. *International Journal of Science and Technology,* 2**,** 707-709.

Attahdaniel, E., P. O. Enwerem, P. G. Lawrence, C. U. Ofiwe , Olusunle, S. O. O. and Adetunji, A. R. 2020. Green synthesis and characterization of sodium cyanide from cassava (*Manihot esculenta* CRANTZ). *FUW Trends in Science & Technology Journal,* 5**,** 247-251.

Barthet, V. J. and Bacala, R. 2010. Development of optimized extraction methodology for cyanogenic glycosides from flaxseed (*Linum usitatissimum*). *Journal of AOAC International,* 93**,** 478-484.

Basu, S., Bose, C., Ojha, N., Das, N., Das, J., Pal, M. and Khurana, S. 2015. Evolution of bacterial and fungal growth media. *Bioinformation,* 11**,** 182-184.

Bayitse, R. 2015. Lactic Acid Production from Biomass: Prospect for Bioresidue Utilization in Ghana: Technological Review. *International Journal of Applied Science and Technology,* 5**,** 164-174.

Bayitse, R., Tornyie, F. and Bjerre, A.-B. 2017. CASSAVA CULTIVATION, PROCESSING AND POTENTIAL USES IN GHANA. *In:* Klein, C. (ed.) *Handbook on Cassava.* Nova Science Publishers, Inc.

Bhalla, T. C., Kumar, V. and Kumar, V. 2017. Microbial Remediation of Cyanides. *In:* Rathoure, D. A. K. (ed.) *Bioremediation Current Research and Applications.* 1st ed.: IK International.

Bolarinwa, I. F. 2013. *Cyanogenic Glycosides in Plant Foods.* Doctor of Philosophy, The University of Leeds.

Bolarinwa, I. F., Oke, M. O., Olaniyan, S. A. and Ajala, A. S. 2016. A Review of Cyanogenic Glycosides in Edible Plants. *In:* Soloneski, S. andLarramendy, M. L. (eds.) *Toxicology - New Aspects to This Scientific Conundrum.* London: IntechOpen.

Boontawan, P. 2010. *Development of lactic acid production process from cassava by using lactic acid bacteria.* Degree of Doctor of Philosophy in Microbiology, Suranaree University of Technology.

Borandeh, S., van Bochove, B., Teotia, A. and Seppala, J. 2021. Polymeric drug delivery systems by additive manufacturing. *Advanced Drug Delivery Reviews,* 173**,** 349-373.

Brito, V. H. S., Ramalho, R. T., Rabacow, A. P. M., Moreno, S. E. and Cereda, M. P. 2009. Colorimetric method for free and potential cyanide analysis of cassava tissue. *Gene Conserve,* 8.

Britz, H. 2019. Successful Cassava Farming. Available from: https://premiumbusinessplans.co.za/successful-cassava-farming/ 2021].

Broderick, K. E., Chan, A., Balasubramanian, M., Feala, J., Reed, S. L., Panda, M., Sharma, V. S., Pilz, R. B., Bigby, T. D. and Boss, G. R. 2008. Cyanide produced by human isolates of Pseudomonas aeruginosa contributes to lethality in Drosophila melanogaster. *Journal of Infectious Diseases,* 197**,** 457-64.

Bruckner, A., Raspotnig, G., Wehner, K., Meusinger, R., Norton, R. A. and Heethoff, M. 2017. Storage and release of hydrogen cyanide in a chelicerate (*Oribatula tibialis*). *Proceedings of the National Academy of Sciences,* 114**,** 3469-3472.

Buasaengchan, S., Pengprecha, S., Vadhanasin, P., Kriengkri and Kaewtrakulpong 2019. The Reason why we can't use Cassava leaf for Commercial Purpose in Thailand. *International Journal of Innovative Technology and Exploring Engineering,* 8**,** 117-122.

Budsabathip, P. 2013. Characterization of lactic acid producing bacteria from Thai sources. *Journal of Applied Pharmaceutical Science,* 3**,** 033-038.

Burns, A., Gleadow, R., Cliff, J., Zacarias, A. and Cavagnaro, T. 2010. Cassava: The Drought, War and Famine Crop in a Changing World. *Sustainability,* 2**,** 3572-3607.

Calabia, B. P. and Tokiwa, Y. 2007. Production of D-lactic acid from sugarcane molasses, sugarcane juice and sugar beet juice by Lactobacillus delbrueckii. *Biotechnology Letters,* 29**,** 1329-32.

Caspar, J. and Spiteller, P. 2015. A Free Cyanohydrin as Arms and Armour of Marasmius oreades. *ChemBioChem,* 16**,** 570-573.

Castada, H. Z., Liu, J., Ann Barringer, S. and Huang, X. 2020. Cyanogenesis in Macadamia and Direct Analysis of Hydrogen Cyanide in Macadamia Flowers, Leaves, Husks, and Nuts Using Selected Ion Flow Tube-Mass Spectrometry. *Foods,* 9.

Chan, J. K.-F. 1985. *Synthesis of cyanohydrins EP0132320A1*. 84304395.1. 30 January 1985.

Chaouali, N., Gana, I., Dorra, A., Khelifi, F., Nouioui, A., Masri, W., Belwaer, I., Ghorbel, H. and Hedhili, A. 2013. Potential Toxic Levels of Cyanide in Almonds (*Prunus amygdalus*), Apricot Kernels (Prunus armeniaca), and Almond Syrup. *International Scholarly Research Notices,* 2013**,** 610648.

Chibueze Izah, S., Bassey, S. E., Ohimain, E. I. and Contreras, J. M. 2018. Impacts of Cassava Mill Effluents in Nigeria. *Journal of Plant and Animal Ecology,* 1**,** 14-42.

Chikezie, P. C. and Ojiako, O. A. 2013. Cyanide and Aflatoxin Loads of Processed Cassava (*Manihot esculenta*) Tubers (Garri) in Njaba, Imo State, Nigeria. *Toxicology International,* 20**,** 261-267.

Cho, H. J., Do, B. K., Shim, S. M., Kwon, H., Lee, D. H., Nah, A. H., Choi, Y. J. and Lee, S. Y. 2013. Determination of cyanogenic compounds in edible plants by ion chromatography. *Toxicological Research,* 29**,** 143-147.

Choudhary, H., Nishimura, S. and Ebitani, K. 2015. Synthesis of high-value organic acids from sugars promoted byhydrothermally loaded Cu oxide species on magnesia. *Applied Catalysis B: Environmental,* 162**,** 1-10.

Chuasuwan, C. 2017. Thailand industry outlook 2017-2019: Cassava Industry. Thailand: Krungsri Research.

Coelho, L. F., Lima, C. J. B. d., Rodovalho, C. M., Bernardo, M. P. and Contiero1, J. 2011. Lactic acid production by new Lactobacillus plantarum LMISM6 grown in molasses: optimization of medium composition. *Brazilian Journal of Chemical Engineering,* 28**,** 27-36.

Cuvaca, I. B., Eash, N. S., Zivanovic, S., Lambert, D. M., Walker, F. and Rustrick, B. 2015. Cassava (Manihot esculenta Crantz) Tuber Quality as Measured by Starch and Cyanide (HCN) Affected by Nitrogen, Phosphorus, and Potassium Fertilizer Rates. *Journal of Agricultural Science,* 7**,** 36-49.

Dadfarnia, S., Haji Shabani, A. M., Tamadon, F. and Rezaei, M. 2006. Indirect determination of free cyanide in water and industrial waste water by flow injection-atomic absorption spectrometry. *Microchimica Acta,* 158**,** 159-163.

Das, S., Biswas, S., Mukherjee, S., Bandyopadhyay, J., Samanta, S., Bhowmick, I., Hazra, D. K., Ray, A. and Parui, P. P. 2014. Cyanide selective off-on fluorescent chemosensor with in-vivo imaging in 100% water: solid probe preferred over in-situ generation. *RSC Advances,* 4**,** 9656-9659.

DataMIntelligence. 2021. *Hydrogen Cyanide Market* [Online]. Available: https://www.datamintelligence.com/research-report/hydrogen-cyanide-market [Accessed 2021].

Davis, S., Murray, J. and Katsiadaki, I. 2017. Cyanide in the aquatic environment and its metabolism by fish.

de Oliveira, E. J., de Oliveira, S. A. S., Otto, C., Alicai, T., de Freitas, J. P. X., Cortes, D. F. M., Pariyo, A., Liri, C., Adiga, G., Balmer, A., Klauser, D. and Robinson, M. 2020. A novel seed treatment-based multiplication approach for cassava planting material. *PLoS One,* 15**,** e0229943.

Deepa, H. A., Raj, A. and Asha, P. 2016. Evaluation on Production and Economics of Acrylonitrile by Sohio Process. *International Journal of Engineering Research & Technology,* 4**,** 6.

Diallo, Y., Gueye, M. T., Ndiaye, C., Sakho, M., Kane, A., Barthelemy, J. P. and Lognay, G. 2014. A New Method for the Determination of Cyanide Ions and Their Quantification in Some Senegalese Cassava Varieties. *American Journal of Analytical Chemistry,* 5**,** 181-187.

Ding, Z., Zhang, Y., Xiao, Y., Liu, F., Wang, M., Zhu, X., Liu, P., Sun, Q., Wang, W., Peng, M., Brutnell, T. and Li, P. 2016. Transcriptome response of cassava leaves under natural shade. *Scientific Reports,* 6**,** 1-14.

Dong, W., Shen, Z., Peng, B., Gu, M., Zhou, X., Xiang, B. and Zhang, Y. 2016. Selective Chemical Conversion of Sugars in Aqueous Solutions without Alkali to Lactic Acid Over a Zn-Sn-Beta Lewis Acid-Base Catalyst. *Scientific Reports,* 6**,** 1-8.

Drochioiu, G., Oniscu, C., Sunel, V., Popa, K., Cuciac, C. and Cozma, D. 2003. Cyanide assay based on its novel reaction with resorcinol and picric acid. *The European Journal of Mineral Processing and Environmental Protection,* 3**,** 291-296.

Duo, J., Zhanga, Z., Yao, G., Huo, Z. and Jin, F. 2016. Hydrothermal conversion of glucose into lactic acid with sodium silicate as a base catalyst. *Catalysis Today,* 263**,** 112-116.

Dusica, I., Bojana, K., Tea, B., Radmilo, C., Djuro, V., Jovanka, L. and Slavica, S. 2012. Effect of microwave heating on content of cyanogenic glycosides in linseed. *Ratarstvo i povrtarstvo,* 49**,** 63-68.

ECETOC, E. C. f. E. a. T. o. C.-. 2007. Cyanides of Hydrogen, Sodium and Potassium, and Acetone Cyanohydrin (CAS No. 74-90-8, 143-33-9, 151-50-8 and 75-86-5). Brussels.

eGyanKosh. 2017. *UNIT 3 ACID-BASE TITRATIONS-II* [Online]. India: IGNOU. Available: https://egyankosh.ac.in/bitstream/123456789/15642/1/Unit-3.pdf [Accessed 2022].

Eiteman, M. A. and Ramalingam, S. 2015. Microbial production of lactic acid. *Biotechnology letters,* 37**,** 955-972.

Eletta, O. A. A., Ajayi, O. A., Ogunleye, O. O. and Akpan, I. C. 2016. Adsorption of cyanide from aqueous solution using calcinated eggshells: Equilibrium and optimisation studies. *Journal of Environmental Chemical Engineering,* 4**,** 1367-1375.

FRI, F. R. I. 2012. Work Package 4: Ensuring the safety and quality of processed cassava products in market-oriented production: Report on the Review of previous experiences and works on cyanogenic glycosides in cassava processing. Ghana: CSIR-FRI/NRI CASSAVA GMARKET PROJECT.

Fukushima, A. R., Nicoletti, M. A., Rodrigues, A. J., Pressutti, C., Jeandro Almeida, Brandão, T., Ito, R. K., Leoni, L. A. B. and Spinosa, H. D. S. 2016. Cassava Flour: Quantification of Cyanide Content. *Food and Nutrition Sciences,* 7**,** 592-599.

Gail, E., Gos, S., Kulzer, R., Lorösch, J., Rubo, A., Sauer, M., Kellens, R., Reddy, J., Steier, N. and Hasenpusch, W. 2011. Cyano Compounds, Inorganic. *Ullmann's Encyclopedia of Industrial Chemistry.* Wiley-VCH Verlag GmbH & Co. KGaA, Weinheim.

Gervason A, M., Ben O, O., Bibianne W, W., Edith W. T, W. and Jared M, O. 2017. Evaluation of Cyanide Levels in Two Cassava Varieties (*Mariwa* and *Nyakatanegi*) Grown in Bar-agulu, Siaya County, Kenya. *Journal of Food and Nutrition Research,* 5**,** 817-823.

Ghaffar, T., Irshad, M., Anwar, Z., Aqil, T., Zulifqar, Z., Tariq, A., Kamran, M., Ehsan, N. and Mehmood, S. 2014. Recent trends in lactic acid biotechnology: A brief review on production to purification. *Journal of Radiation Research and Applied Sciences,* 7**,** 222-229.

Ghasemi, M., Najafpour, G., Rahimnejad, M., Beigi, P. A., Sedighi, M. and Hashemiyeh, B. 2009. Effect of different media on production of lactic acid from whey by Lactobacillus bulgaricus. *African Journal of Biotechnology,* 8**,** 081-089.

Govender, K. 2015. Africa explores cassava potential. Available from: https://phys.org/news/2015-04-africa-explores-cassava-potential.html 2021].

Guédé, S. S., Traoré, S. and Brou, K. 2013. Assessment of Cyanide Content in Cassava (Manihot esculenta Crantz) Varieties and Derived Products from Senegal. *International Journal of Nutrition and Food Sciences,* 2**,** 225-231.

Gustafson, A. Y. 2015. *Wastewater to renewable energy at a tapioca factory in Vietnam. In-situ evaluation of anaerobic covered pond treating high strength industrial wastewater.* Master of Science in Engineering, Lund University.

Hayek, S. A. and Ibrahim, S. A. 2013. Current Limitations and Challenges with Lactic Acid Bacteria: A Review. *Food and Nutrition Sciences,* 04**,** 73-87.

He, T., Jiang, Z., Wu, P., Yi, J., Li, J. and Hu, C. 2016. Fractionation for further conversion: from raw corn stover to lactic acid. *Scientific Reports,* 6**,** 1-11.

Howeler, R. H. and Oates, C. G. 2000. Strategic environmental assessment: An Assessment of the Impact of Small holder Cassava Production and Processing Practices on the Environment.

Ifeabunike, O., Nwaedozie, J. and Aghanwa, C. 2017. Proximate Analysis, Hydrogen Cyanide and Some Essential Mineral Content of Sweet Cassava Variety (*Manihot utilisima*) and Bitter Cassava Variety (*Manihot palmata*) Cultivated in Kachia Local Government Area of Kaduna State, Nigeria. *International Journal of Biochemistry Research & Review,* 19**,** 1-12.

Indrastuti, Y. E., Estiasih, T., Christanti, R. A., Pulungan, M. H., Zubaedah, E. and Harijono 2018. Microbial and some chemical constituent changes of high cyanide cassava during simultant spontaneous submerged and solid state fermentation of" gadungan pohung. *International Food Research Journal,* 25**,** 487-498.

Information, N. C. f. B. 2020. *PubChem Compound Summary for CID 768, Hydrogen cyanide* [Online]. Available: https://pubchem.ncbi.nlm.nih.gov/compound/Hydrogen-cyanide [Accessed 2020].

Itoba-Tombo, E. F., Nchu, S. K. O. N. F. and Mudumbi1, J. B. 2019. Potential Challenges of Cassava Cultivation in South Africa. *16th South Africa International Conference on Agricultural, Chemical, Biological and Environmental Sciences (ACBES-19).* SOUTH AFRICA.

Izah, S. C. 2018. Estimation of Potential Cassava Mill Effluents Discharged into Nigerian Environment *Environmental Analysis & Ecology Studies,* 2**,** 189-195.

Jaszczak, E., Polkowska, Z., Narkowicz, S. and Namiesnik, J. 2017. Cyanides in the environment-analysis-problems and challenges. *Environmental Science and Pollution Research,* 24**,** 15929-15948.

Jideofor, I. M. 2015. Chemical adjustment of effluent from cassava processing plant prior to safe disposal plant prior to safe disposal. *Nigerian Journal of Technology,* 34**,** 883-889.

Jin, F. and Enomoto, H. 2008. Application of hydrothermal reaction to conversion of plant-origin biomasses into acetic and lactic acids. *Journal of Materials Science,* 43**,** 2463-2471.

Karande, R. D., Abitha, V. K., Rane, A. V. and Mishra, R. K. 2016. Journal of Materials Science and Engineering with Advanced Technology. *Journal of Materials Science and Engineering with Advanced Technology,* 12**,** 1-37.

Kishida, H., Jin, F., Yan, X., Moriya, T. and Enomoto, H. 2006. Formation of lactic acid from glycolaldehyde by alkaline hydrothermal reaction. *Carbohydrate Research,* 341**,** 2619-2623.

Klaic, R., Sallet, D., Kuhn, R. C., Salbego, P., Centenaro, G. S., Jacques, R. J. S., Guedes, V. C., Jahn, S. L. and Mazutti, M. A. 2014. Optimization of Fermentation Media for the Growth of a Fungus Used as Bioherbicide. *XX Congresso Brasileiro de Engenharia Química.*

Komesu, A., de Oliveira, J. A. R., Martins, L. H. d. S., Wolf Maciel, M. R. and Maciel Filho, R. 2017a. Lactic acid production to purification: A review. *BioResources,* 12**,** 4364-4383.

Komesu, A., Wolf Maciel, M. R. and Maciel Filho, R. 2017b. Separation and Purification Technologies for Lactic Acid – A Brief Review. *BioResources,* 12**,** 6885-6901.

Kong, L., Li, G., Wang, H., He, W. and Ling, F. 2008. Hydrothermal catalytic conversion of biomass for lactic acid production. *Journal of Chemical Technology and Biotechnology,* 83**,** 383-388.

Korkmaz, D. 2001. Precipitation Titration: Determination of Chloride by the Mohr Method. *Methods,* 2**,** 1-6.

Kouakou, J., Nanga, S. N., Plagne-Ismail, C., Pali, A. M. and Ognakossan, K. E. 2016. *Cassava: production and processing,* Yaoundé (Cameroun), Engineers Without Borders, Cameroon (ISF Cameroun) and The Technical Centre for Agricultural and Rural Cooperation (CTA).

Krishna, B. S., Nikhilesh, G. S. S., Tarun, B., V, N. S. K. and Gopinadh, R. 2018. Industrial production of lactic acid and its applications. *International Journal of Biotech Research,* 1**,** 42-54.

Kuy, S. and Boonyarattanakalin, S. 2019. Lactic acid production from alkaline hydrothermal reaction of cassava starch. *Songklanakarin Journal of Science and Technology,* 41**,** 506-512.

La, M., Hao, Y., Wang, Z., Han, G. C. and Qu, L. 2016. Selective and Sensitive Detection of Cyanide Based on the Displacement Strategy Using a Water-Soluble Fluorescent Probe. *Journal of Analytical Methods in Chemistry,* 2016**,** 1462013.

Lambri, M., Fumi, M. D., Roda, A. and Faveri, D. M. D. 2013. Improved processing methods to reduce the total cyanide content of cassava roots from Burundi. *African Journal of Biotechnology,* 12**,** 2685-2691.

Lansche, J., Awiszus, S., Latif, S. and Müller, J. 2020. Potential of Biogas Production from Processing Residues to Reduce Environmental Impacts from Cassava Starch and Crisp Production-A Case Study from Malaysia. *Applied Sciences,* 10**,** 2975.

Lasprilla, A. J., Martinez, G. A., Lunelli, B. H., Jardini, A. L. and Filho, R. M. 2012. Poly-lactic acid synthesis for application in biomedical devices - a review. *Biotechnology Advances,* 30**,** 321-328.

Lawal, N. S., Ogedengbe, K. and Oamen, E. C. 2019. Cassava Mill Wastewater Treatment by a Combination of Physical and Nature-Based Processes: A Pilot Study. *Applied Journal of Environmental Engineering Science,* 5**,** 349-356.

Lawal, N. S., Ogedengbe, K., Ojo, O. O. S. and Odufowokan, A. A. 2020. Assessment of a submerged membrane bioreactor with composite ceramic filters for cassava wastewater treatment. *Research in Agricultural Engineering,* 66**,** 72-79.

Lei, X., Wang, F.-F., Liu, C.-L., Yang, R.-Z. and Dong, W.-S. 2014. One-pot catalytic conversion of carbohydrate biomass to lactic acidusing an ErCl3catalyst. *Applied Catalysis A: General,* 482**,** 78-83.

Li, L., Yan, L., Shen, F., Qiu, M. and Qi, X. 2017. Mechanocatalytic Production of Lactic Acid from Glucose by Ball Milling. *Catalysts,* 7**,** 170-177.

Li, S., Deng, W., Li, Y., Zhang, Q. and Wang, Y. 2019. Catalytic conversion of cellulose-based biomass and glycerol to lactic acid. *Journal of Energy Chemistry,* 32**,** 138-151.

Long, L., Yuan, X., Cao, S., Han, Y., Liu, W., Chen, Q., Han, Z. and Wang, K. 2019. Determination of Cyanide in Water and Food Samples Using an Efficient Naphthalene-Based Ratiometric Fluorescent Probe. *ACS Omega,* 4**,** 10784-10790.

Lopes, M. S., Jardini, A. L. and Filho, R. M. 2012. Poly (Lactic Acid) Production for Tissue Engineering Applications. *20th International Congress of Chemical and Process Engineering CHISA 2012* Prague, Czech Republic.

Lopez Gomez, A. V. and Martinez Calatayud, J. 1998. Determination of cyanide by a flow injection analysis-atomic absorption spectrometric method. *Analyst,* 123**,** 2103-7.

Ma, C., Jin, F., Cao, J. and Wu, B. 2010. Hydrothermal Conversion of Carbohydrates into Lactic Acid with Alkaline Catalysts. *4th International Conference on Bioinformatics and Biomedical Engineering.* Chengdu, China: IEEE.

Mabasa, K. G. 2007. *Epidemiology of cassava mosaic disease and molecular characterization of cassava mosaic viruses and their associated whitefly (BEMISIA TABACI) vector in SOUTH AFRICA.* Master of Science, University of the Witwatersrand, Johannesburg.

Makwarela, M. and Rey, C. 2006. Cassava Biotechnology, a southern African Perspective. *Biotechnology and Molecular Biology Review,* 1**,** 2-11.

Martín, C., Wei, M., Xiong, S. and J.Jönsson, L. 2017. Enhancing saccharification of cassava stems by starch hydrolysis prior to pretreatment. *Industrial Crops and Products,* 97**,** 21-31.

Maślanka, S., KOS, A., BAŃCZYK, M., CZOPEK, I. and ADAM, Ł. 2015. Study of concentration of lactic acid obtained in the process of lactic fermentation of lactose contained in the spent whey using Lactobacillus. *Chemik,* 69**,** 247-251.

Masutani, K. and Kimura, Y. 2014. PLA Synthesis. From the Monomer to the Polymer. *In:* Jiménez, A., Peltzerand, M. andRuseckaite, R. (eds.) *Poly(lactic acid) Science and Technology: Processing, Properties, Additives and Applications.* RSC Publishing.

Mombo, S., Dumat, C., Shahid, M. and Schreck, E. 2017. A socio-scientific analysis of the environmental and health benefits as well as potential risks of cassava production and consumption. *Environmental Science and Pollution Research,* 24**,** 5207-5221.

Montagnac, J. A., Davis, C. R. and Tanumihardjo, S. A. 2009. Processing Techniques to Reduce Toxicity and Antinutrients of Cassava for Use as a Staple Food. *Comprehensive Reviews in Food Science and Food Safety,* 8**,** 17-27.

Mousavi, A. 2018. *Analysis of cyanide in mining waters.* Master in Program of Chemical Engineering, Lappeenranta university of technology.

Mudombi, C. R. 2010. *An ex ante economic evaluation of genetically modified cassava in South Africa.* MSc Agric (Agricultural Economics), University of Pretoria.

Mushumbusi, C. B. 2018. *Cyanide levels in raw sweet cassava varieties and people's perception on cyanide poisoning in Kagera and Morogoro regions of Tanzania.* Master of science Sokoine university of agriculture.

Mushumbusi, C. B., Max, R. A., Bakari, G. G., Mushi, J. R. and Balthazary, S. T. 2020. Cyanide in Cassava Varie ties and Peo ple's Perce ption on Cyanide Pois oning in Selected Regio ns of Tanzania. *Journal of Agricultural Studies,* 8**,** 180-193.

Mustarichie, R., Sulistyaningsih, S. and Runadi, D. 2020. Antibacterial Activity Test of Extracts and Fractions of Cassava Leaves (*Manihot esculenta* Crantz) against Clinical Isolates of *Staphylococcus epidermidis* and *Propionibacterium acnes* Causing Acne. *International Journal of Microbiology,* 2020**,** 1975904.

Nandiyanto, A. B. D., Oktiani, R. and Ragadhita, R. 2019. How to Read and Interpret FTIR Spectroscope of Organic Material. *Indonesian Journal of Science & Technology,* 4**,** 97-118.

Narayanan, G., Vernekar, V. N., Kuyinu, E. L. and Laurencin, C. T. 2016. Poly (lactic acid)-based biomaterials for orthopaedic regenerative engineering. *Advanced Drug Delivery Reviews,* 107**,** 247-276.

Narayanan, N., Roychoudhury, P. K. and Srivastava, A. 2004. L (+) lactic acid fermentation and its product polymerization. *Electronic Journal of Biotechnology,* 7**,** 167-178.

Ndam, Y. N., Mounjouenpou, P., Kansci, G., Kenfack, M. J., Meguia, M. P. F., Eyenga, N. S. N. N., Akhobakoh, M. M. and Nyegue, A. 2019. Influence of cultivars and processing methods on the cyanide contents of cassava (*Manihot esculenta* Crantz) and its traditional food products. *Scientific African,* 5.

Ndubuisi, N. D. and Chidiebere, A. C. U. 2018. Cyanide in Cassava: A Review. *International Journal of Genomics and Data Mining,* 118**,** 1-10.

Ngugi, M. P., Murugi, N. J., Oduor, O. R., Mgutu, A. J., Ombori, R. O. and Cheriyot, R. C. 2015. Determination of Cyanogenic Compounds Content in Transgenic Acyanogenic Kenyan Cassava (*Manihot esculenta* Crantz) Genotypes: Linking Molecular Analysis to Biochemical Analysis. *Journal of Analytical & Bioanalytical Techniques,* 6.

Nhassico, D., Muquingue, H., Cliff, J., Cumbana, A. and Bradbury, J. H. 2008. Rising African cassava production, diseases due to high cyanide intake and control measures. *Journal of the Science of Food and Agriculture,* 88**,** 2043-2049.

NHM, N. H. M.-. 2017. *Map of the spread of cassava over time* [Online]. Available: https://www.nhm.ac.uk/resources/nature-online/life/plants-fungi/seeds-of-trade/images/maps/cassava.gif [Accessed 2019].

Nuwamanya, E., Baguma, Y. and Rey, M. E. C. 2016. An African perspective: developing an African bioresource-based industry – the case for cassava. *In:* Virgin, I. andMorris, E. J. (eds.) *Creating Sustainable Bioeconomies The bioscience revolution in Europe and Africa.* 1st ed. London: Taylor & Francis.

Nuwamanya, E., Chiwona-Karltun, L., Kawuki, R. S. and Baguma, Y. 2012. Bio-ethanol production from non-food parts of cassava (Manihot esculenta Crantz). *Ambio,* 41**,** 262-270.

Nyirenda, K. K. 2021. Toxicity Potential of Cyanogenic Glycosides in Edible Plants. *In:* Erkekoglu, P. andOgawa, T. (eds.) *Medical Toxicology.* London: IntechOpen.

Obueh, H. and Odesiri-Eruteyan, E. 2016. A Study on the Effects of Cassava Processing Wastes on the Soil Environment of a Local Cassava Mill. *Journal of Pollution Effects & Control,* 4.

Oghenejoboh, K. M. 2015. Effects of Cassava Wastewater on the Quality of Receiving Water Body Intended for Fish Farming. *British Journal of Applied Science & Technology,* 6**,** 164-171.

Okudoh, V., Trois, C., Workneh, T. and Schmidt, S. 2014. The potential of cassava biomass and applicable technologies for sustainable biogas production in South Africa: A review. *Renewable and Sustainable Energy Reviews,* 39**,** 1035-1052.

Olaoye, R., Afolayan, O., Mustapha, O. and Adeleke, H. 2018. The Efficacy of Banana Peel Activated Carbon in the Removal of Cyanide and Selected Metals from Cassava Processing Wastewater. *Advances in Research,* 16**,** 1-12.

Omomowo, I. O., Omomowo, O. I., Adeeyo, A. O., Adebayo, E. A. and Oladipo, E. K. 2015. Bacteriological Screening and Pathogenic Potential of Soil Receiving Cassava Mill Effluents. *International Journal of Basic and Applied Science,* 3**,** 26-36.

Omotayo, A. R., EL-Ishaq, A. and Babatunde, A. S. 2015. Assessment of Cyanide Content in White, Light Yellow and Deep Yellow Cassava Grit (Gari) Sold in Damaturu Metropolis. *American Journal of Food Science and Health,* 1**,** 109-113.

Orazov, M. and Davis, M. E. 2015. Tandem catalysis for the production of alkyl lactates from ketohexoses at moderate temperatures. *Proceedings of the National Academy of Sciences,* 112**,** 11777-11782.

Orozco, F. G., Valadez-González, A., Domínguez-Maldonado, J. A., Zuluaga, F., Figueroa-Oyosa, L. E. and Alzate-Gaviria, L. M. 2014. Lactic Acid Yield Using Different Bacterial Strains, Its Purification, and Polymerization through Ring-Opening Reactions. *International Journal of Polymer Science,* 2014**,** 365310.

Oshima, H., Ueno, E., Saito, I. and Matsumoto, H. 2003. Quantitative Determination of Cyanide in Foods by Spectrophotometry using Picric Acid Test Strips. *Japanese Journal of Food Chemistry* 10**,** 96-100.

Otekunrin, O. A. and Sawicka, B. 2019. Cassava, a 21st Century Staple Crop: How can Nigeria Harness Its Enormous Trade Potentials? *Acta Scientific Agriculture,* 3**,** 194-202.

Panou, M. and Gkelis, S. 2020. Cyano-assassins: Widespread cyanogenic production from cyanobacteria. *BioRxiv*.

Pereira, I. G., Vagula, J. M., Marchi, D. F., Barão, C. E., R., G., Almeida, S., Visentainer, J. V., Maruyama, S. A. and Júnior, O. O. S. 2016. Easy Method for Removal of Cyanogens from Cassava Leaves with Retention of Vitamins and Omega-3 Fatty Acids. *Journal of the Brazilian Chemical Society,* 27**,** 1290-1296.

Polthanee, A. and Wongpichet, K. 2017. Effects of Planting Methods on Root Yield and Nutrient Removal of Five Cassava Cultivars Planted in Late Rainy Season in Northeastern Thailand. *Agricultural Sciences,* 8**,** 33-45.

Rashid, R. 2008. *Optimization and modeling of lactic acid production from pineapple waste* Universiti Teknologi Malaysia.

Rawat, K., Nirmala, C. and Bisht, M. S. 2015. Processing Techniques for Reduction of Cyanogenic Glycosides from Bamboo Shoots. *10th World Bamboo Congress.* Korea.

Recalde-Ruiz, D. L., Andrés-García, E. and Díaz-García, M. E. 2000. Fluorimetric flow injection and flow-through sensing systems for cyanide control in waste water. *The Analyst,* 125**,** 2100-2105.

Reddy, G., Altaf, M., Naveena, B. J., Venkateshwar, M. and Kumar, E. V. 2008. Amylolytic bacterial lactic acid fermentation - a review. *Biotechnology Advances,* 26**,** 22-34.

Research, Z. M. 2019. *Lactic Acid Market - Global Industry Analysis* [Online]. Available: https://www.zionmarketresearch.com/report/lactic-acid-market [Accessed 2021].

Saha, S., Ghosh, A., Mahato, P., Mishra, S., Mishra, S. K., Suresh, E., Das, S. and Das, A. 2010. Specific recognition and sensing of CN^- in sodium cyanide solution. *Organic Letters,* 12**,** 3406-3409.

Sánchez, C., Egüés, I., García, A., Llano-Ponte, R. and Labidi, J. 2012. Lactic acid production by alkaline hydrothermal treatment of corn cobs. *Chemical Engineering Journal,* 181-182**,** 655-660.

Saunders, D. A. 2012. When plants bite back: A broadly applicable method for the determination of cyanogenic glycosides as hydrogen cyanide in plant-based foodstuffs. *Chemistry in New Zealand,* 4**,** 129-132.

Sekab. 2021. *Acetaldehyde– A basic chemical to be found in many everyday products around us* [Online]. Available: https://www.sekab.com/en/products-services/product/acetaldehyde/ [Accessed 2021].

Shackelford, G. E., Haddaway, N. R., Usieta, H. O., Pypers, P., Petrovan, S. O. and Sutherland, W. J. 2018. Cassava farming practices and their agricultural and environmental impacts: a systematic map protocol. *Environmental Evidence,* 7**,** 1-7.

Sharif, N. F. A., Razak, S. I. A. and Rahman, W. A. W. A. 2014. Cassava leaves as packaging materials *Cellulose Chemistry And Technology,* 48**,** 585-590.

Sharif, N. F. A., Saiful Izwan Abd Razak, Rahman, W. A. W. A., Nayan, N. H. M., Rahmat, A. R. and Yahya, M. Y. 2015. Preparation and characterization of cassava leaves/cassava starch acetate biocomposite sheets. *BioResources,* 10**,** 4339-4349.

Shen, Z., Gao, Y., Kong, L., Gu, M., Xia, M., Dong, W., Zhang, W., Zhou, X. and Zhang, Y. 2021. Selective Conversion of Scenedesmus into Lactic Acid over Amine-Modified Sn-β. *ACS Omega,* 6**,** 284-293.

Shittu, T. A., Alimi, B. A., Wahab, B., Sanni, L. O. and Abass, A. B. 2016. Cassava Flour and Starch: Processing Technology and Utilization. *In:* Sharma, H. K., Njintang, N. Y., Singhal, R. S. andKaushal, P. (eds.) *Tropical Roots and Tubers: Production, Processing and Technology.* First ed.: John Wiley & Sons, Ltd.

Sitompul, J., Setyawan, D., Kim, D. Y. J. and Lee, H. W. Synthesis of PDLLA/PLLA-bentonite nanocomposite through sonication. AIP Conference Proceedings, 2016. AIP Publishing, p.020080.

Sobrun, Y., Bhaw-Luximon, A., Jhurry, D. and Puchooa, D. 2012. Isolation of lactic acid bacteria from sugar cane juice and production of lactic acid from selected improved strains. *Advances in Bioscience and Biotechnology,* 3**,** 398-407.

Spencer, D. S. C. and Ezedinma, C. 2017. Cassava cultivation in sub-Saharan Africa. *Achieving sustainable cultivation of cassava Volume 1.* Cambridge: Burleigh Dodds Science Publishing

Srihawong, W., Kongsil, P., Petchpoung, K. and Sarobol, E. 2015. Effect of genotype, age and soil moisture on cyanogenic glycosides content and root yield in cassava (Manihot esculenta Crantz). *Agriculture and Natural Resources,* 49**,** 844-855.

Subramanian, M. R., Talluri, S. and Christopher, L. P. 2015. Production of lactic acid using a new homofermentative Enterococcus faecalis isolate. *Microbial Biotechnology,* 8**,** 221-229.

Tallarico, S., Costanzo, P., Bonacci, S., Macario, A., Di Gioia, M. L., Nardi, M., Procopio, A. and Oliverio, M. 2019. Combined Ultrasound/Microwave Chemocatalytic Method for Selective Conversion of Cellulose into Lactic Acid. *Scientific Reports,* 9**,** 1-8.

Tesleva, E. P., Gil, L. B. and Solovyan, A. V. Thermodeformational Behavior of Cubic Crystals of Sodium Cyanide. VII International Scientific Practical Conference "Innovative Technologies in Engineering", 2016 Yurga, Russian Federation. IOP Publishing Ltd, 6.

Tewe, O. O. and Iyayi, E. A. 1989. *Cyanogenic Glycosides,* Boca Raton, Florida, CRC-Press, Inc.

Tivana, L. 2012. *Cassava Processing: Safety and Protein Fortification.* Doctoral Degree, Lund University.

Tivana, L. D., Francisco, J. D. C., Zelder, F., Bergenståhl, B. and Dejmek, P. 2014. Straightforward rapid spectrophotometric quantification of totalcyanogenic glycosides in fresh and processed cassava products. *Food Chemistry,* 158**,** 20-27.

Trevisan, A. P., Lied, E. B., Fronza, F. L., Devens, K. U. and Gomes, S. D. 2019. Cassava Wastewater Treatment by Coagulation/Flocculation Using Moringa oleifera Seeds *Chemical Engineering Transactions,* 74**,** 367-372.

Trontel, A., Baršić, V., Slavica, A., Santek, B. and Novak, S. 2010. Modelling the Effect of Different Substrates and Temperature on the Growth and Lactic Acid Production by *Lactobacillus amylovorus* DSM 20531T in Batch Process. *Food Technology and Biotechnology,* 48**,** 352-361.

Ubwa, S. T., Otache, M. A., Igbum, G. O. and Shambe, T. 2015. Determination of Cyanide Content in Three Sweet Cassava Cultivars in Three Local Government Areas of Benue State, Nigeria. *Food and Nutrition Sciences,* 06**,** 1078-1085.

Umuhozariho M, G., Shayo N, B., Msuya J, M. and PSallah , Y. K. 2014. Cyanide and selected nutrients content of different preparations of leaves from three cassava species. *African Journal of Food Science,* 8**,** 122-129.

Veselá, A. B. 2015. *Study of function and molecular architecture of fungal nitrilases applicable in biocatalysis.* Charles University in Prague.

Voss, D., Dietrich, R., Stuckart, M. and Albert, J. 2020. Switchable Catalytic Polyoxometalate-Based Systems for Biomass Conversion to Carboxylic Acids. *ACS Omega,* 5**,** 19082-19091.

Waisundara, V. Y. 2018. Introductory Chapter: Cassava as a Staple Food. *In:* Waisundara, V. Y. (ed.) *Cassava.* IntechOpen.

Wang, F.-F., Jie Liu, H. L., Liu, C.-L., Yang, R.-Z. and Dong, W.-S. 2015. Conversion of cellulose to lactic acid catalyzed by erbium-exchanged montmorillonite K10. *Green Chemistry,* 17**,** 2455-2463.

Wang, F.-F., Wu, H.-Z., Ren, H.-F., Liu, C.-L., Xu, C.-L. and Dong, W.-S. 2016. Er/β-zeolite-catalyzed one-pot conversion of cellulose to lactic acid. *Journal of Porous Materials,* 24**,** 697-706.

Wang, X., Song, Y., Huang, C., Liangb, F. and Chena, B. 2014. Lactic acid production from glucose over polymer catalysts in aqueous alkaline solution under mild conditions. *Green Chemistry,* 16**,** 4234-4240.

Wang, Y., Deng, W., Wang, B., Zhang, Q., Wan, X., Tang, Z., Wang, Y., Zhu, C., Cao, Z., Wang, G. and Wan, H. 2013. Chemical synthesis of lactic acid from cellulose catalysed by lead(II) ions in water. *Nature Communications,* 4**,** 1-7.

Wangari, M. F. 2013. *Potential toxic levels of cyanide in cassava (manihot esculenta CRANTZ) grown in some parts of Kenya.* Master of Science in Chemistry, Kenyatta University.

Watthier, E., Andreani, C. L., Torres, D. G. B., Kuczman, O., Tavares, M. H. F., Lopes, D. D. and Gomes, S. D. 2019. Cassava Wastewater Treatment in Fixed-Bed Reactors: Organic Matter Removal and Biogas Production. *Frontiers in Sustainable Food Systems,* 3.

Wee, Y.-J., Kim, J.-N. and Ryu, H.-W. 2006. Biotechnological Production of Lactic Acid and Its Recent Applications. *Food Technology and Biotechnology,* 44**,** 163-172.

Wilberforce, J. O. O. and Ngele, S. O. 2016. Comparative Assay of Cyanide Content in Cassava from Selected Parts of Imo State, Nigeria. *World Journal of Medical Sciences,* 13**,** 204-207.

Woffenden, M., Noller, B. N., Noonan, K., Breuer, P., Cooper, P. and Donato, D. 2008. *Cyanide management*, Commonwealth of Australia.

Yahaya, I. and Seferoglu, Z. 2018. Fluorescence Dyes for Determination of Cyanide. *Photochemistry and Photophysics - Fundamentals to Applications* Ankara, Turkey.

Yan, X., Jin, F., Tohji, K., Kishita, A. and Enomoto, H. 2010. Hydrothermal conversion of carbohydrate biomass to lactic acid. *AIChE Journal,* 56**,** 2727-2733.

Yang, G.-Y., Ke, Y.-H., Ren, H.-F., Liu, C.-L., Yang, R.-Z. and Dong, W.-S. 2016. The conversion of glycerol to lactic acid catalyzed by ZrO2-supported CuO catalysts. *Chemical Engineering Journal,* 283**,** 759-767.

Yang, L., Su, J., Carl, S., Lynam, J. G., Yang, X. and Lin, H. 2015. Catalytic conversion of hemicellulosic biomass to lactic acid inpH neutral aqueous phase media. *Applied Catalysis B: Environmental,* 162**,** 149-157.

Yu, X. Z. 2014. Uptake, assimilation and toxicity of cyanogenic compounds in plants: facts and fiction. *International Journal of Environmental Science and Technology,* 12**,** 763-774.

Yu, Y., Shu, T. and Dong, C. 2017. A convenient colorimetric and ratiometricfluorescent probe fordetection of cyanide based on BODIPY derivative in aqueous media. *Analytical Chemistry Research,* 12**,** 34-39.

Yun, J. S., Wee, Y. J., Kim, J. N. and Ryu, H. W. 2004. Fermentative production of DL-lactic acid from amylase-treated rice and wheat brans hydrolyzate by a novel lactic acid bacterium, Lactobacillus sp. *Biotechnology Letters,* 26**,** 1613-1616.

Zhang, H., Hu, Y., Qi, L., Jian He, H. L. and Yang, S. 2018. Chemocatalytic Production of Lactates from Biomass Derived Sugars. *International Journal of Chemical Engineering,* 2018**,** 18 pages.

Zhu, W., Lestander, T. A., Örberg, H., Wei, M., Hedman, B., Ren, J., Xie, G. and Xiong, S. 2015. Cassava stems: a new resource to increase food and fuel production. *Gcb Bioenergy,* 7**,** 72-83.

Zidenga, T., Siritunga, D. and Sayre, R. T. 2017. Cyanogen Metabolism in Cassava Roots: Impact on Protein Synthesis and Root Development. *Frontiers in Plant Science,* 8**,** 220.

Zuk, M., Pelc, K., Szperlik, J., Sawula, A. and Szopa, J. 2020. Metabolism of the Cyanogenic Glucosides in Developing Flax: Metabolic Analysis, and Expression Pattern of Genes. *Metabolites,* 10**,** 288.